INTRA-VALLEY TOPOGRAPHICAL CONTROL OF NOCTURNAL VALLEY WINDS

by

Robert D. O'Neal
Thomas B. McKee

Department of Atmospheric Science
Colorado State University
Fort Collins, Colorado

Colorado State University

Department of Atmospheric Science

Paper No. 416

INTRA-VALLEY TOPOGRAPHICAL CONTROL OF NOCTURNAL VALLEY WINDS

Robert D. O'Neal

Thomas B. McKee

This research was supported by the
National Science Foundation
under grant number ATM-830428
and the Colorado State University
Agricultural Experiment Station

Department of Atmospheric Science
Colorado State University
Fort Collins, Colorado 80523

July 1987

Atmospheric Science Paper No. 416

Climatology Report No. 87-2

ABSTRACT

INTRA-VALLEY TOPOGRAPHICAL CONTROL OF NOCTURNAL VALLEY WINDS

Mountain-valleys throughout the world exhibit diurnal wind systems under synoptically undisturbed conditions. Along-valley temperature and pressure gradients are established under these circumstances creating valley wind systems which reverse sign twice daily. The purpose of this research was to investigate the role that valley topography plays during the nocturnal cooling of air in the valley volume, particularly when advective processes are small such as early in the cooling period.

Commencing with the First Law of Thermodynamics and utilizing energy budgets, a unique method has been derived for the cooling rate of an air volume. In a dry environment the rate of cooling is proportional to an energy term, expressed as the difference between the net longwave radiation escaping through the top of the valley atmosphere and the ground heat flux in the valley, multiplied by a topographical term, K. The topographical parameter is defined for a cross section to be the ratio of valley width from ridgetop to ridgetop divided by the cross-sectional area.

A changing valley configuration produces a variation in the topographical parameter which allows for differential cooling rates among the valley cross sections. If the topography changes in a systematic manner, an along-valley temperature gradient will be established which will hydrostatically produce a corresponding pressure gradient driving the nocturnal valley wind. The sign of the

topographically-induced temperature gradient hinges entirely on the change of the topographic parameter along-valley. Advective changes aside, a decreasing K down-valley produces relatively cooler air in the upper portion of the valley compared to the lower portion which leads to a strong down-valley wind. An increasing K in the down-valley direction produces the opposite temperature regime and consequently light down-valley winds.

The topographic parameter was calculated for five Colorado mountain-valleys using digital elevation data and compared to tethersonde wind observations available in four of them. Good agreement was found between the changing topographic parameter and the observed strength of the valley wind system. The ability of the topographical parameter to create a localized temperature gradient within individual valleys eliminates the need to include the plain effect as an important feature in the creation of the local mountain-valley wind system.

ACKNOWLEDGMENTS

The authors greatly appreciated the constructive criticism and recommendations of Dr. Richard Johnson and Dr. Freeman Smith in improving the final version of this report. Dr. Elmar Reiter was instrumental in providing many of the European references cited in this research.

A special thanks goes to Mr. John Kleist who provided assistance with the computer work, Ms. Odie Bliss who was invaluable in putting this all together and Ms. Judy Sorbie who drafted several of the figures. This research was funded by the National Science Foundation under grant number ATM-8304328 and the Colorado State University Agricultural Experiment Station.

TABLE OF CONTENTS

LIST OF TABLES

LIST OF FIGURES

CHAPTER I

INTRODUCTION

As the world's population swells in the latter portion of the twentieth century, environmental issues garner an increasing amount of attention from physical and sociological scientists alike. A leading contender among today's concerns is the foulness of the air given to us both as a benefit and a burden of modern technology. The pollution of the fluid which houses our everyday lifestyles demonstrates the need for a greater understanding of the causes and the effects of atmospheric motion.

Mountain meteorology has been an area of research for many years and as industrial activity and population increase in this region, the need for more information will accelerate. Despite its scenic beauty, mountainous terrain is not immune to air quality problems. The layer of woodsmoke trapped in a mountain valley by a temperature inversion is a familiar sight to the high country skier. Proper ventilation of this air can only be accomplished through thermal mixing of the daytime boundary layer or mechanical mixing by the wind.

The diurnal circulations found in mountain-valleys are well documented throughout the literature. In order to separate the local effects from the larger synoptic flow, the majority of research in this area has focused on days with clear, undisturbed weather and weak upper-level winds. The resultant slope and valley wind systems have been studied and theorized by many authors beginning with Wagner (1938) in

the 1930's. He theorized that unequal heating and cooling differences between the mountain-valley and adjacent plain cause up-valley winds during the day and down-valley winds at night. The speed and depth of the valley wind layer appears to be a characteristic unique to each valley. Whiteman (1980) took 375 tethersonde soundings in western Colorado valleys over the course of four years and found that each valley was capable of reproducing its own wind regime night after night under favorable synoptic conditions.

Many factors appear to be important to the development or absence of the valley wind system. Among them are:

1) along-valley pressure gradient
2) mechanical or natural constrictions in the valley
3) volume of down-valley reservoirs
4) angle of merging valleys

Of principal interest to mountain meteorology is the pressure gradient whose presence may depend on the nature of the other three quantities.

Valley geometry has long been recognized as contributing to a horizontal temperature gradient in the valley which in turn causes a horizontal pressure gradient driving the wind. According to Wagner (1938) the pressure gradient is the result of the combined effects of the inclinations of valley bottom and ridge line. Steinacker (1984) concluded that the primary reason for the valley wind regime is found in the geometric features of the orography. Vergeiner and Dreiseitl (1987) explain that the daily range of temperature is much larger in the interior of valleys than over the foreland because of pure geometry. A certain percent of the air volume beneath the crest height (dependent on the slope of the valley sidewalls) is blocked out in a mountainous region compared to an equal area over the plains.

Whiteman's observations would seem to indicate that there is an intrinsic feature of each valley which helps to uniquely determine its characteristic wind speed. The purpose of this paper is to develop an analytic method which brings out the importance of valley topography during the nocturnal cooling regime. Inherently varying topography along the valley axis will influence the local cooling rate of the valley air which can lead to a temperature gradient in the valley atmosphere. A temperature gradient leads to a pressure gradient through the hydrostatic relationship thereby establishing a valley wind. Knowledge of the along-valley topography can be utilized as an aid in the determination of the strength and direction of the temperature gradient. This can be combined with energy budget considerations to estimate whether a valley will exhibit strong nocturnal winds (a "draining" valley) or weak nocturnal winds (a "pooling" valley). The theory is tested on several western Colorado mountain-valleys where tethersonde wind observations are available.

CHAPTER II

LITERATURE REVIEW

Diurnal valley winds are generally divided into two categories. Winds blowing parallel to the valley axis are termed valley winds. Slope winds typically blow parallel to the inclination of the valley sidewalls. Up-valley and up-slope winds are characteristic of the daytime hours while down-valley and down-slope winds are usually found at night. The valley and slope wind terminology used in this research is illustrated in Figure 1.

The history of the theoretical development of valley and slope wind systems up to 1980 is well summarized by Whiteman (1980). Synoptic conditions, valley geometry, and the forcing functions behind mountain-valley wind systems are reviewed from Wagner's (1938) early theory up through Whiteman's own research program in Colorado. Consequently, the ensuing discussion will focus on a portion of the mountain-valley literature published since 1980.

In 1978, the Assistant Secretary for the Environment developed a program specifically geared toward Atmospheric Studies in COmplex Terrain (ASCOT). The two main objectives of the ASCOT program presented by Dickerson and Gudiksen (1980) were:

1) To improve fundamental knowledge of transport and dispersion processes in complex terrain.
2) Building on this improvement in the understanding of the physics, provide a methodology for performing air-quality assessments.

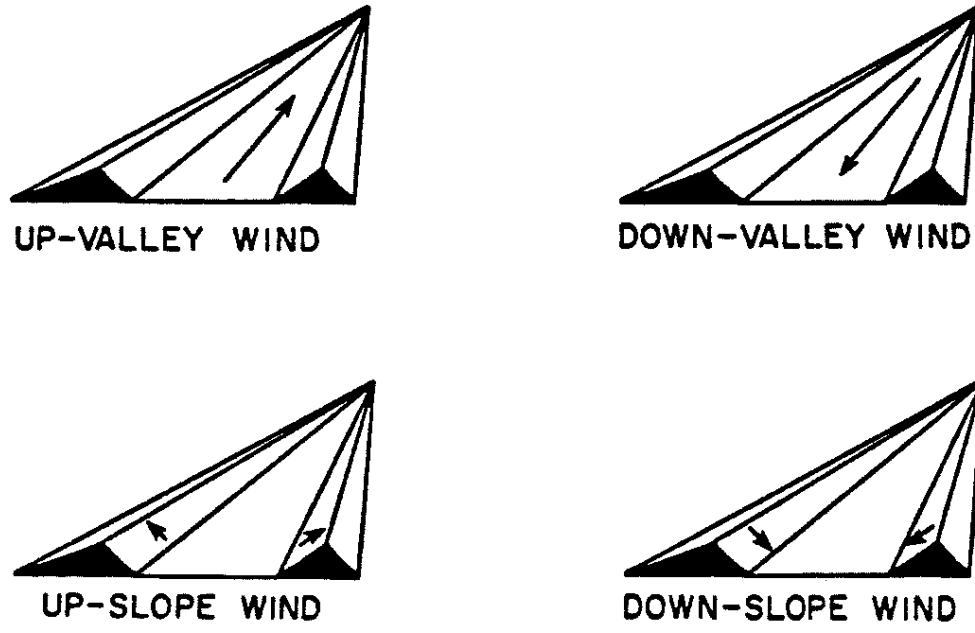

Figure 1. Valley and slope wind terminology. From Whiteman (1980).

As a result of the ASCOT program, an abundance of new data was collected from several field projects in the western United States. Yamada (1981) was one of the first scientists to tap the ASCOT data source. His three-dimensional nocturnal drainage flow model compares results with the wind data collected in the 1979 ASCOT study at the California Known Geothermal Resources Area. The model predicts a wind speed maximum in the surface layer as the flow travels downslope. Observed speeds, however, are much smaller and more uniform with height. Yamada surmises this discrepancy may be due to canopy effects and poor vertical resolution of the tethersondes near the earth's surface. Garrett (1983) has formulated a one-dimensional slope flow model for research and operational applications. Drainage wind and temperature profiles are calculated and compared to observations from Australia and various ASCOT experiments from 1979-1981. The model performs well in uniform slope areas but fares poorly in complex terrain.

ASCOT 82 was conducted during the summer of 1982 in Brush Creek, a 600 meter deep valley in western Colorado. Bader (1985) researched the diurnal evolution of the boundary layer over northwest Colorado in which he utilized a numerical model to help understand the ASCOT 82 data. He concluded that the valley wind structure, the geostrophic wind direction and the mesoscale boundary layer evolution were interrelated. Whiteman and Barr (1986) have also presented results from ASCOT 82 in which they have derived a relationship between atmospheric mass transport and the nocturnal valley-wind. A network of five stations along an eight kilometer stretch of the valley axis exhibit a jet wind maximum which decreases somewhat in strength and rises in above ground level height with down-valley distance. Analyses from ASCOT 84, situated in Brush

Creek during the fall of 1984, are now beginning to appear in professional publications.

In addition to the ASCOT field work, Hennemuth (1987) reports that the European community has also been conducting mountain-valley experiments during the late 1970's and early 1980's. Among them have been the Alpine Experiment (ALPEX) organized by the WMO, the Mesoscale Experiment in the Region Kufstein-Rosenheim (MERKUR), an investigation of the slope wind layer in the HAWEI experiment of 1978, and the Dischma valley climate investigation (DISKUS) in 1980.

The mountain-wind experiment DISKUS took place in the Dischma Valley near Davos, Switzerland in August 1980 (Hennemuth 1987) and is of particular interest to mountain meteorology because through the collection of air temperature, wind and surface energy balance quantities, a unique look at the energy budget of an entire valley atmosphere is presented. This study was intended to look at the daytime heating of a valley so nocturnal measurements of the energy budget are not available. Data collected during the first intensive observing period of the MERKUR project has been analyzed by Freytag (1985) to study the horizontal temperature gradient and the energetics of the Inn Valley atmosphere. Freytag's case study looked at 33 consecutive hours of heating and cooling from which he concluded that there is no similarity between the development of the daytime and nighttime wind development due in large part to the differing roles temperature advection plays in the cycle.

Vergeiner and Dreiseitl (1987) recently published an excellent overview of the current body of knowledge in the areas of mountain-valley and slope winds. Their observations and thoughts include

descriptions of the physical concepts driving the observed phenomena and comparisons to recent field data. A lengthy set of references, many which may be unknown to the American meteorologist, are listed at the end of the paper.

Several attempts have been made to characterize the complicated orography found in mountain-valleys. Petkovsek (1978) uses parameters such as the linear openness of basins and the inflow and outflow of air in the basin to develop two independent methods for evaluating the height of the cold air pool found in these basins. The theory tests reasonably well with actual observations for some Slovenia basins in northwest Yugoslavia. Petkovsek 's follow-up paper (1980) notes that the aforementioned techniques do not hold for narrow, deep and ramificated basins where redefined characteristics need to be studied. Steinacker (1984) uses energy budget reasoning based on area-height distributions in the valley to explain the large diurnal variation in barometric mean temperature between the valley and the plain. The inclusion of static stability in the model equations is deemed vital to fully explain the temperature change solely on geometry. Areal quantities are defined to be the orographic catchment areas in the valley bounded by a chosen contour line.

Dynamic models of the valley-plain circulation are introduced by Egger (1987) and Vergeiner (1987) in an attempt to capture the basic physical processes at work in this diurnal wind flow. Part I of Egger 's work describes a simple minimum resolution grid point model where the valley volume effect has been incorporated through enhanced heating/cooling in the valley. A serious drawback to this model is the representation of the valley flow by one numerical box which makes it

unable to cope with varying flow characteristics within the valley. Part II tries to resolve the problem in part I by introducing a flow resolving model with increased horizontal resolution in the valley. Profiles of wind and temperature along the valley and plain entrance are studied and found to agree in principal with observations. Vergeiner's (1987) model for quasi-periodic valley winds is constructed for an ideal plain-valley-basin system typical of a large alpine valley. Solutions of mass flux are computed for this system and from these results, heating time lags along-valley, pressure differences from plain to basin and the strength of the along-valley wind are estimated.

Mountain-valley research has identified geometrical differences between valley and plain as the cause of the diurnal circulation between these two features. Vergeiner and Dreiseitl (1987) state that the horizontal temperature contrast between plain and valley, reversing sign twice daily, builds up a corresponding pressure contrast hydrostatically, thereby causing up- and down-valley winds. Whiteman's (1980) work noted, however, that there are wide variations in the strength of the resulting valley winds. What causes some valleys to have weak along-axis flows while others can maintain relatively strong valley winds? No attempt has yet been undertaken to use the actual valley geometry as an aid to qualitatively determine whether a valley can sustain the required pressure gradient to drive the valley winds. In order to maintain down-valley winds, as in the nocturnal case, a higher pressure must exist up-valley relative to the pressure down-valley. The reverse must be true in the daytime case. The research presented here strives to demonstrate how the temperature gradient along-valley varies as a function of the valley geometry, differing from

previous methods in that the valley shape is allowed to change. Petkovsek (1978) laments that a completely digitalized relief would enable us to get more precise determinations of the inclination of cooling areas, and also their size. The current research program utilizes the digital relief available for Colorado to more accurately determine valley parameters and compare them to theory.

CHAPTER III

THEORETICAL DEVELOPMENT

The valley wind system under undisturbed conditions is primarily air currents trying to equalize horizontal pressure gradients which have built up hydrostatically from temperature differences due to unequal heating or cooling in the valley air volume. In the nocturnal case studied here, a temperature gradient along valley will establish itself only if the valley air cools at different rates within the valley volume. This cooling begins during a period of time around sunset when the temperature structure within a valley is relatively uniform as the diurnal wind system is reversing direction.

Fleagle (1950) and Freytag (1985) have developed expressions for the rate of temperature change in a valley but neither one explicitly accounts for the valley geometry. Through the development of an expression for $\partial T/\partial t$, the current research attempts to derive an explicit geometrical parameter which contributes to the valley cooling. The local temperature change can subsequently be linked to the temperature and pressure gradient in order to show how the valley topography is related to the along valley wind.

A. Valley Cooling of an Air Volume

Steinacker (1984) remarks that the volume of air which must be considered when dealing with the energy budget of the valley atmosphere cannot be simply derived from a cross section of the Inn valley. It is

necessary to include all side valleys the circulation of which is linked to the main valley. Heeding this caveat, the theory developed in this paper pertains to valleys or sections of valleys with no major side intrusions.

The rate of potential temperature change for a parcel of air is

$$\frac{dq}{dt} = \frac{c_p T}{\theta} \frac{d\theta}{dt} \tag{1}$$

where q is the heat change per unit mass of air, t is time, c_p is the specific heat at constant pressure, T is temperature and θ is potential temperature.

Equation (1) originated from the Bernoulli equation which expresses the transformations between mechanical and thermodynamic forms of energy for the flow of a compressible fluid. Whiteman (1980) applied a scale analysis technique (Holton 1979) appropriate for the time and space scales used in studying a valley atmosphere. The terms not included in equation (1) were found to be at least two orders of magnitude less than the ones retained above. Equation (1) is also recognized as another version of the First Law of Thermodynamics.

In order to apply equation (1) to an entire valley volume the mass of air $m = \rho V$ in the volume must be considered. Then equation (2) is

$$\frac{dQ}{dt} = \frac{mc_p T}{\theta} \frac{d\theta}{dt} = \frac{\rho c_p T}{\theta} V \frac{d\theta}{dt} \tag{2}$$

where Q is the total heat change in a mass of air, ρ is the density of air and V is the volume of the air.

The idealized valley cross section portrayed in Figure 2 shows that the volume of air undergoing a potential temperature change in the

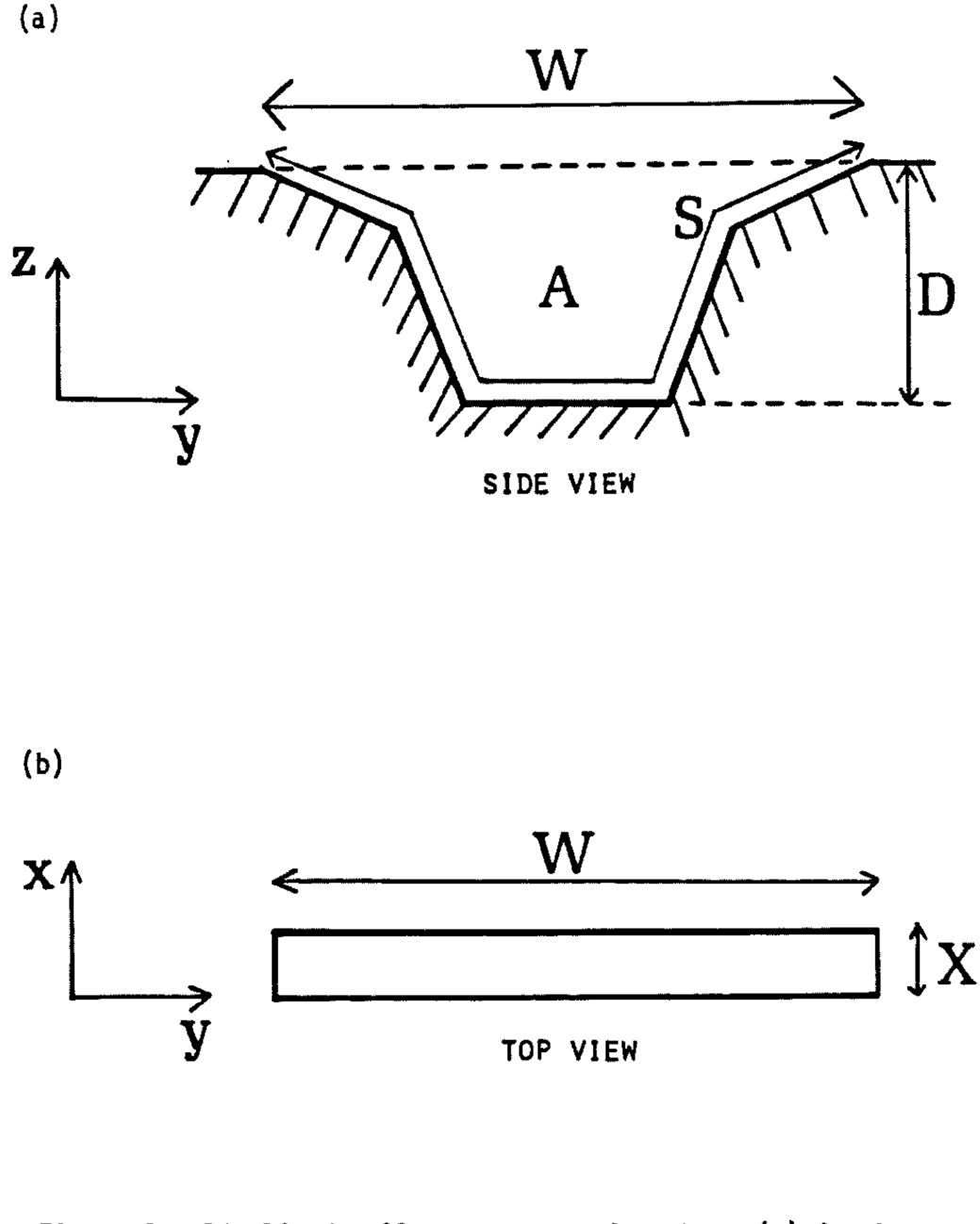

Figure 2. Idealized valley cross section where (a) is the side view and (b) is the top view. W = valley width from ridgetop to ridgetop. A = cross-sectional area of valley. S = distance along cross section surface from ridgetop to ridgetop. X = along valley length.

valley is V = (AX) where A is the cross-sectional area below the ridgetops and X is an arbitrary along-valley length. Equation (2) then becomes

$$\frac{dQ}{dt} = \frac{\rho c_p T}{\theta} (AX) \frac{d\theta}{dt} \qquad (3)$$

in which all variables are volume averages.

The left-hand side of equation (3) is the diabatic heat flux which acts to change the potential temperature of the given volume of air. This heat flux consists of sensible heat H conducted out of the air, radiative divergence and latent heat of evaporation LE. Observations indicate that the locally driven nocturnal wind system is best developed under conditions of a dry, clear atmosphere. Under these circumstances the latent heat will be insignificant.

Since sensible heat conduction (H) is a function of temperature gradient, the valley volume will be cooled primarily by conduction from the atmosphere near the ground into the valley surface. The flux of sensible heat acts only in the y-z plane where the surface area is (SX) (see Figure 2). S is the length of the line integral constructed along the valley cross section surface from ridgetop to ridgetop. Thus equation (3) is

$$\frac{dQ}{dt} = \frac{\rho c_p T}{\theta} (AX) \frac{d\theta}{dt} = H(SX) + \begin{matrix}\text{radiative} \\ \text{divergence}\end{matrix} \qquad (4)$$

where H and the radiative divergence are valley-averaged quantities.

The radiative divergence is merely the cooling an atmospheric volume undergoes due to a net loss of longwave radiation. In terms of the valley volume under consideration this is the difference between the net longwave radiation escaping through the top of the valley

atmosphere, R_T, and the net longwave radiation from the ground surface in the valley, R_S. Another line integral permits the length from ridgetop to ridgetop to be calculated as W (see Figure 2). Radiative divergence in a valley cross section is

$$\text{Radiative divergence} = R_T(WX) - R_S(SX) \tag{5}$$

where R_T and R_S are valley-averaged quantities.

Sellers (1965) states that the surface energy balance can be expressed as

$$R_S = H + LE + G \tag{6}$$

where L is the latent heat of vaporization, E is the evaporation rate and G represents the ground/soil heat flux.

Under the dry environment in which the valley wind system is best developed, the nocturnal latent heat flux will be nearly equal to zero (Clark 1970). Edson (1980) analyzed diurnal data from the plains-based Wangara field experiment to determine the relative importance of each term in the surface energy budget. His results for the nocturnal case found that the ground heat flux was approximately one half of the net radiation while the sensible heat flux made up the other half.

Preliminary surface energy budget estimates (Whiteman et al. 1987) for Brush Creek during ASCOT 1984 indicate that the nocturnal net radiation loss is composed of approximately one-third sensible heat flux and two-thirds ground heat flux. The latent heat of evaporation was confirmed to be small in this semi-arid valley. Hennemuth (1987) collected daytime surface energy budget data in an alpine valley for the

net radiation and sensible heat flux terms. Unfortunately there is currently a dearth of information pertinent to nocturnal energy budget partitioning in mountain-valley locations. This should be assuaged as the field data from the ASCOT 1984 experiment in Brush Creek continues to be analyzed and reported.

The surface energy budget for a valley cross section (see Figure 2) is written as

$$R_S(SX) = H(SX) + LE(SX) + G(SX) \quad . \tag{7}$$

Combining equation (7) with the radiative divergence and assuming no latent heat flux leads to

$$\begin{matrix}\text{Radiative} \\ \text{divergence}\end{matrix} = R_T(WX) - H(SX) - G(SX) \quad . \tag{8}$$

Equation (8), with a rearrangement of terms, can now be substituted back into the expression for the rate of temperature change of an air volume (equation 4) to arrive at

$$\frac{d\theta}{dt} \approx \left[\frac{\theta}{c_p \rho \overline{T}}\right]\left[\frac{R_T(WX) - G(SX)}{AX}\right] \quad . \tag{9}$$

Therefore, the total rate of potential temperature change is the product of two terms. The first term on the right-hand side of equation (9) is essentially the heat capacity of a given volume of air at a particular density and the second term is the rate at which energy is being removed from the volume.

As the ratio of W to S approaches unity for a valley cross section, S can be approximated by W in equation (9). With the aid of Figure 3,

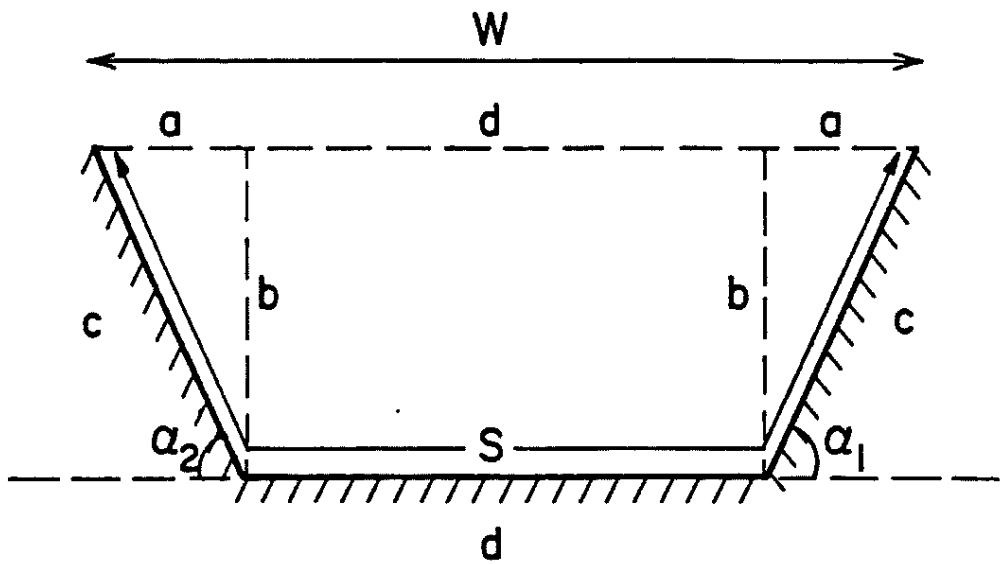

Figure 3. Trigonometric variables in an idealized valley cross section. $\alpha_1 = \alpha_2$. d = valley floor width, c = sidewall slope length, b = valley depth. S and W are defined in Figure 2.

which illustrates an idealized valley cross section broken into its constituent simple shapes, the ratio of W and S is

$$\frac{W}{S} = \frac{2c \cos\alpha + d}{2c + d} \quad . \tag{10}$$

Equation (10) implies that as the valley floor width increases, (W/S) approaches one independent of the sidewall slope angle. Equation (10) also approaches one as the slope angle decreases to zero. In order to determine the accurateness of approximating S by W, the limiting case of no valley floor (d=0) will be tested as a function of several realistic sidewall slope angles. The results are presented below in Table 1.

Table 1.

Calculated W/S ratios as a function of sidewall slope angle (α) with a valley floor equal to zero.

α (degrees)	W/S
0	1.000
5	0.996
10	0.985
15	0.966
20	0.940
25	0.906
30	0.866

Hence, for most valleys, the total cooling rate may be written

$$\frac{d\theta}{dt} \approx \left[\frac{\theta}{c_p \rho T}\right]\left[\left(\frac{WX}{AX}\right)(R_T - G)\right] \quad . \tag{11}$$

Equation (11) states that the important parameter for valley cooling is the ratio of valley width to the cross-sectional area which is the same as the ratio of the area on top to the volume beneath a cross section.

The total derivative for potential temperature may be expanded to explicitly include advection:

$$\frac{\partial \theta}{\partial t} \approx \left[\frac{\theta}{c_p \rho T}\right]\left[\left(\frac{WX}{AX}\right)(R_T - G)\right] - u\frac{\partial \theta}{\partial x} - v\frac{\partial \theta}{\partial y} - w\frac{\partial \theta}{\partial z} \quad . \qquad (12)$$

Equation (12) illustrates that the local cooling of a given valley air volume is due to a combination of local topography, along-valley advection, across-valley advection and vertical advection. Several authors have examined and discussed the effect of temperature advection and its role in the thermal energy balance (Freytag 1985, Hennemuth 1987, Vergeiner et al. 1987.) The purpose of this research is to investigate the impact valley topography has on local cooling and its subsequent capacity to establish a temperature and pressure gradient along the valley axis. The cooling rate developed here will pertain to the early evening period when advection is small. Under strong temperature advection the local topographically-driven cooling rate will no longer portray a true picture of the overall cooling of a given air volume.

Because the local cooling is hydrostatically tied to the pressure gradient, it is more convenient to work with dry bulb air temperature T instead of potential temperature θ. A relationship between T and θ valid for many valleys in the world is outlined in Appendix A. The result is

$$\theta \approx T + \frac{g}{c_p} z \qquad (13)$$

where z is the height above sea level in meters and g is the gravitational acceleration.

Taking the derivative of equation (13) with respect to time and utilizing the assumption from Appendix A that $(T/\theta)\approx 1$, equation (12) becomes

$$\frac{\partial T}{\partial t} \approx \left[\frac{1}{c_p \rho}\right]\left[\left(\frac{WX}{AX}\right)(R_T - G)\right] \quad . \tag{14}$$

Equation (14) says that if steady state energy losses from R_T and G are assumed during the cooling period, the temperature change of an air volume will be controlled by the valley geometry, namely (W/A). In order to qualitatively understand the effect valley topography can have on cooling an air volume it is instructive to examine a couple of theoretical values of (W/A) using idealized valley shapes.

An idealized valley cross section with a rectangular shape (see Figure 4a) has a (W/A) equal to 1/D. Equation (14) indicates that the cooling is then inversely proportional to the depth of the valley i.e. a shallow valley will cool air at a faster rate than a relatively deep valley. In reality, a valley will never contain sidewalls near 90^{o} and Figure 4a is more representative of a flat plain with a large width. In this case D is the depth of the cooled boundary layer and $\partial T/\partial t$ is the cooling rate found over a plain in the absence of topography.

A second idealized valley cross section is triangular in shape with a (W/A) equal to 2/D (see Figure 4b). Equation (14) states that this valley shape will exhibit twice the cooling rate of the flat plain case assuming an equal energy budget partitioning. Thus, the cross-sectional valley configuration and its resultant parameters play an important role in controlling the capability of an air volume to cool. In general, (W/A) can be approximated by some fractional multiple of 1/D. As this

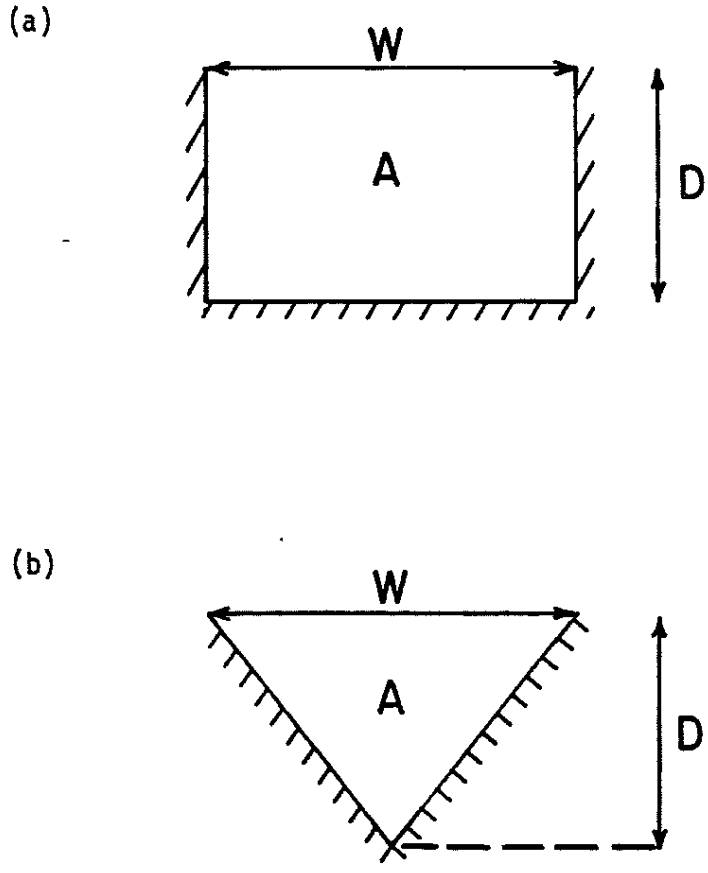

Figure 4. (a) Rectangular idealized valley cross section. A = WD. (b) Triangular idealized valley cross section. A = ½WD.

fraction increases, the strength of the local cooling, $\partial T/\partial t$, increases. In chapter V, calculations of 1/D, 2/D and 3/D for five Colorado valleys are presented and compared to (W/A) in order to demonstrate this enhanced cooling.

Thus it appears from the above discussion and equation (14) that the magnitude of (W/A) will strongly influence the cooling rate. Tables 2-6 present the measured parameters of valley depth (D) and (W/A) for five actual Colorado valleys as a function of along-valley distance X in order to determine the magnitude of the cooling rate. The cooling rate in column 3 is the expected $\partial T/\partial t$ due to the actual topography in the valley (from equation 14) while the cooling rate in column 5 is the $\partial T/\partial t$ for an equivalent flat plain (W/A = 1/D) case. Column 6 is the ratio of the two cooling rates which demonstrates the added effect valley topography has on the cooling of air in the valley versus the plain.

Cooling rates from equation (14) are calculated assuming the density of air is approximately 1 kg/m^3 and c_p is 1004 J/(kg·K). High-confidence values of the nocturnal energy budget components are notoriously hard to procure (André and Mahrt 1982, Vergeiner and Dreiseitl 1987). However, preliminary results from the Brush Creek Valley (Whiteman et al. 1987) indicate that soil heat flux, G, is typically 40 W/m^2 at night while the net surface radiation, R_S, is around 65 W/m^2. Kyle (1987) has also been studying the ASCOT 84 data in Brush Creek and he estimates a radiative divergence in the valley of 15 W/m^2 depending on the gradient between the ambient air temperature and the ground radiating temperature. Utilizing the definition of radiative divergence (equation 5) R_T is estimated to be 80 W/m^2 for the calculated cooling rates.

Table 2.

Measured parameters and calculated cooling rates for Brush Creek as a function of along-valley distance (0 km = head of valley).

(1) X (km)	(2) W/A (m^{-1})	(3) Cooling rate from W/A (°C/hr)	(4) D (m)	(5) Cooling rate from 1/D (°C/hr)	(6) Ratio of cooling rates Col. (3) / Col. (5)
0	0.0145	2.08	215	0.67	3.1
2	0.0105	1.51	360	0.40	3.8
4	0.0078	1.12	415	0.35	3.2
6	0.0063	0.90	460	0.31	2.9
8	0.0053	0.76	500	0.29	2.6
10	0.0052	0.75	520	0.28	2.7
12	0.0052	0.75	550	0.26	2.8
14	0.0050	0.72	600	0.24	3.0
16	0.0037	0.53	645	0.22	2.4
18	0.0035	0.50	625	0.23	2.2

Table 3.

Measured parameters and calculated cooling rates for South Fork White River as a function of along-valley distance (0 km = head of valley).

(1)	(2)	(3)	(4)	(5)	(6)
X (km)	W/A (m^{-1})	Cooling rate from W/A (°C/hr)	D (m)	Cooling rate from 1/D (°C/hr)	Ratio of cooling rates $\frac{\text{Col. (3)}}{\text{Col. (5)}}$
0	0.0055	0.79	850	0.17	4.6
1	0.0078	1.12	780	0.18	6.2
2	0.0055	0.79	850	0.17	4.6
4	0.0040	0.57	790	0.18	3.2
6	0.0024	0.34	825	0.17	2.0
8	0.0025	0.36	830	0.17	2.1
10	0.0021	0.30	870	0.16	1.9

Table 4.

Measured parameters and calculated cooling rates for Upper Colorado River as a function of along-valley distance (0 km = head of valley).

(1)	(2)	(3)	(4)	(5)	(6)
X (km)	W/A (m^{-1})	Cooling rate from W/A (°C/hr)	D (m)	Cooling rate from 1/D (°C/hr)	Ratio of cooling rates $\frac{\text{Col. (3)}}{\text{Col. (5)}}$
0	0.0032	0.46	640	0.22	2.1
2	0.0023	0.33	820	0.17	1.9
4	0.0027	0.39	800	0.18	2.2
6	0.0025	0.36	850	0.17	2.1
8	0.0022	0.32	870	0.16	2.0
10	0.0018	0.26	1080	0.13	2.0
12	0.0017	0.24	1040	0.14	1.7
14	0.0020	0.29	1010	0.14	2.1
16	0.0018	0.26	970	0.15	1.7
18	0.0020	0.29	890	0.16	1.8

Table 5.

Measured parameters and calculated cooling rates for Yampa Valley as a function of along-valley distance (0 km = head of valley).

(1) X (km)	(2) W/A (m^{-1})	(3) Cooling rate from W/A (°C/hr)	(4) D (m)	(5) Cooling rate from 1/D (°C/hr)	(6) Ratio of cooling rates $\frac{\text{Col. (3)}}{\text{Col. (5)}}$
0	0.0028	0.40	580	0.25	1.6
2	0.0031	0.44	620	0.23	1.9
4	0.0037	0.53	605	0.24	2.2
6	0.0055	0.79	580	0.25	3.2
8	0.0033	0.47	635	0.23	2.0
10	0.0047	0.67	630	0.23	2.9
12	0.0046	0.66	750	0.19	3.5

Table 6.

Measured parameters and calculated cooling rates for Gore Creek as a function of along-valley distance (0 km = head of valley).

(1) X (km)	(2) W/A (m^{-1})	(3) Cooling rate from W/A (°C/hr)	(4) D (m)	(5) Cooling rate from 1/D (°C/hr)	(6) Ratio of cooling rates Col. (3) / Col. (5)
0	0.0019	0.27	1070	0.13	2.1
2	0.0026	0.37	1010	0.14	2.6
4	0.0027	0.39	935	0.15	2.6
6	0.0036	0.52	770	0.19	2.7
8	0.0030	0.43	760	0.19	2.3
10	0.0052	0.75	550	0.26	2.9
12	0.0036	0.52	670	0.21	2.5

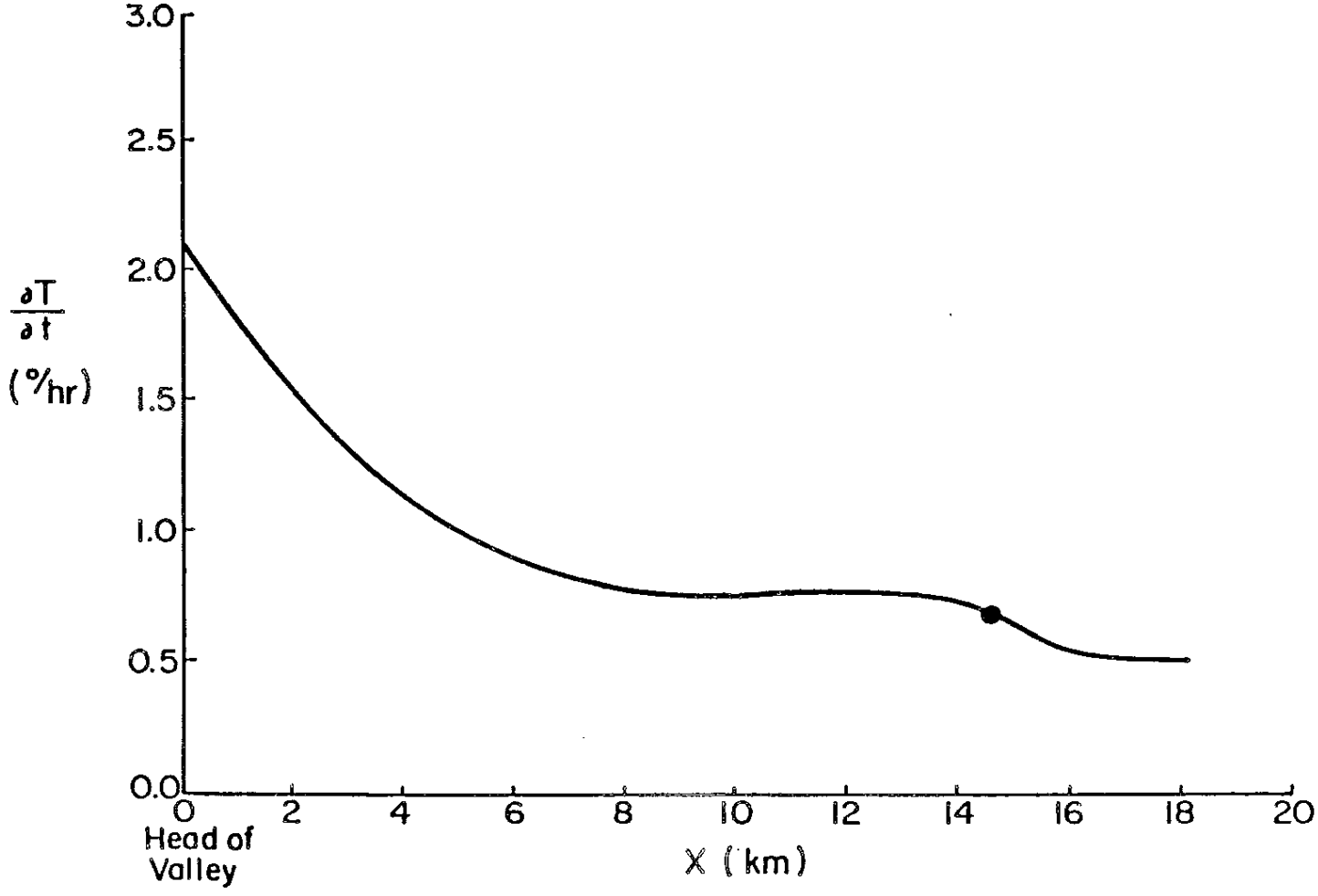

Figure 5a. Brush Creek's theoretically calculated cooling rate (°C/hr) due to valley topography as a function of along-valley distance. Dot is sounding site location.

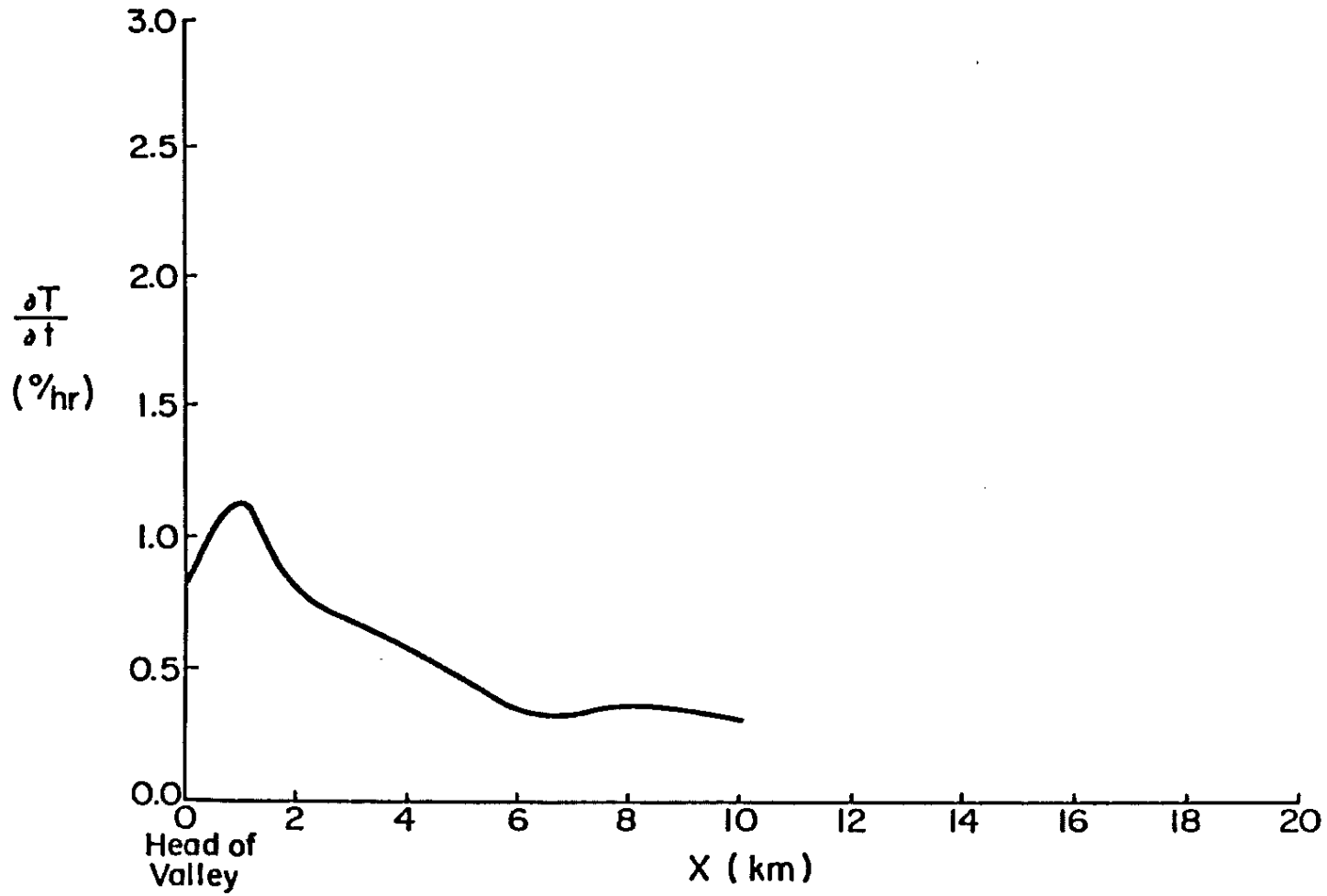

Figure 5b. Same as Figure 5a but for South Fork White River.

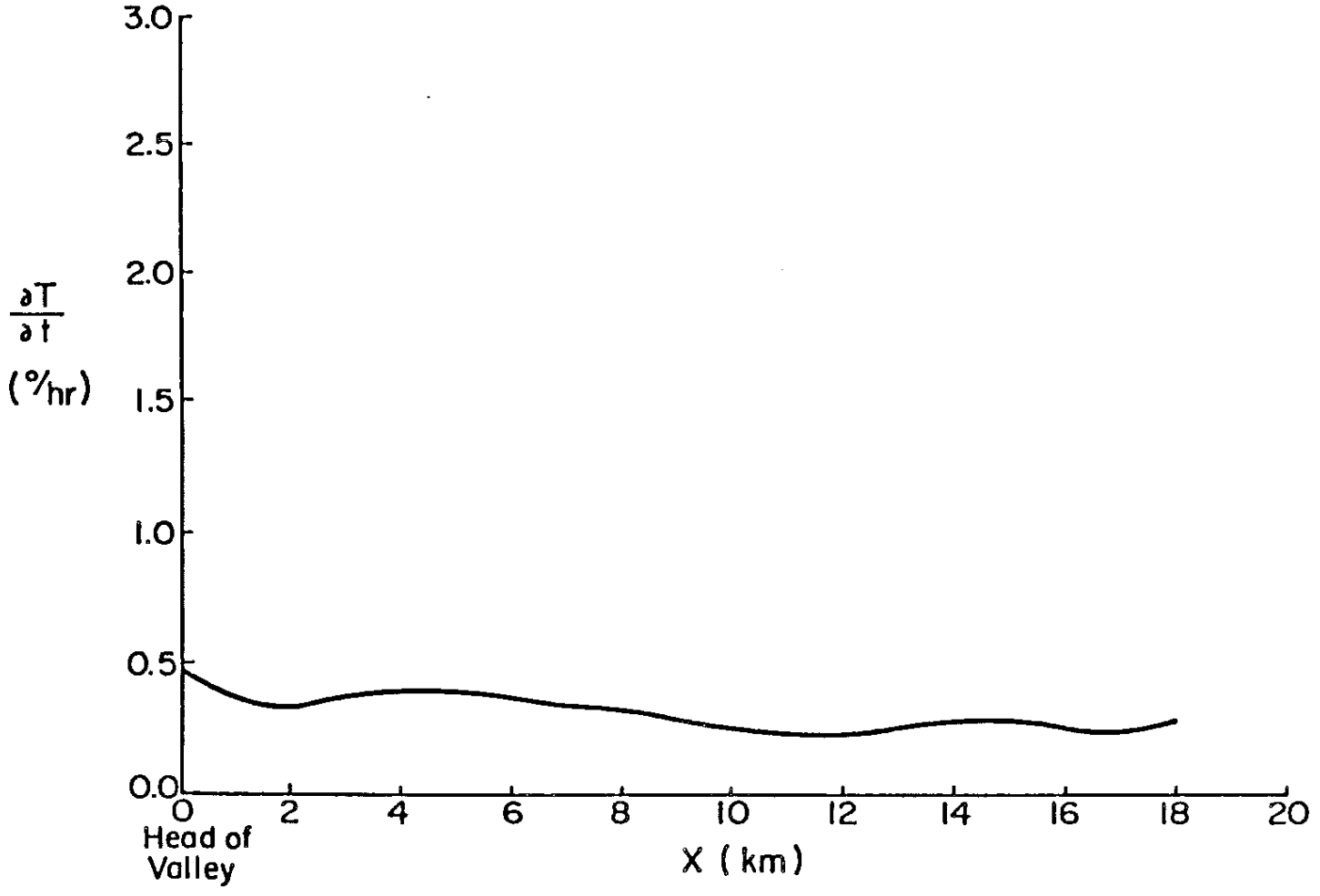

Figure 5c. Same as Figure 5a but for Upper Colorado River.

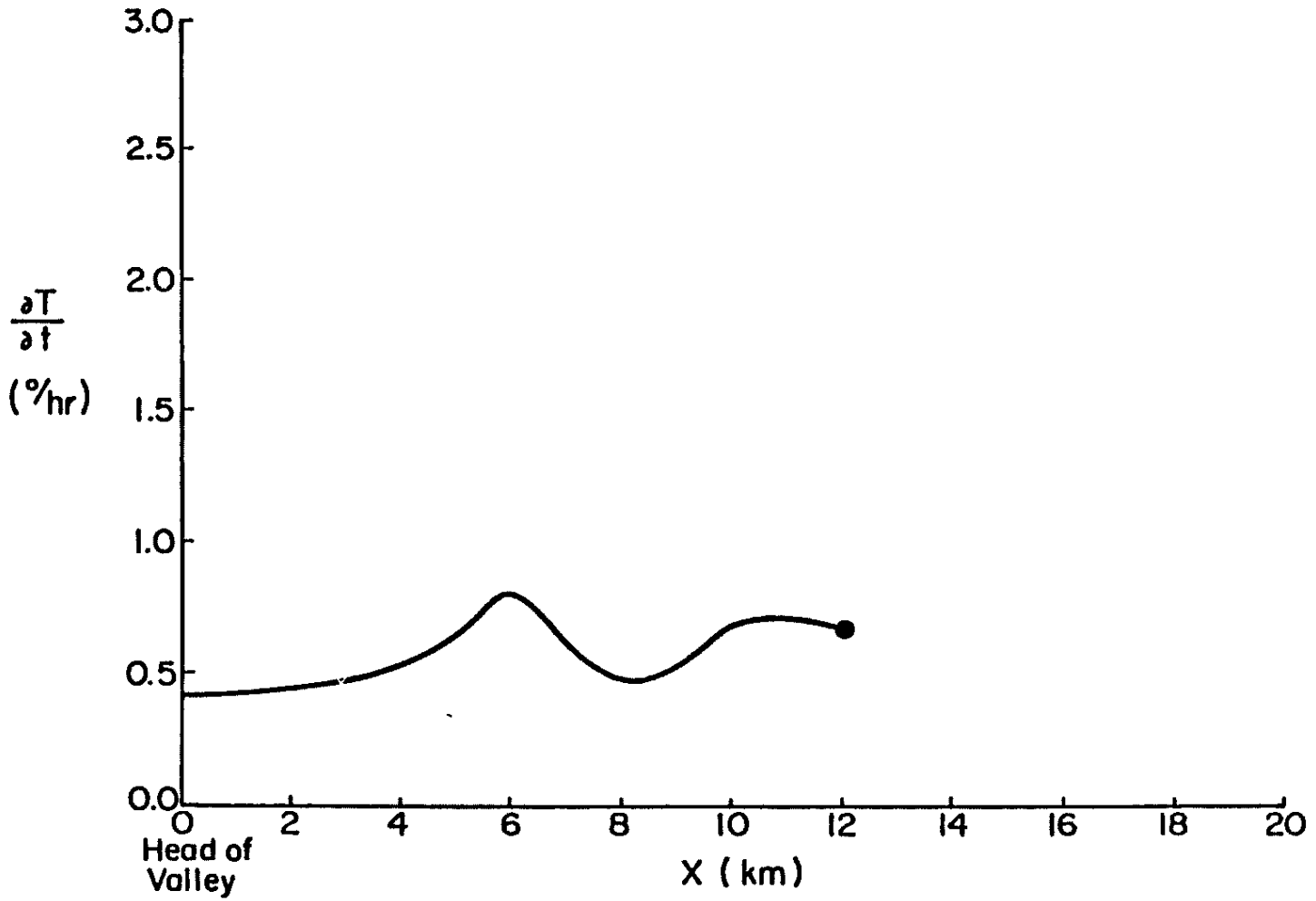

Figure 5d. Same as Figure 5a but for Yampa Valley.

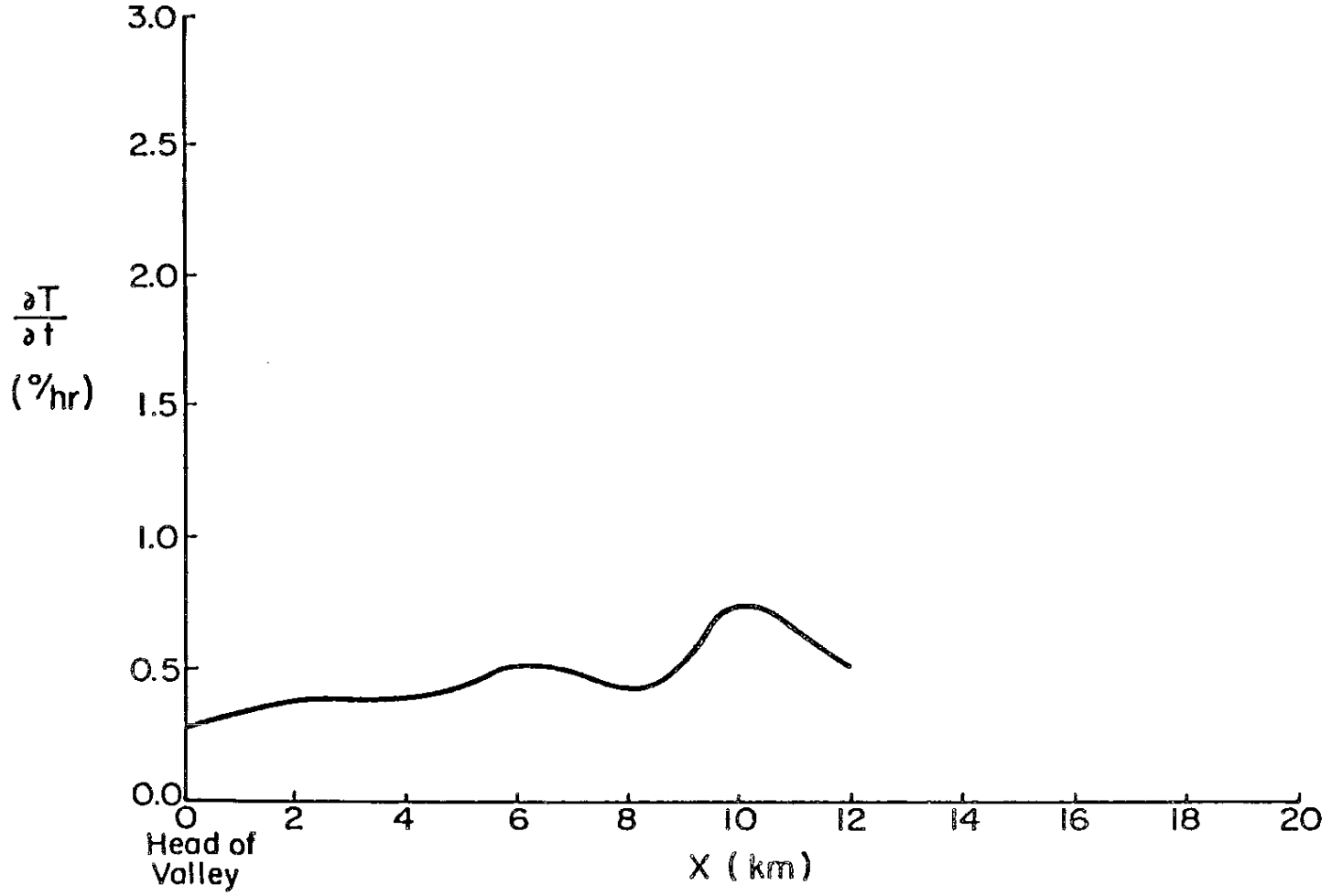

Figure 5e. Same as Figure 5a but for Gore Creek.

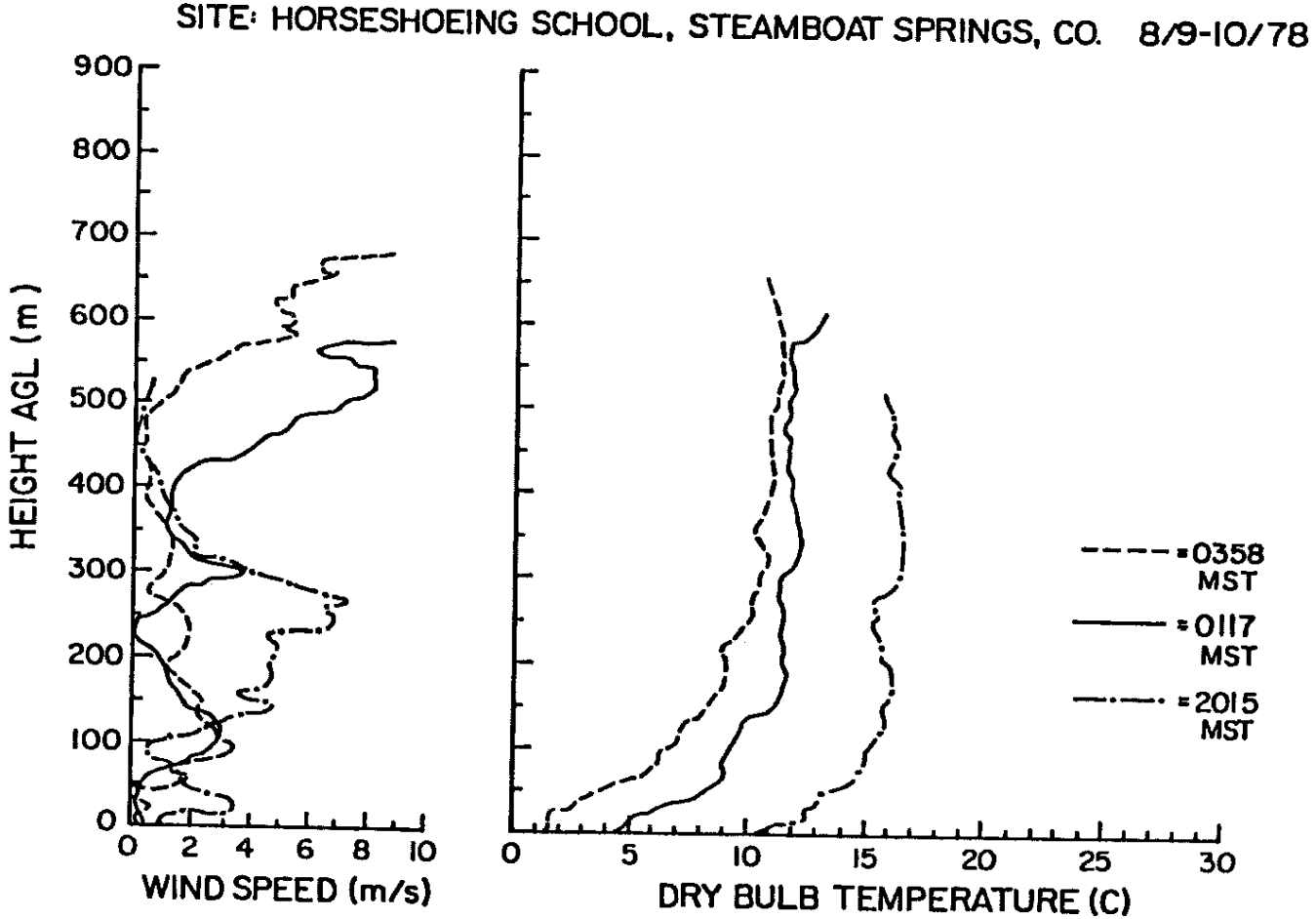

Figure 6a. Nocturnal time series of tethersonde soundings taken by Whiteman (1980) in the Yampa Valley.

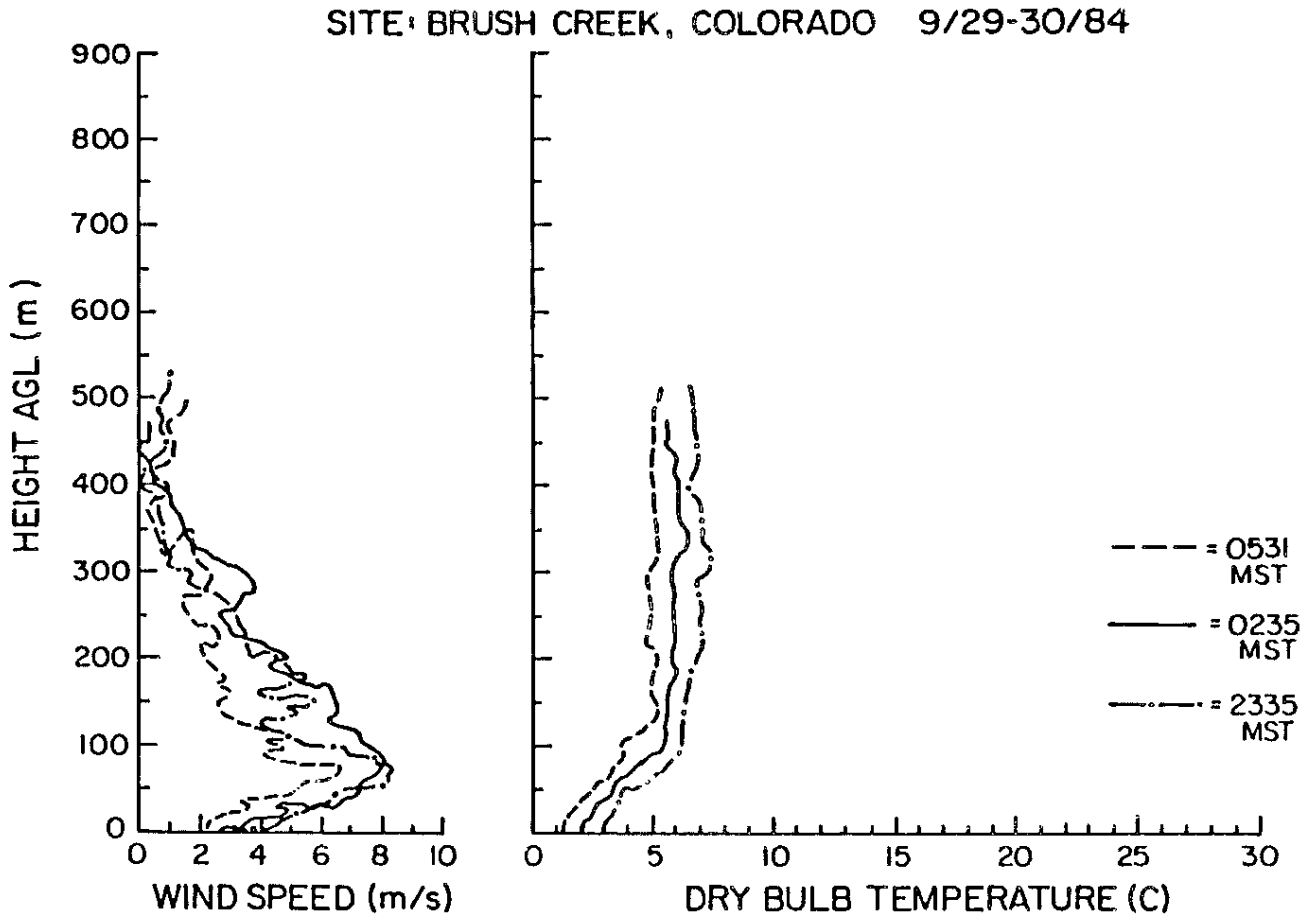

Figure 6b. Nocturnal time series of tethersonde soundings taken by CSU in Brush Creek.

The theoretically calculated cooling rates due to valley topography (column 3) are also presented in graphical form as a function of down-valley distance in Figures 5a-e. Both Brush Creek and the South Fork of the White River tend to show strong, steadily decreasing down-valley temperature cooling rates while the Upper Colorado River has, at best, a weak down-valley gradient. The Gore and the Yampa Valleys exhibit an increasing temperature gradient down valley despite the sinusoidal interruption present at the eight kilometer mark which, as will be explained later, is due to the intrusion of a side creek. From these tables and graphs it appears that the critical aspect in determining whether or not a valley can set up a down-valley temperature gradient is the behavior of (W/A) along the valley axis. A decreasing (W/A) down valley sets-up a down-valley temperature gradient (Brush Creek) while an increasing (W/A) down valley creates an up-valley temperature gradient (Yampa Valley).

As stated earlier, column 3 in Tables 2-6 represents the expected theoretical local cooling rate within a valley as a function of along-valley distance. Two Colorado valleys exhibiting different wind regimes were selected as test cases to determine if these cooling rates are actually observed. A nocturnal time series of tethersonde soundings taken by Whiteman (1980) in the Yampa Valley (Figure 6a) are characteristic of a trapping valley (light nocturnal winds) while the series of Colorado State University soundings in Brush Creek (Figure 6b) characterize a draining valley (strong nocturnal winds).

The time series for the Yampa valley shows the winds to be generally light (under 2 m/s) through the first 300 meters of the sounding. Within this layer a rather uniform cooling rate of

approximately 0.75°C per hour is observed. This corresponds well to the expected cooling rate of 0.66°C per hour calculated from the sounding location's topography (Figure 5d). Above 300 meters the wind speeds tend to increase and the cooling profiles behave somewhat differently. As will be shown later (Figure 13c), the height of the western ridgeline at this site is roughly 300 meters above the valley floor.

The above observations in the Yampa Valley bring out a critical point regarding the theoretical development of equation (14). This cooling rate is only applicable to the air cooled within the valley volume. Air above the ridgelines may remain coupled to the synoptic flow and therefore will not be subjected to the more localized valley cooling. By the same reasoning, air once cooled locally by the valley topography must remain within the valley volume in order for the along-valley cooling rates to create a bona fide temperature gradient as suggested in Tables 2-6 and Figures 5a-e. A common way for topographically-cooled air to leave the valley volume occurs when one or both ridgelines drop significantly in the down-valley direction.

Three successive soundings in Brush Creek collected at three hour intervals cool approximately 1°C per three hours. The expected cooling rate in this 600 meter deep portion of the valley is 0.75°C per hour (Figure 5a) which would seem to suggest another process is at work inhibiting the maximum possible production of cold air in this valley volume. The strong wind speeds (up to 8 m/s) appear to indicate that considerable mixing is helping to reduce the local formation of cold air. Whiteman and Barr's (1986) analysis of Brush Creek data find that in order to conserve mass in the valley volume subsidence from the top of the valley atmosphere must occur. Subsidence in a stable atmosphere

such as Brush Creek's (Figure 6b) will produce local warming thereby decreasing the cooling rate.

B. Along-Valley Temperature Gradient

Cooling of a valley cross section proceeds at various rates depending on the valley topography and the difference between net radiation at the top of the atmosphere and soil heat flux. The data analyses presented above suggest that an along valley temperature gradient $\partial T/\partial x$ is closely correlated to the changing valley topography. Commencing with equation (14) a formal relationship between these two parameters is derived below.

Since R_T and G have been defined as time and space averaged quantities for a valley volume, the rate of temperature change is integrated from an initial time, t_o, and temperature, T_o, to some later time, t, and temperature, T. The resulting expression is

$$T - T_o \approx \left[\frac{1}{c_p \rho}\right] K\,(R_T - G)(t - t_o) \qquad (15)$$

where K = (W/A) has been defined as the valley topographic parameter.

The along-valley coordinate has been defined as x (see Figure 2), therefore the temperature gradient along the valley axis is

$$\frac{\partial T}{\partial x} - \frac{\partial T_o}{\partial x} \approx \left[\frac{1}{c_p \rho}\right]\left[K \frac{\partial}{\partial x}(R_T - G) + (R_T - G)\,\frac{\partial K}{\partial x}\right](t - t_o)\ . \qquad (16)$$

Equation (16) may be simplified by assuming that at some initial time $t_o = 0$ the valley atmosphere is well-mixed in the along-valley direction so that $\partial T_o/\partial x$ may be ignored. Variations of R_T along the

valley axis are expected to be small if clouds are not present. Variations of G will also be small unless significant changes occur in surface conditions. Therefore, in an effort to isolate the topographic parameter K and its effect on the temperature gradient, energy budget gradients will be considered small in the following analysis. The resulting along-valley temperature gradient may then be approximated by

$$\frac{\partial T}{\partial x} \approx \left[\frac{1}{c_p \rho}\right]\left[(R_T - G)\,\frac{\partial K}{\partial x}\right] t \quad . \tag{17}$$

Thus the critical aspect in the formation of a temperature gradient from topographic effects is the behavior of K along-valley. If K decreases in the down-valley direction then relatively cooler air will be formed up-valley. If K increases in the down-valley direction then relatively warmer air will be formed up-valley. This sign convention presumes the diabatic terms have been assigned negative values consistent with a heat loss.

One further comment on the temperature gradient expression is in order at this time. Equation (17) implies that the temperature gradient would strengthen throughout the night as t increases. In reality this will not occur because the temperature gradient will hydrostatically lead to a pressure gradient thus creating a valley wind.

Equation (17) is the temperature gradient of an entire volume averaged quantity of air and is expected to be quite small. Choosing a cooling time of one hour and selecting an average $\partial K/\partial x$ equal to 5×10^{-7} m^{-2} from the Colorado valleys examined, an along-valley temperature gradient of roughly 0.1 $^{o}C/km$ is calculated. This presumes the same values of ρ, c_p, R_T and G are utilized that were used for the computation of $\partial T/\partial t$ in Tables 2-6.

In summary, the changing topography in a valley, $\partial K/\partial x$, is able to create an along-valley temperature gradient without any "knowledge" of an adjacent plain. The volume reduction within a valley itself is enough to create an along valley temperature gradient under the conditions outlined above. The following chapter outlines a method whereby $\partial K/\partial x$ can be calculated for any valley where digital topography is available.

CHAPTER IV

DESCRIPTION OF ANALYTIC METHOD

A. Objectives of the Method

The theory developed in the last chapter rests upon the knowledge of two geometric parameters pertaining to a valley structure. Valley width, W, and cross-sectional area, A, can be calculated planimetrically from topographic maps of an appropriate scale. However, this is time consuming and labor intensive, factors which helped initiate the development of a more efficient technique.

In order to calculate $\partial K/\partial x$ it was determined that a series of cross sections taken at a sufficiently resolved dx along the valley axis should be constructed. The easiest way to build these cross sections is with digital topographic data fed into a computer program geared toward this end. Therefore an automated graphical routine has been developed to draw valley profiles and calculate the relevant geometrical features. To the author's knowledge this technique has only been used once before in the area of mountain-valley meteorology. Hennemuth (1987) used a digital topographic map with a resolution of 125 by 125 meters to determine the terms of the surface energy balance in the heating of a small alpine valley. Whiteman and Barr (1986) used 1:24,000-scale topographic maps to calculate cross-sectional areas in Brush Creek, Colorado.

The valley cross sections were drawn up the main sidewalls as perpendicular to the height contours as possible. Cross sections were demarcated at the crest height which was defined as the highest point on each side of the valley where the valley-plain area reduction began. The choice of crest height played a key role in determining the value of both width, W, defined as the distance from crest to crest and cross-sectional area, A, defined to be the area of atmosphere beneath W (see Figure 2).

B. Digital Data Set

Digital files containing computer-readable terrain data of the United States are available from a variety of sources and at many scales depending on specific user needs and financial constraints (Dietrich and Childs, 1982). The National Cartographic Information Center (NCIC) distributes digital data sets produced by the U.S. Geological Survey (USGS) including Digital Line Graphs (DLG) and Digital Elevation Models (DEM) (Elassal and Caruso 1983). Current U.S. coverage by the 1:250,000-scale DEM data is much more extensive than the 1:24,000-scale data while not sacrificing a great deal of resolution. In addition, the larger scale data is readily accessible to the user (four week turn-around time) while the smaller scale data requires a six to twelve month delivery period.

DEM data on the 1:250,000-scale is available in 1^{o} longitude by 1^{o} latitude quadrants with a resolution of three arc-seconds longitude (71 meters at 40^{o} latitude) and three arc-seconds latitude (93 meters). The cost of one of these quads in the summer of 1986 was $75 while an equivalent area of coverage by the 1:24,000-scale DEM would have been

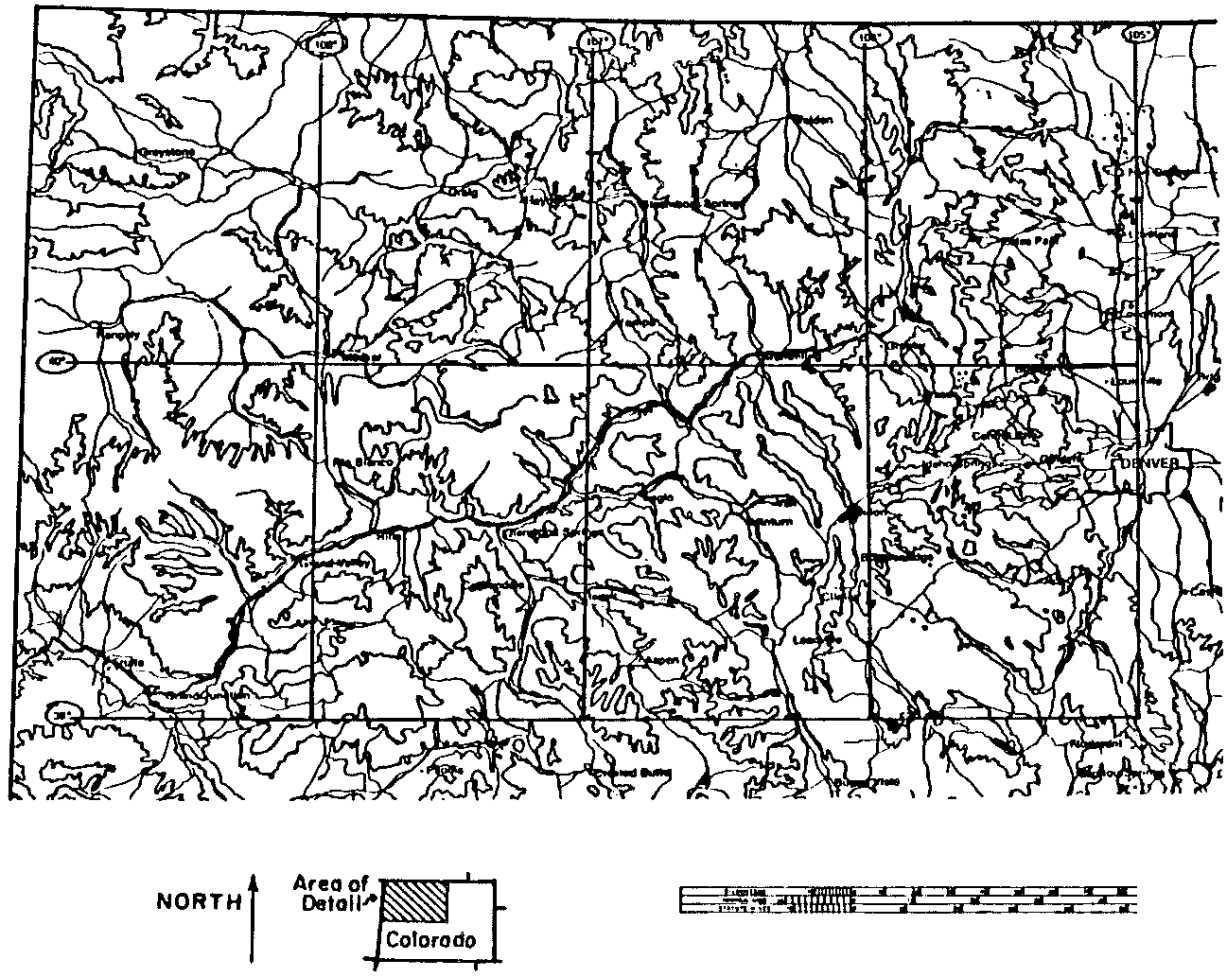

Figure 7. Eight quadrants of the 1:250,000-scale DEM data purchased to calculate topographical parameters in actual valleys throughout northwest Colorado.

$6400 for a resolution of 30 meters in either direction. In order to test the valley geometric factor in a reasonable number of locations, eight quadrants of the 1:250,000-scale data were purchased covering the northwest quarter of Colorado (see Figure 7). This area encompasses many mountain-valleys where wind system field work has been performed (Whiteman 1980, Bader 1985). (Note: henceforth all references to a DEM quad will pertain to the 1:250,000-scale).

The structure of a 1:250,000-scale DEM quadrant is shown in Figure 8. One DEM quad is comprised of a series of 1201 profiles oriented south to north along lines of longitude containing 1201 elevation points (above sea level) per profile. A header record appears before the first point in each profile listing the ground planimetric coordinates, in arc-seconds, for that point so the subsequent 1200 elevation points in that profile can be tagged with a latitude and a longitude.

C. Computer Algorithm

The uniqueness of the research objectives necessitated a computer program specifically designed to accomplish the aforementioned goals. A VAX 11-750 computer housed at Colorado State University's Department of Atmospheric Science served as a home for the DEM data as well as the FORTRAN 77 programs written to construct the cross sections.

The construction of a $\partial K/\partial x$ profile for an entire valley is a seven step process:

(1) Latitude and longitude values (degrees, minutes, seconds) for the valley head and valley bottom endpoints are input. These are easily read from a USGS 1:250,000-scale topographic map.

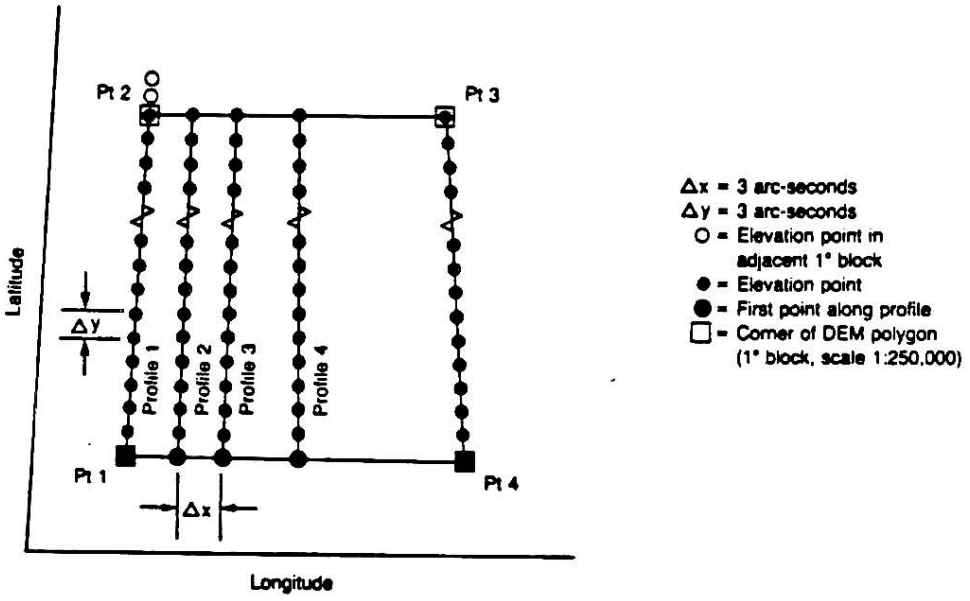

Figure 8. Structure of a 1:250,000 scale digital elevation model. From Elassal and Caruso (1983).

(2) Total distance along the valley segment is automatically calculated and a desired cross-section increment is selected (meters).

(3) The location of each cross section is delineated along the valley segment followed by a prompt asking how far the cross section should extend perpendicularly from the valley segment in each direction (meters). This distance is generally hundreds of meters beyond the crest height to guarantee its inclusion. Sets of cross-section endpoints derived from the above three steps are placed in an array.

(4) Utilizing a set of endpoints from the cross-section array a height profile can be constructed from the DEM data. Elevation values are linearly interpolated every three arc-seconds, consistent with the DEM data, using a weighted distance averaging scheme. This process is repeated for each pair of cross-section endpoints along the valley segment.

(5) Each cross section can be drawn using an NCAR (National Center for Atmospheric Research) graphics plotting package. The vertical scale is exaggerated three times in order to accentuate the profile.

(6) The height profile calculated in step (4) is used to compute the valley parameters W, A and D for each cross section. Cross-sectional area is calculated using Simpson's method.

(7) Steps (1) through (6) are repeated for each valley segment. When this loop is finished, A, W, D or any combination of parameters may be plotted as a function of along-valley distance using NCAR graphics.

For the purpose of the computer algorithm, actual valleys may be considered a series of straight segments following along the valley floor from the headwaters to the end of the well-defined portion of the valley.

A further explanation of the depth parameter, D, is in order. The valley bottom is defined as the lowest point in the profile (step 4 above). Hence it is assumed that in step (3) the distance chosen perpendicular to the valley axis is not so far that it enters into the main body of an adjoining valley thus creating a misleading 'second' valley floor. Two depths are computed for each profile from the elevation difference between the crest heights and the valley bottom. The depth, D, calculated in the program is simply an average of these two values.

In order to evaluate the accurateness of the computer-generated valley parameters W, A, and D and thus the credibility of the program, a hand analysis of two Colorado valleys was performed. Seven to eight cross sections were drawn by hand for each of the Brush Creek and Gore Creek valleys from 1:24,000-scale topographic maps. A planimeter was used to compute the cross sectional area underneath W. Values obtained from this method were within five percent of the automated technique which used the DEM data. Direct comparison of the hand analysis sites with the computer-created profiles was made possible due to a similar but separate program which allowed for manual entering of the cross-section endpoints.

CHAPTER V

DATA ANALYSIS

A valley which exhibits a decreasing $\partial K/\partial x$ down-valley will be able to drain during the night while an increasing $\partial K/\partial x$ implies a valley unable to sustain a nocturnal along-valley wind. In light of this assertion, a number of real valleys in western Colorado were tested to see if this trait was observable. An attempt was made to choose valleys which were reasonably well-behaved, topographically speaking, along part or all of their extent. This behavioral clause was included because the original theory was developed with the constraint that the valley ridgeline could not drop precipitously along the valley axis. If this is the case we can no longer be certain that the air cooled by the reduced geometry of the valley is remaining in the valley volume but instead may be leaving the valley on a constant potential temperature surface further downstream.

The majority of drainage areas were selected because of available wind data in the valley from previous field work (Whiteman 1980). All subsequently referenced sounding sites have come from Whiteman's experiments unless otherwise noted. Another was chosen because of its potentially interesting geological construction and a curiosity to see if a draining or pooling trend existed. Figure 9 illustrates the valley locations studied by the computer program within Colorado.

A few comments on Figures 10-14 accompanying the valleys discussed below are in order at this time. Each valley, with the exception of the

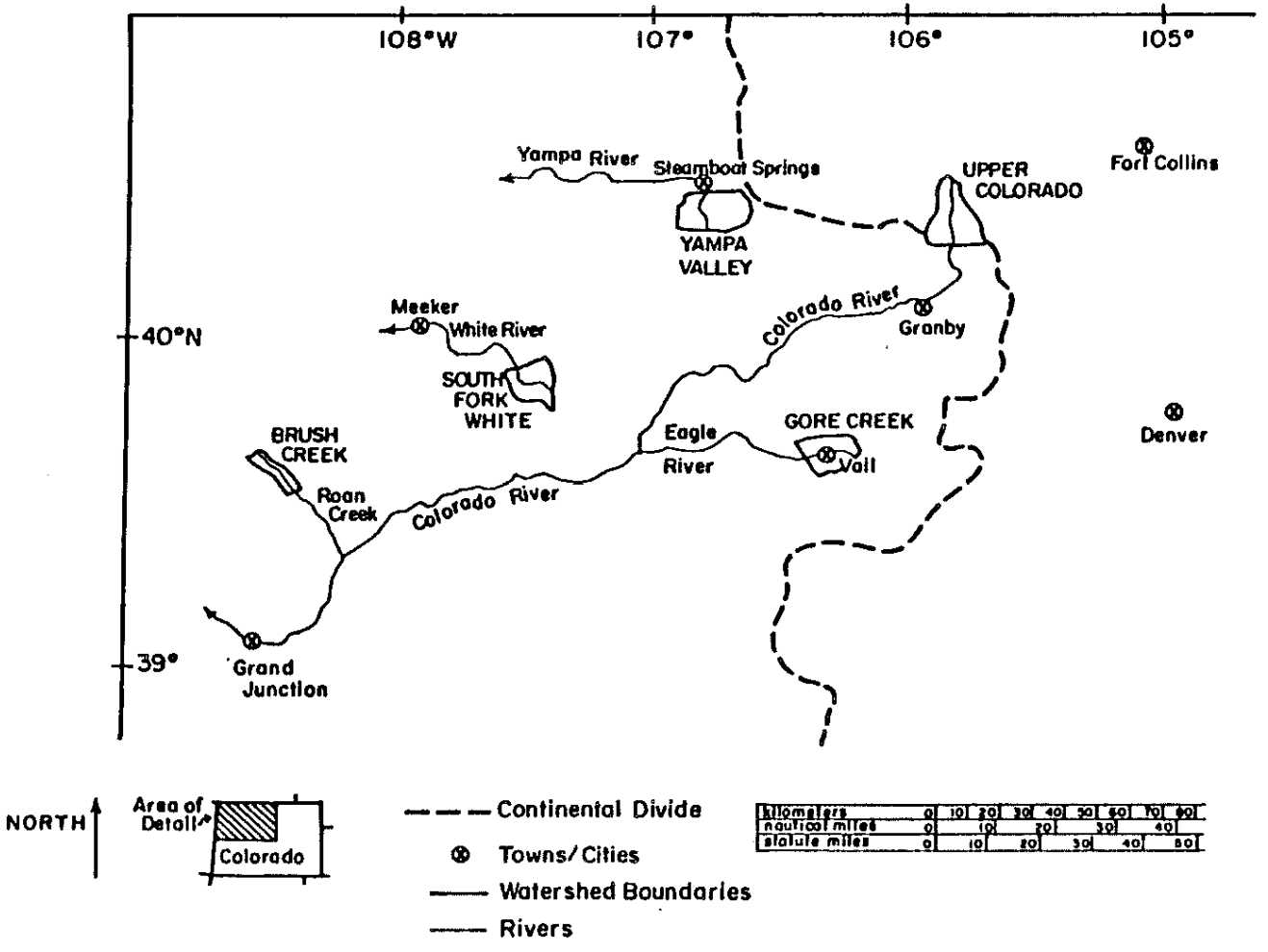

Figure 9. Valley locations studied by automated graphical techniques within Colorado.

Upper Colorado River, contains a set of figures lettered "a" through "h". The Upper Colorado River did not have any recorded wind measurements so tethersonde related plots are not included for this valley and the corresponding figure letters are slightly different. Figure "a" illustrates the valley watershed and location of the sounding site if one was available. Figure "b" is the vertical cross section of the sounding site exaggerated six times. This scale was utilized for consistency of presentation as the maximum abscissa for all valley cross sections was found to be 18,000 meters and the ordinate has a range of 3000 meters. Figure "c" displays a horizontal profile of the valley floor and ridgetops. The ordinate is scaled to the abscissa because it is felt that a one-to-one ratio is important for recognizing ridgeline fluctuations. Figures "d", "e" and "f" are the three calculated valley parameters- depth, width and cross-sectional area respectively. Valley slices were taken in increments of approximately 500 meters which was small enough to get the appropriate detail but large enough to lessen the chance of many spurious sidewall features entering the graphs. Figure "g" is the computation of (W/A) plotted along with 1/D, 2/D and 3/D where D is the actual depth from Figure "d." Figure "h" is a representative tethersonde sounding from the location marked in Figure "a."

A. Draining Valleys

1. Brush Creek

The Brush Creek valley was the best example found in Colorado with which to compare theory to observation. Cut into a flat topped mesa, the ridgelines on both sides of the valley are nearly identical in elevation and horizontal in extent throughout the length of the valley

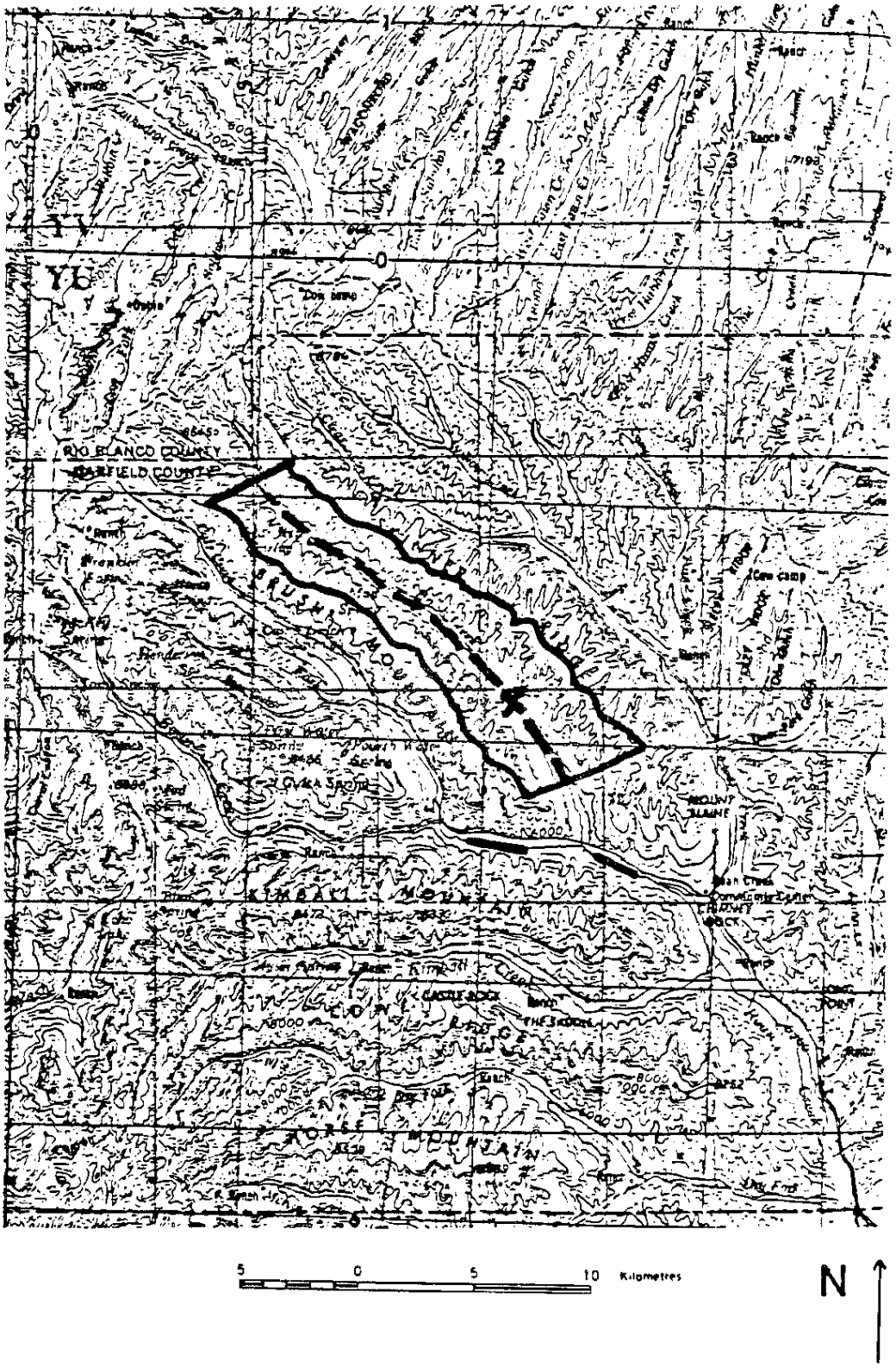

Figure 10a. Portion of Brush Creek Valley studied with computer program (heavy solid line). Dashed line = valley bottom. X = sounding site shown in figure "b." Two lower lines are sections of Roan Creek.

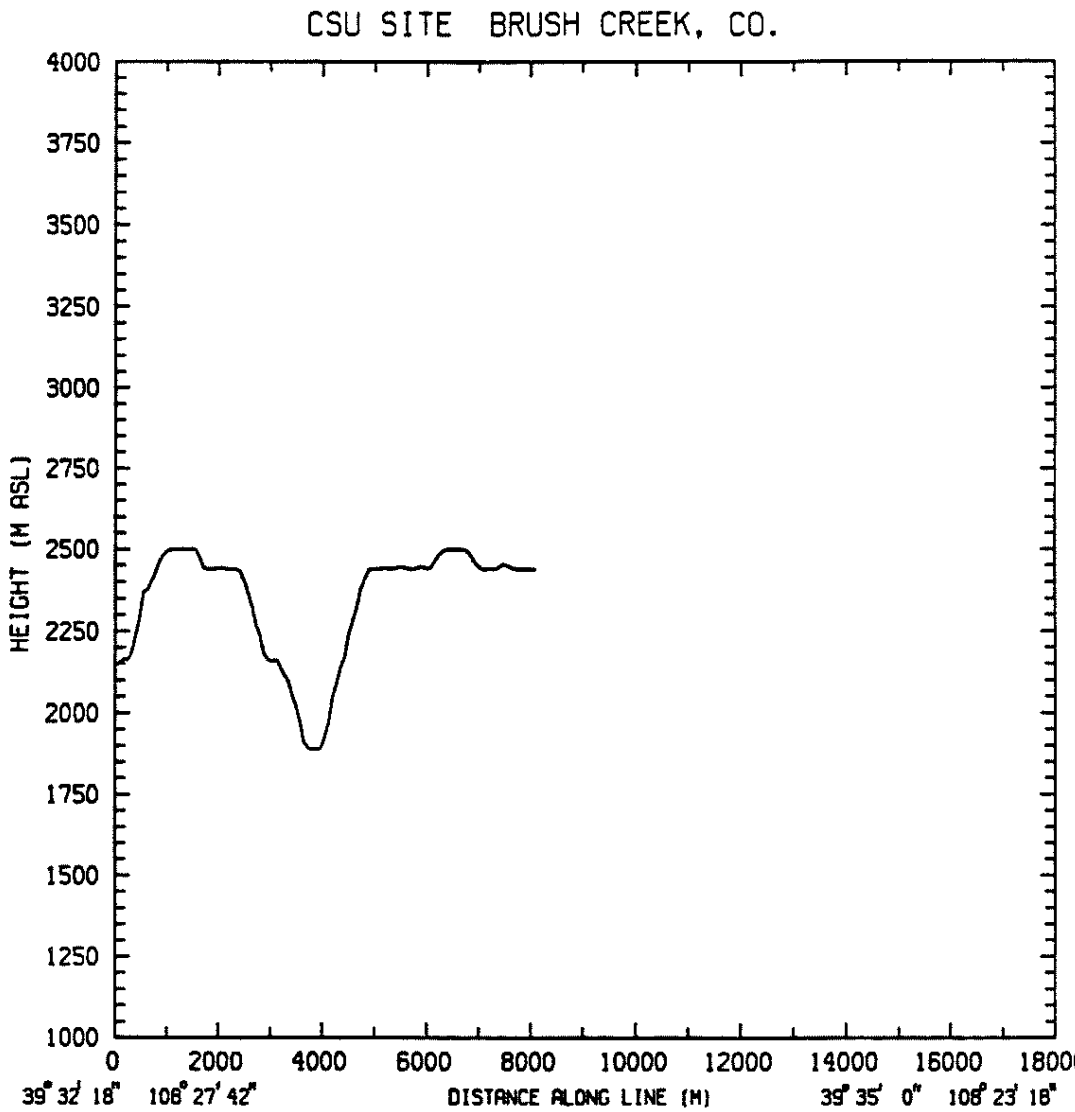

Figure 10b. Vertical cross section of Brush Creek sounding site. Latitude and longitude values for the two cross section endpoints are indicated in lower left and right hand corners of figure. Sidewall slope angle is 29°.

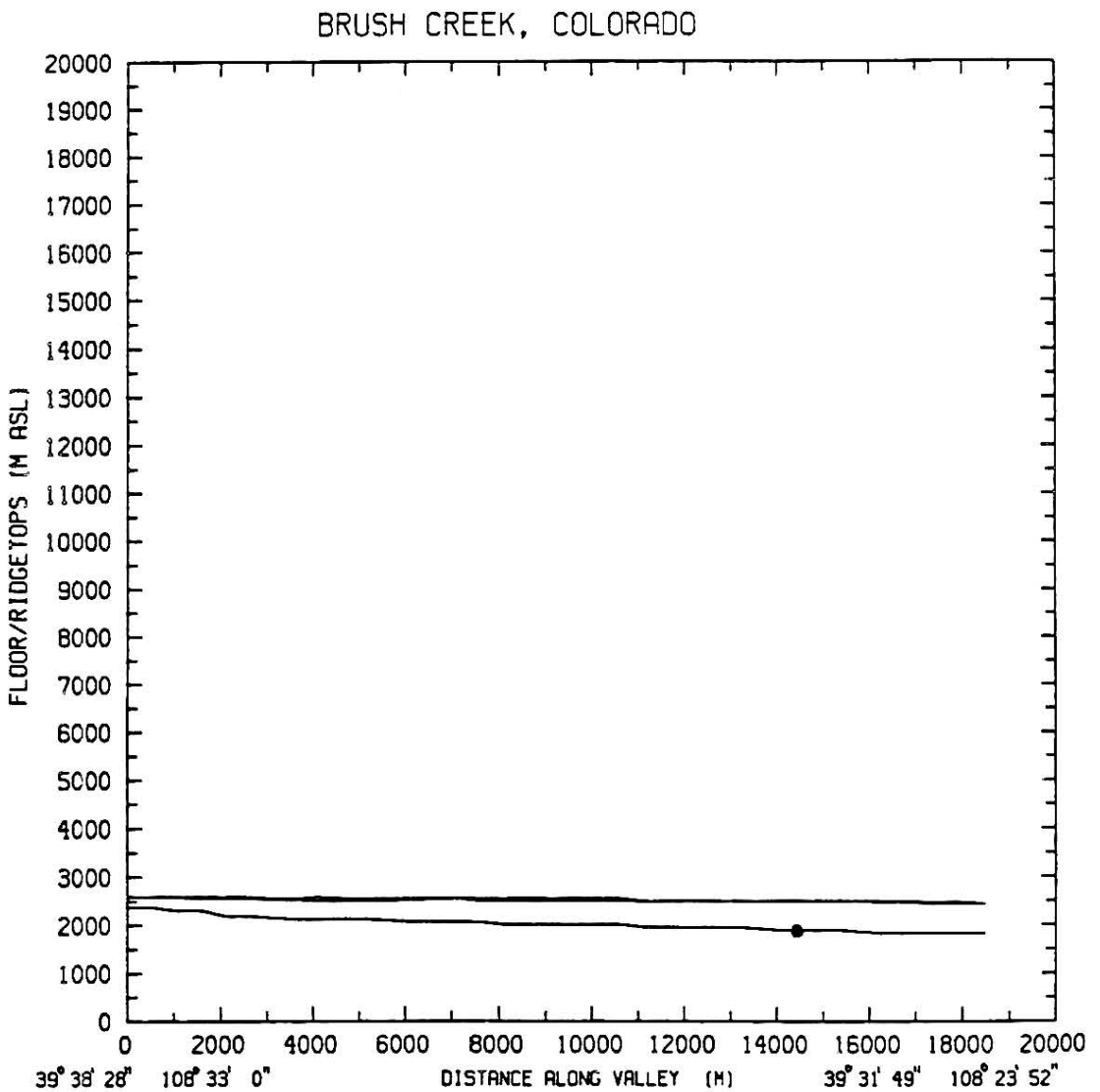

Figure 10c. Horizontal profile of Brush Creek Valley. Upper two lines are ridgetops and lowest line is valley floor. Dot is sounding site location. Latitude and longitude values for first and last points of valley floor are shown in lower left and right corners, respectively.

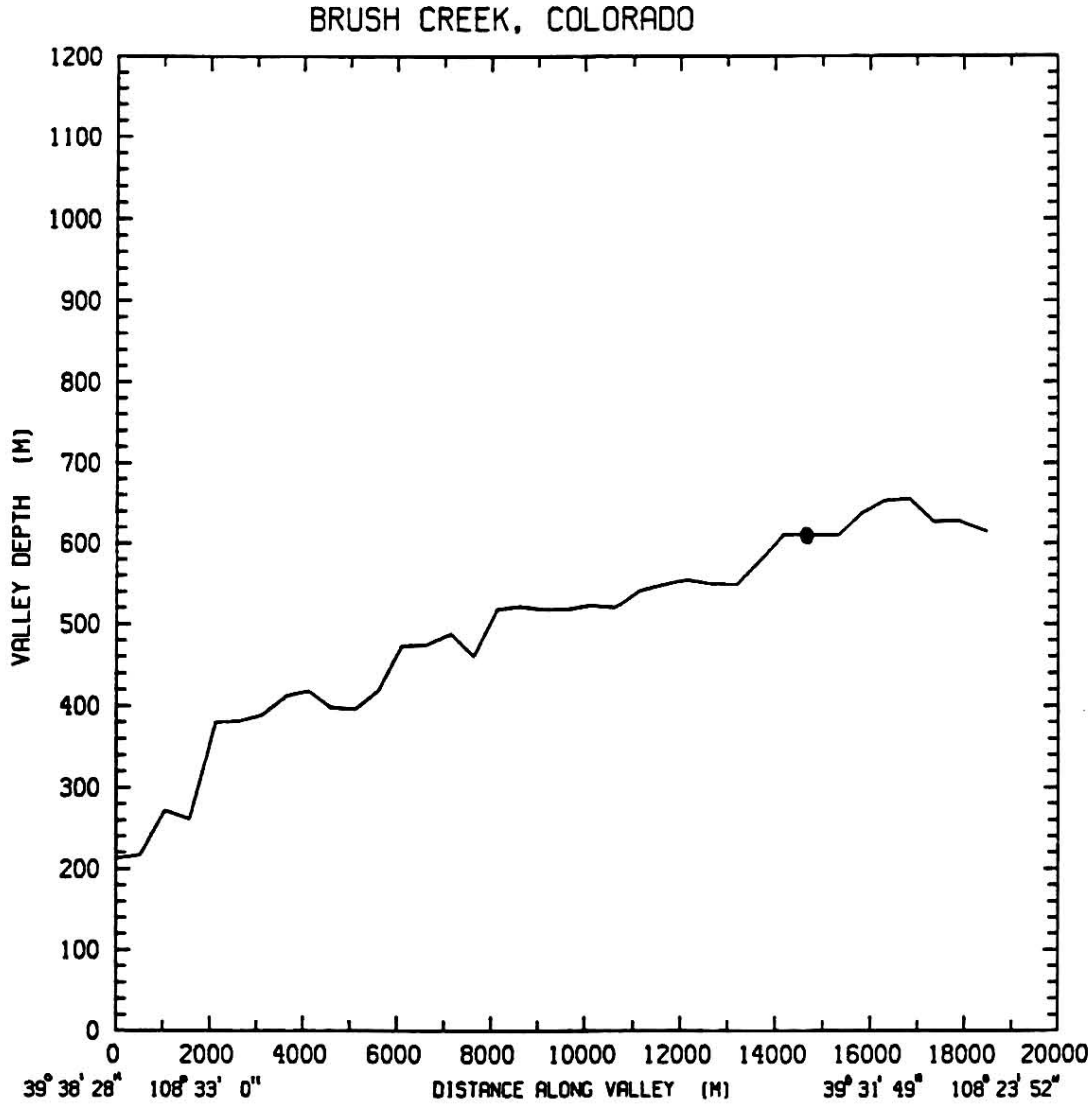

Figure 10d. Along-valley depth, D, for Brush Creek. Dot is sounding site location. Latitude and longitude values for first and last points of valley floor are shown in lower left and right corners, respectively.

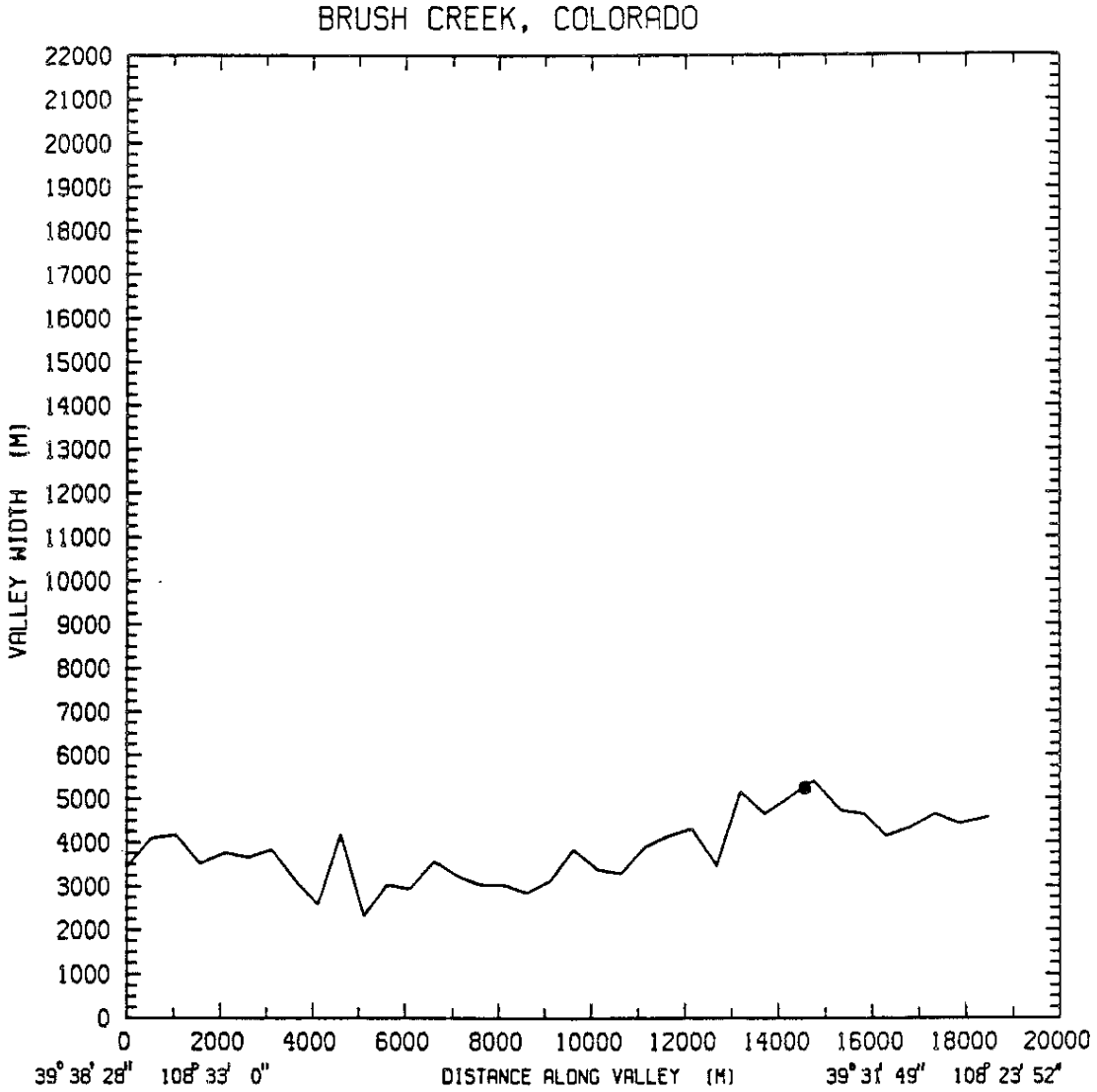

Figure 10e. Along-valley width, W, for Brush Creek. Dot is sounding site location. Latitude and longitude values for first and last points of valley floor are shown in lower left and right corners, respectively.

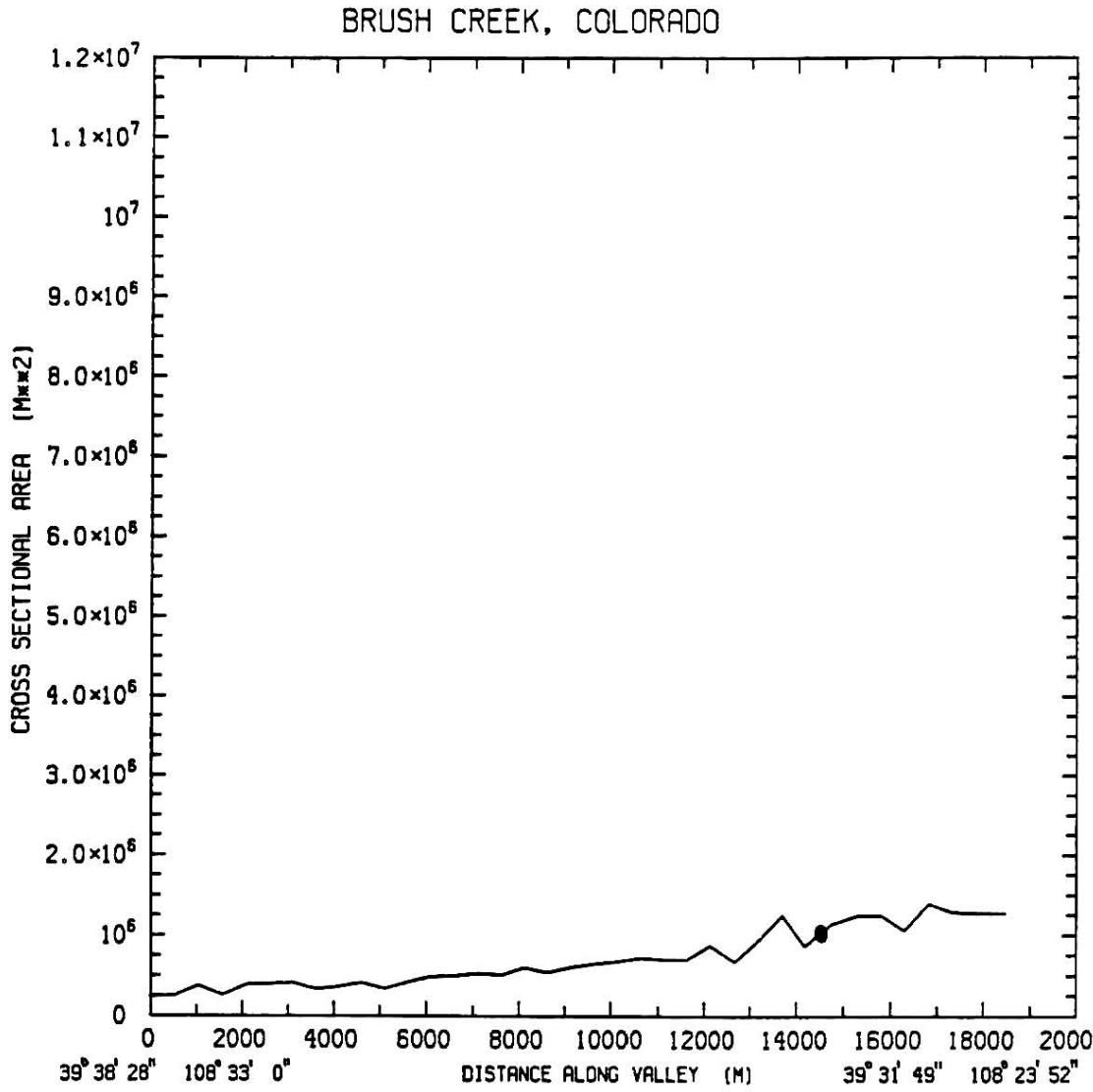

Figure 10f. Along-valley cross-sectional area, A, for Brush Creek. Dot is sounding site location. Latitude and longitude values for first and last points of valley floor are shown in lower left and right corners, respectively.

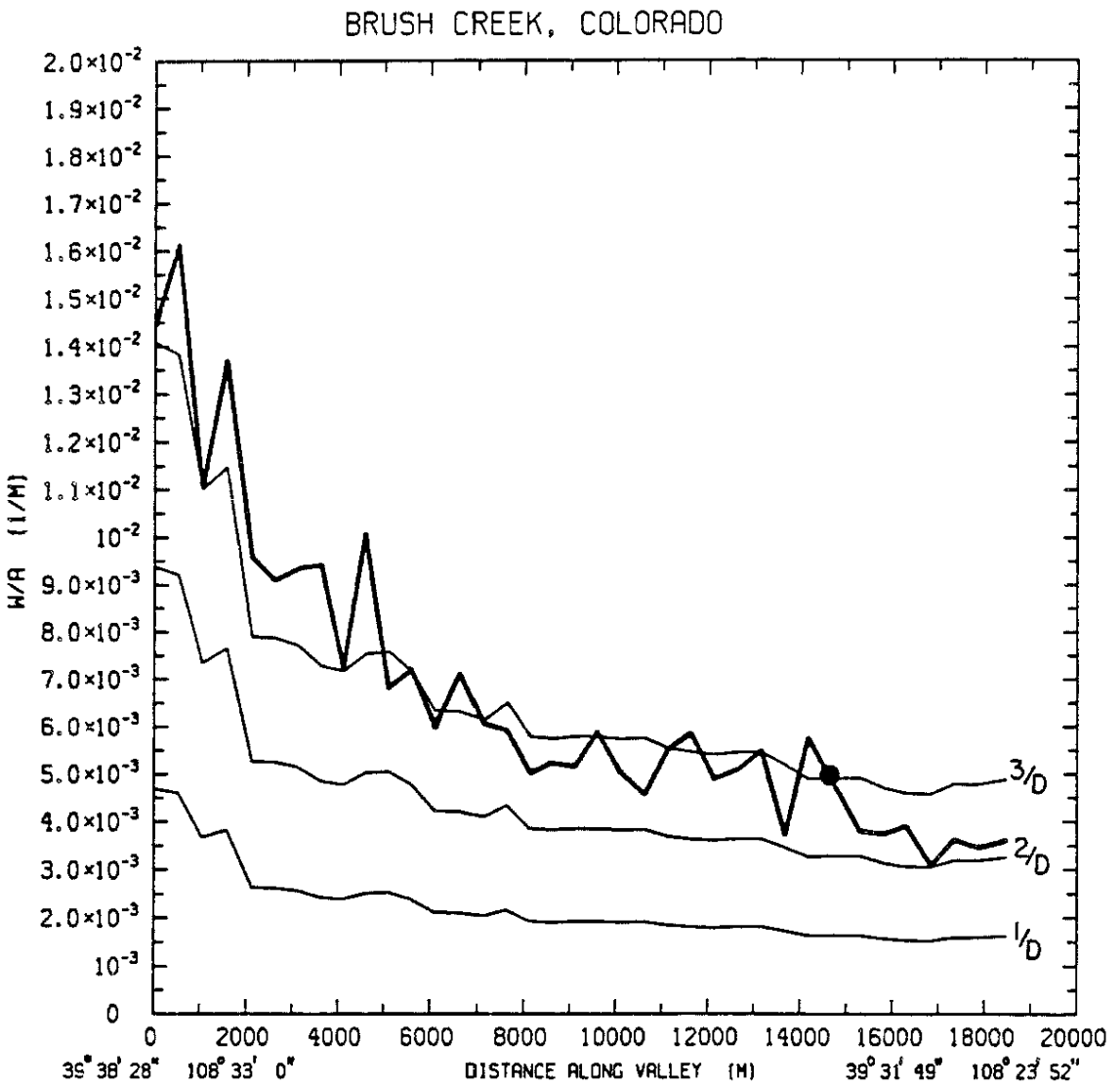

Figure 10g. Along-valley plot of W/A (heavy line) for Brush Creek compared with 1/D, 2/D and 3/D plots where D is the along-valley depth. Dot is sounding site location. Latitude and longitude values for first and last points of valley floor are shown in lower left and right corners, respectively.

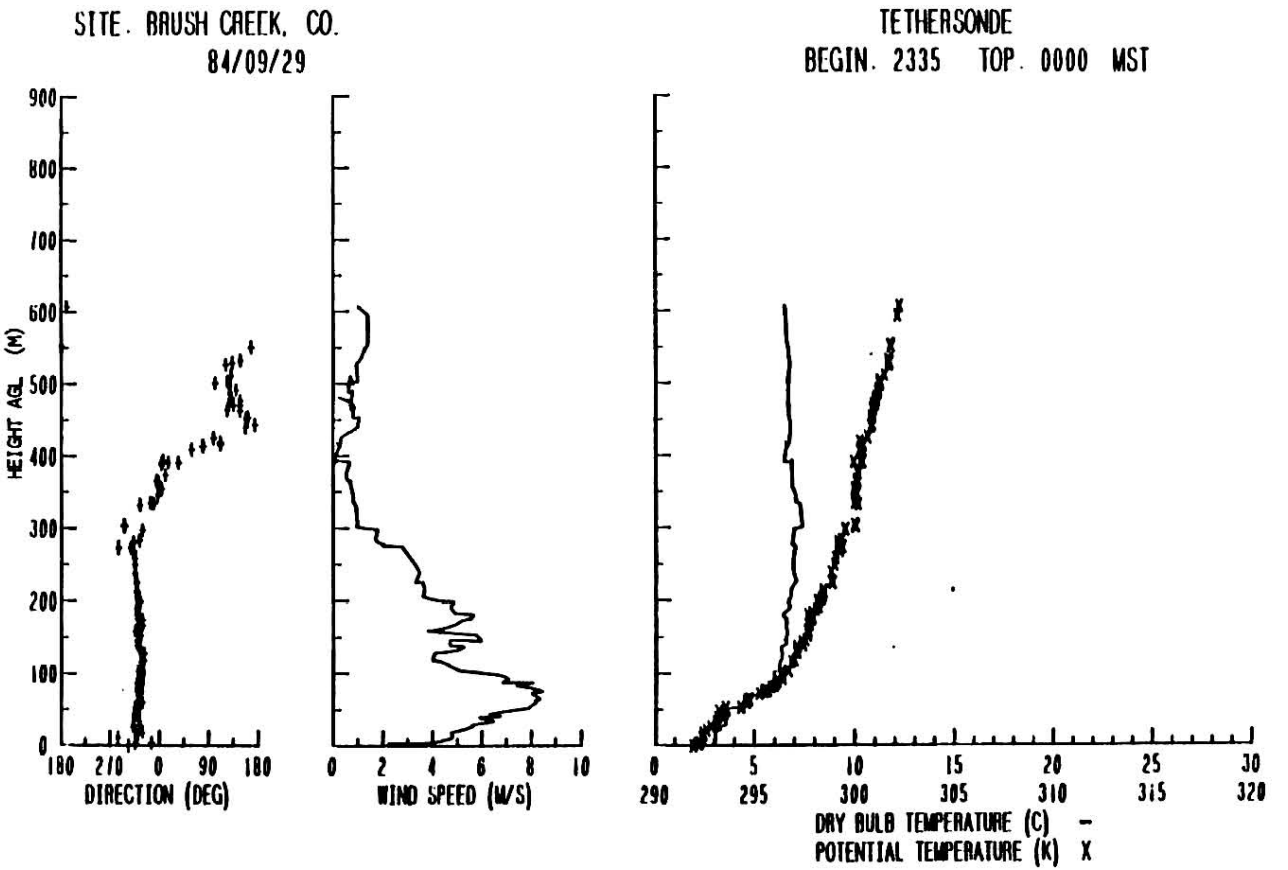

Figure 10h. Representative tethersonde sounding from Brush Creek sounding site.

basin (Figure 10c). In addition, there are no major side valleys or intrusions into Brush Creek to disrupt the idealized geometry.

The resulting (W/A) plot is shown in Figure 10g. A steeply decreasing (W/A) in the first eight kilometers is probably due to the fact that the valley width is decreasing by 25% while over the same distance the area is increasing by 100%, a concurrent trend not found in any other valleys in this research. Figure 10g shows that (W/A) continues to decrease from eight kilometers all the way down-valley, albeit with a more gradual slope, due to the magnitude of the cross-sectional area increase outpacing the magnitude of the width increase.

Colorado State University took tethersonde soundings during the 1984 ASCOT field project coincident with the position of the 14.5 kilometer marker in Brush Creek. A representative sounding from this experiment (Figure 10h) depicts an 8 m/s low-level wind maximum found at the top of the inversion layer, characteristic of a draining valley. One is left to wonder if the nocturnal jet would be significantly stronger in the upper eight kilometers of Brush Creek where the slope of (W/A) is an order of magnitude greater than the lower eleven kilometers?

2. South Fork White River

An 11.5 kilometer stretch of the South Fork of the White River is examined from the merging of Lost Solar Creek and the South Fork to Burro Mountain where the Stillwater sounding site is located (Figure 11a). Northwestward from Burro Mountain the southern ridgeline drops rapidly to the main stem of the White River while the northern ridgeline remains nearly horizontal for several additional kilometers. Figure 11g shows (W/A) decreasing steadily from a maximum of 0.008 m^{-1} to a minimum of 0.002 m^{-1} at the Stillwater site. This is due to the rapid increase

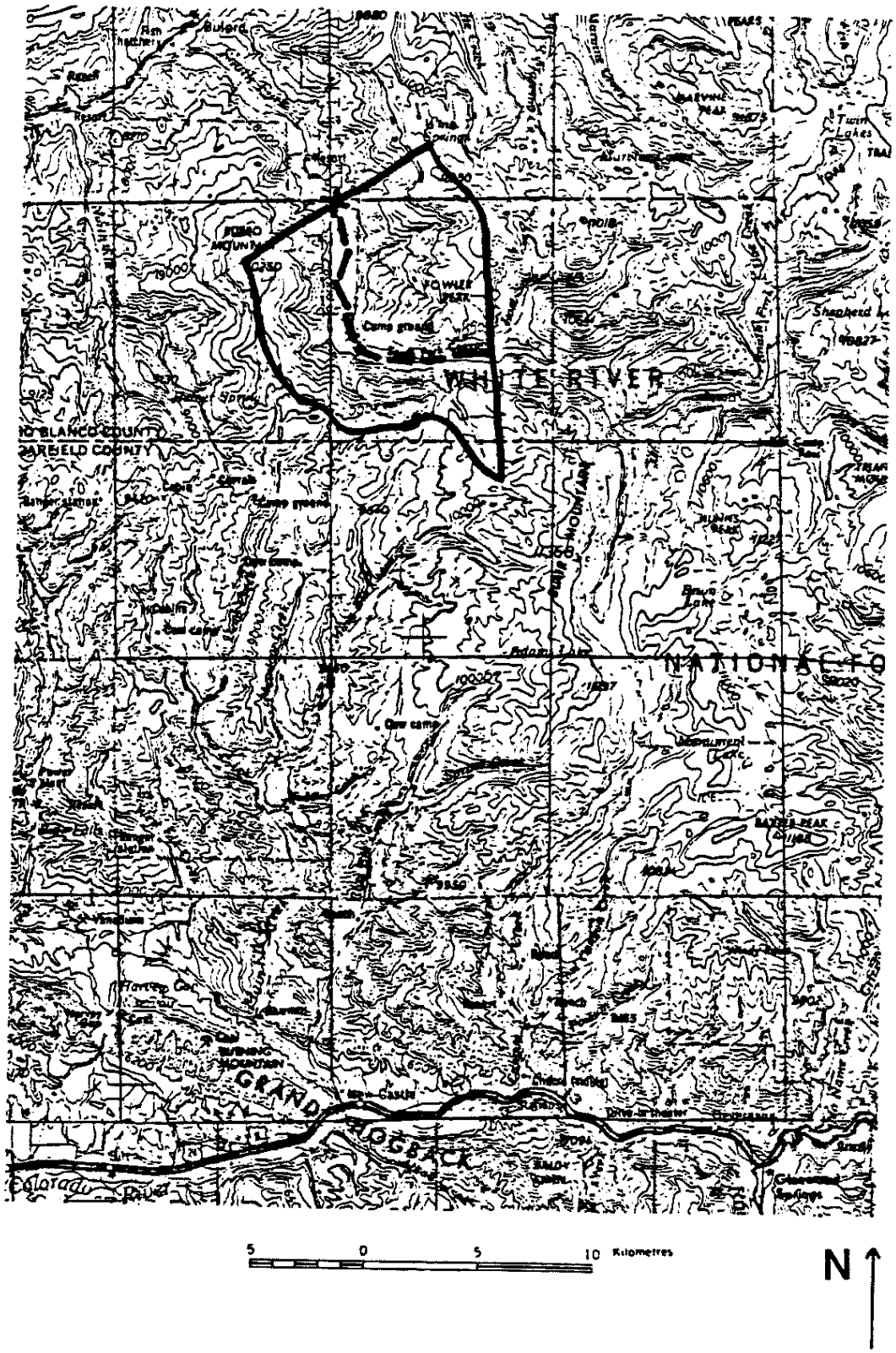

Figure 11a. Same as Figure 10a but for South Fork White River.

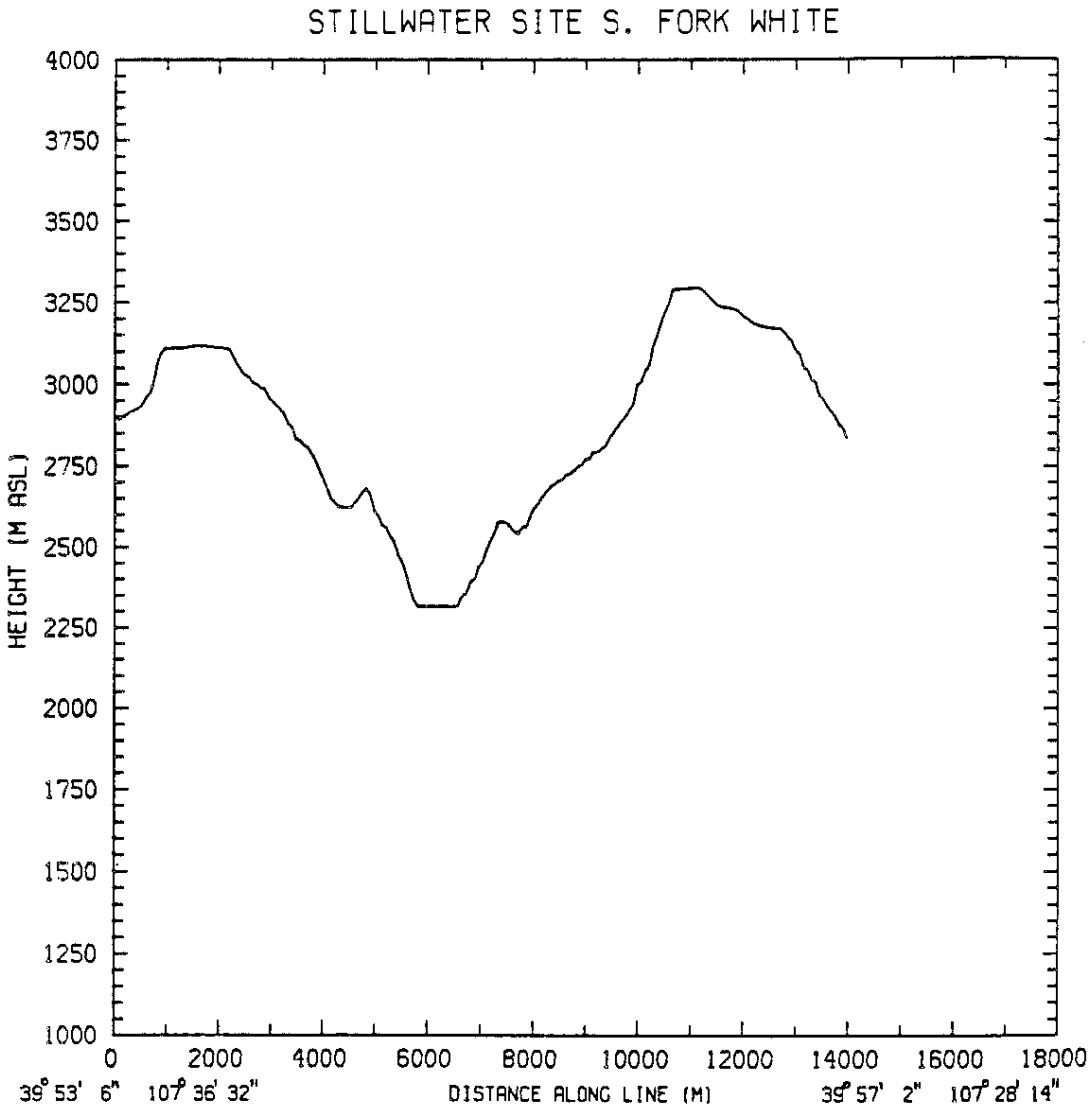

Figure 11b. Same as Figure 10b but for South Fork White River. Sidewall slope angle is 14°.

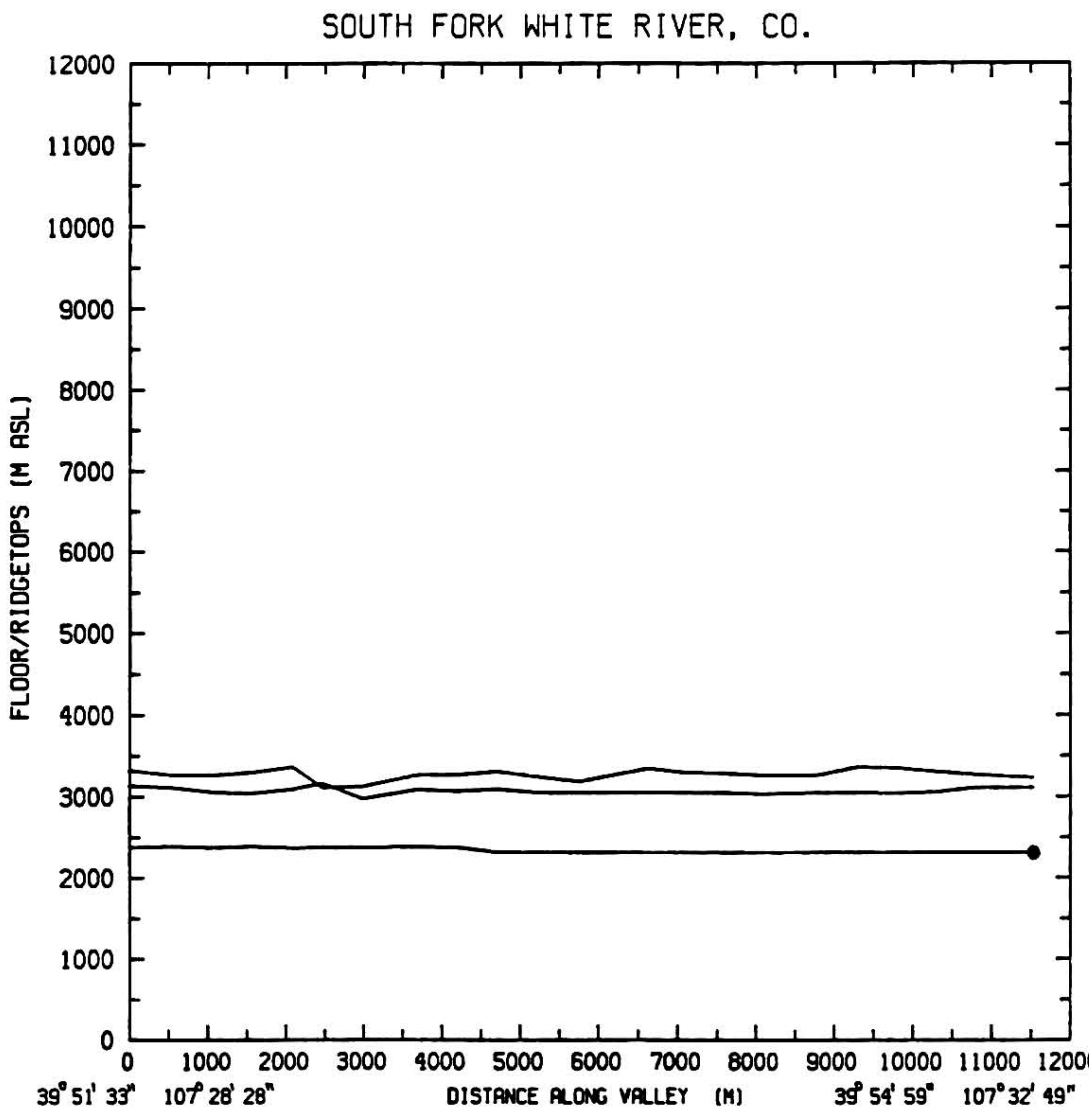

Figure 11c. Same as Figure 10c but for South Fork White River.

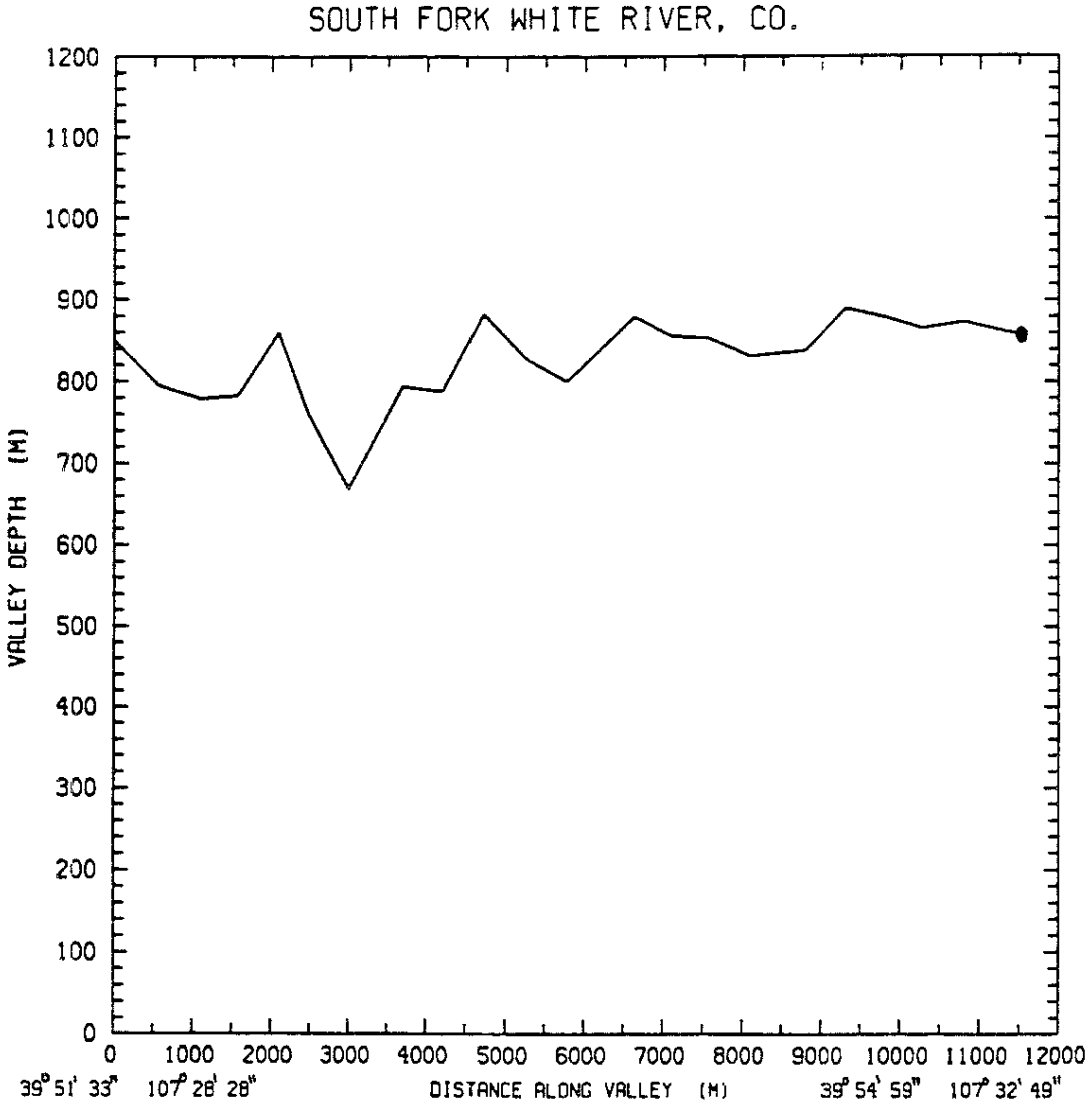

Figure 11d. Same as Figure 10d but for South Fork White River.

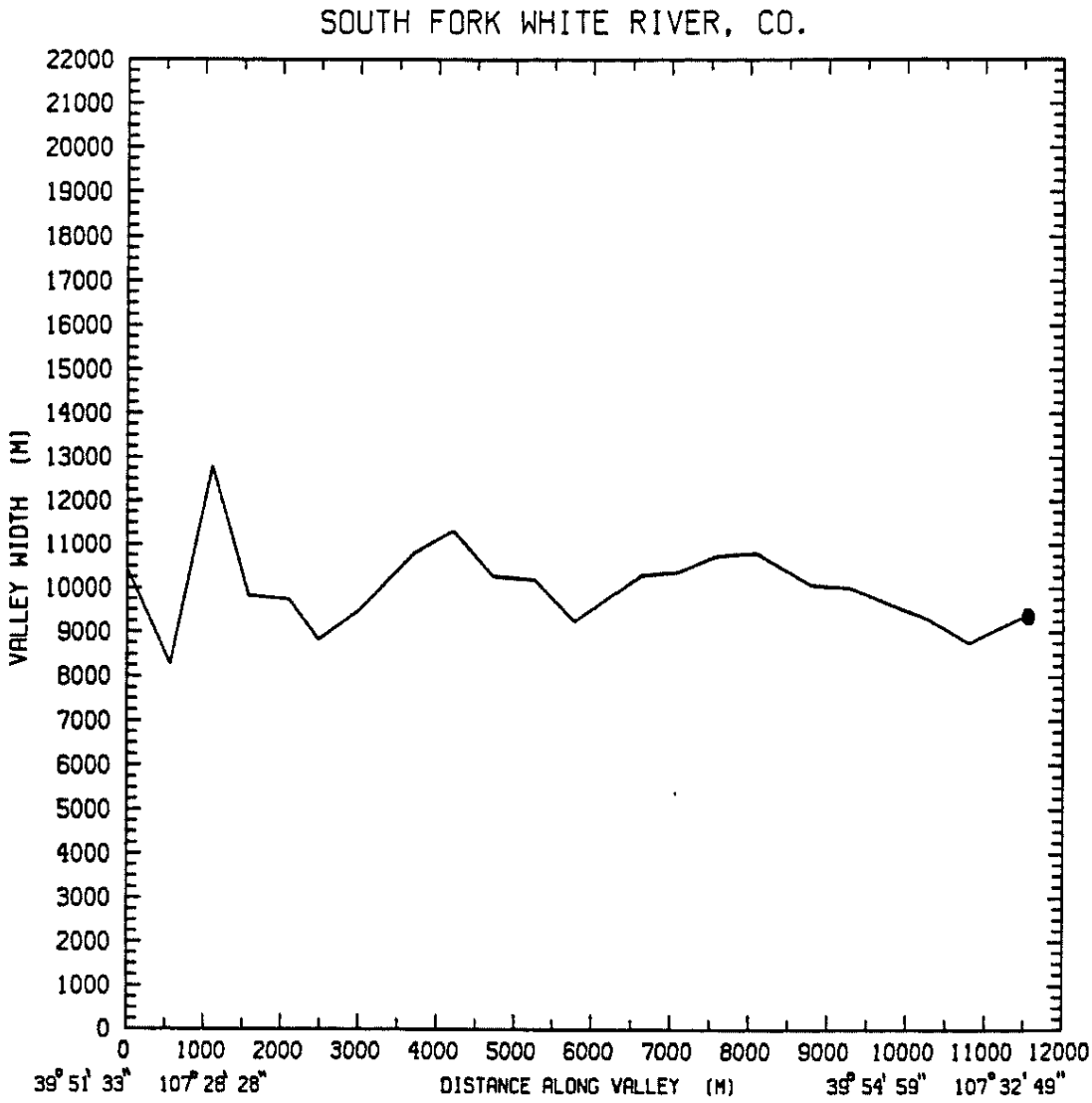

Figure 11e. Same as Figure 10e but for South Fork White River.

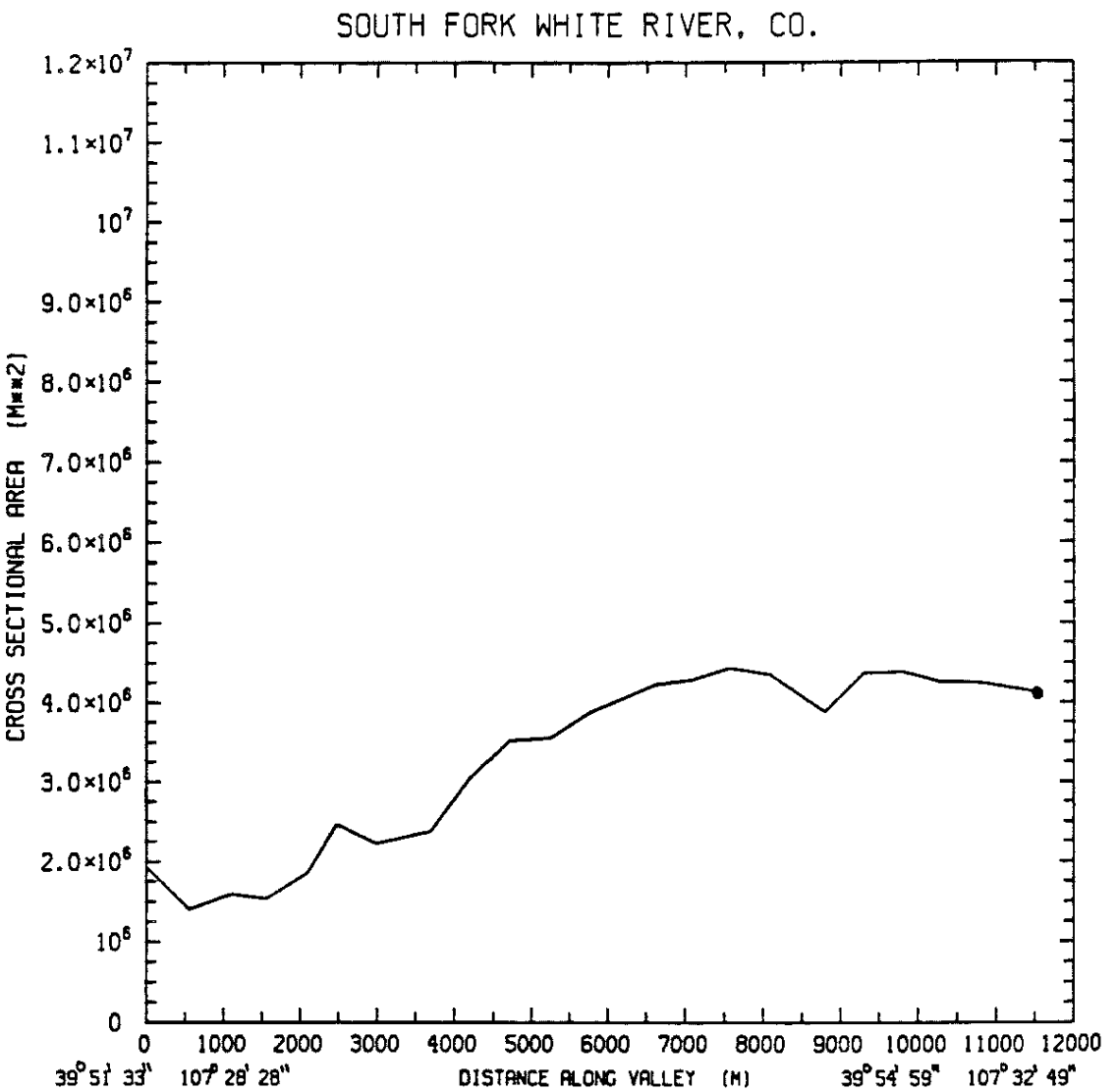

Figure 11f. Same as Figure 10f but for South Fork White River.

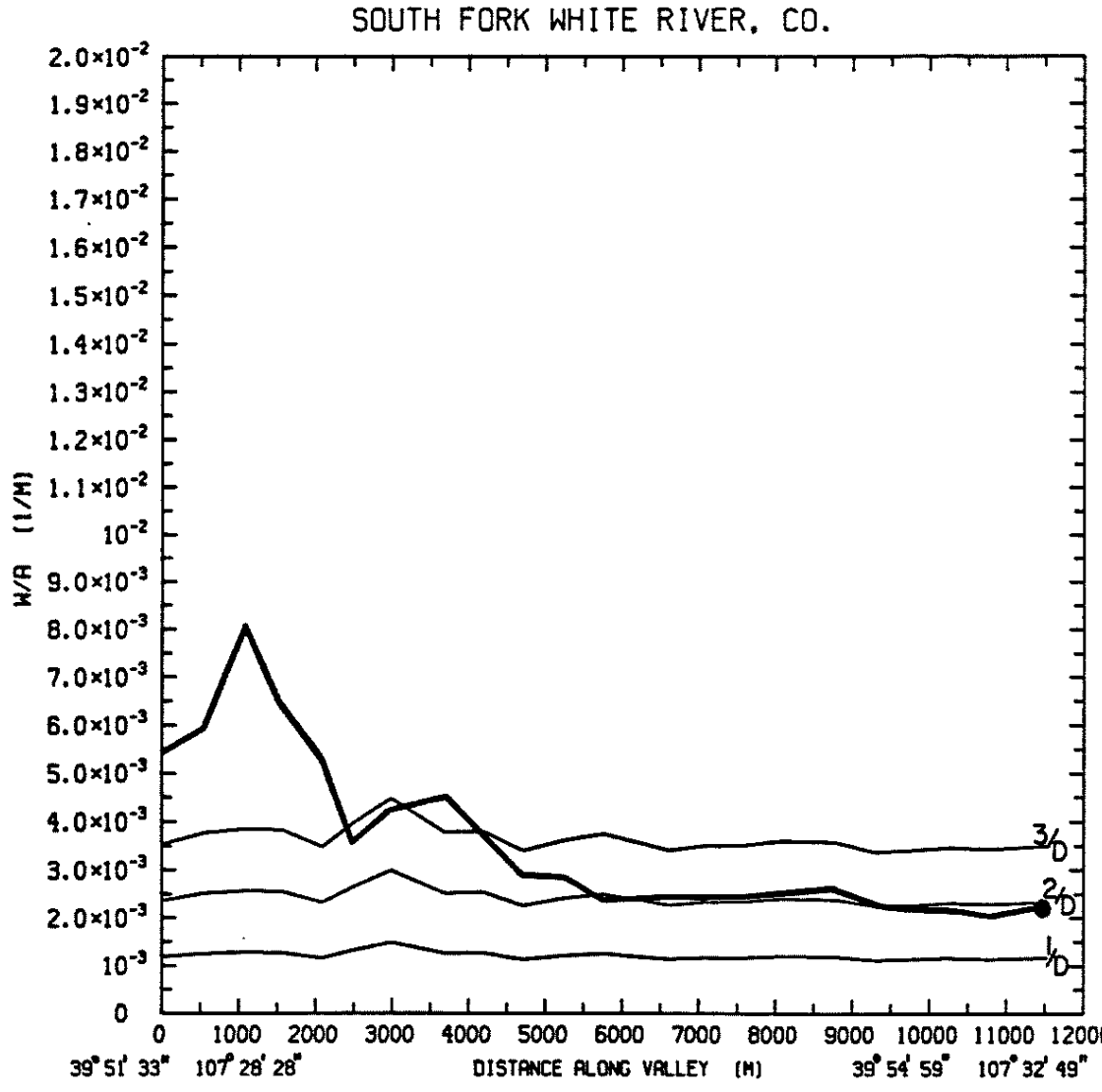

Figure 11g. Same as Figure 10g but for South Fork White River.

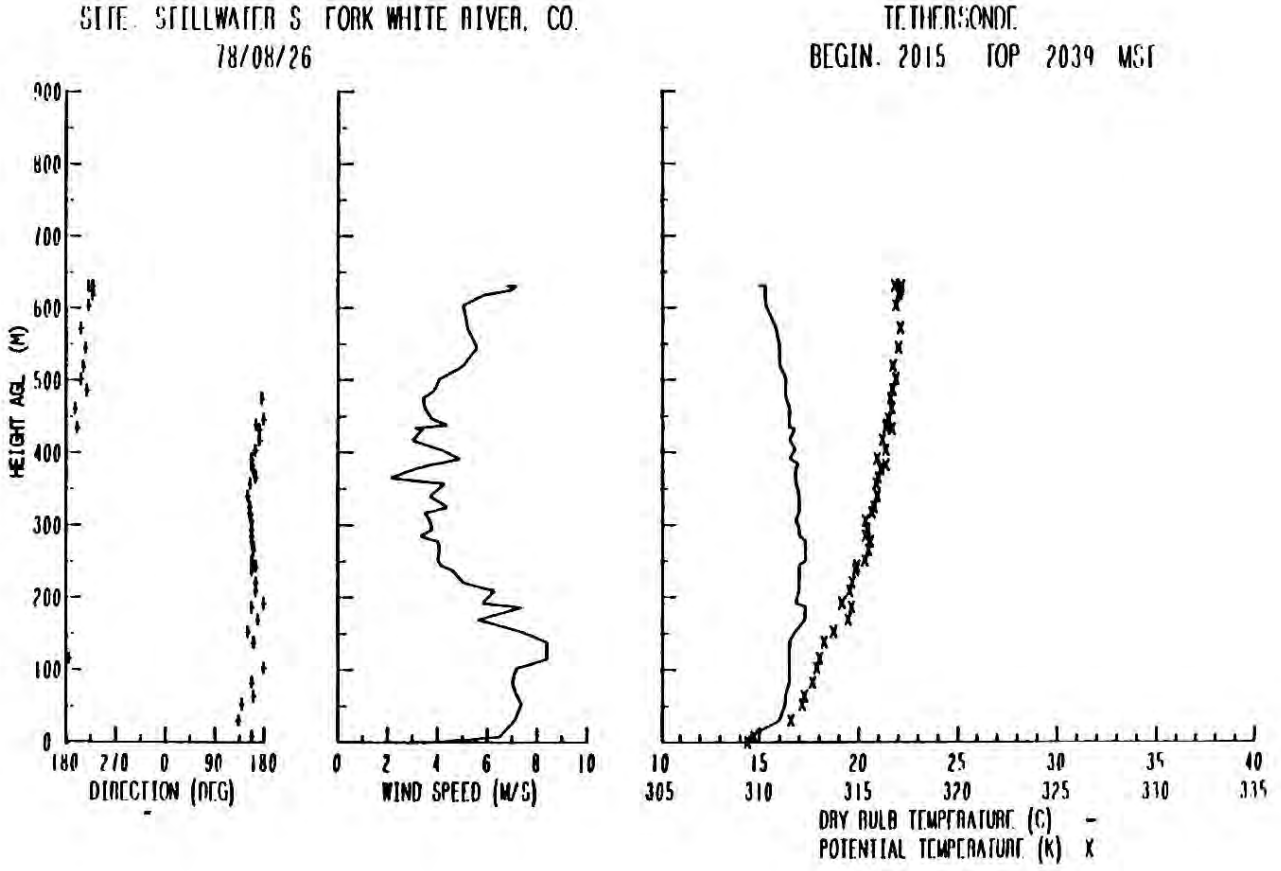

Figure 11h. Same as Figure 10h but for South Fork White River.

in the valley area as the river exits the narrow canyon in the first three or four kilometers of the valley and a relatively unchanging width over the same interval. This favorable topography aids in the development of winds up to 8.5 m/s at the Stillwater sounding site (Figure 11h).

3. Upper Colorado River

The Colorado River, from its source at the Continental Divide to a location eight kilometers north of Grand Lake, drains a rapidly widening and deepening watershed (Figure 12a). These features make this 18.5 kilometer valley an ideal one in which to test the (W/A) hypothesis. Despite a sixfold increase in cross-sectional area down-valley, (W/A) only drops by a factor of two due to the 350% widening of the valley along the same distance. Nevertheless, the Upper Colorado River does exhibit slight drainage characteristics and it would be interesting to verify the topographical predictor through tethered wind observations. At this writing there are no known sources of tethersonde wind data in this region.

B. Pooling Valleys

1. Yampa Valley

A thirteen kilometer stretch of the broad Yampa Valley from a point just north of Blacktail Mountain to the Steamboat Springs ski area is checked for the presence or absence of a wind system. Although the western ridgeline is significantly lower than its eastern counterpart they both remain on a more or less horizontal plane along the entire valley length thus validating comparisons of geometric features along-valley. The depth of the valley atmosphere from the valley floor to the

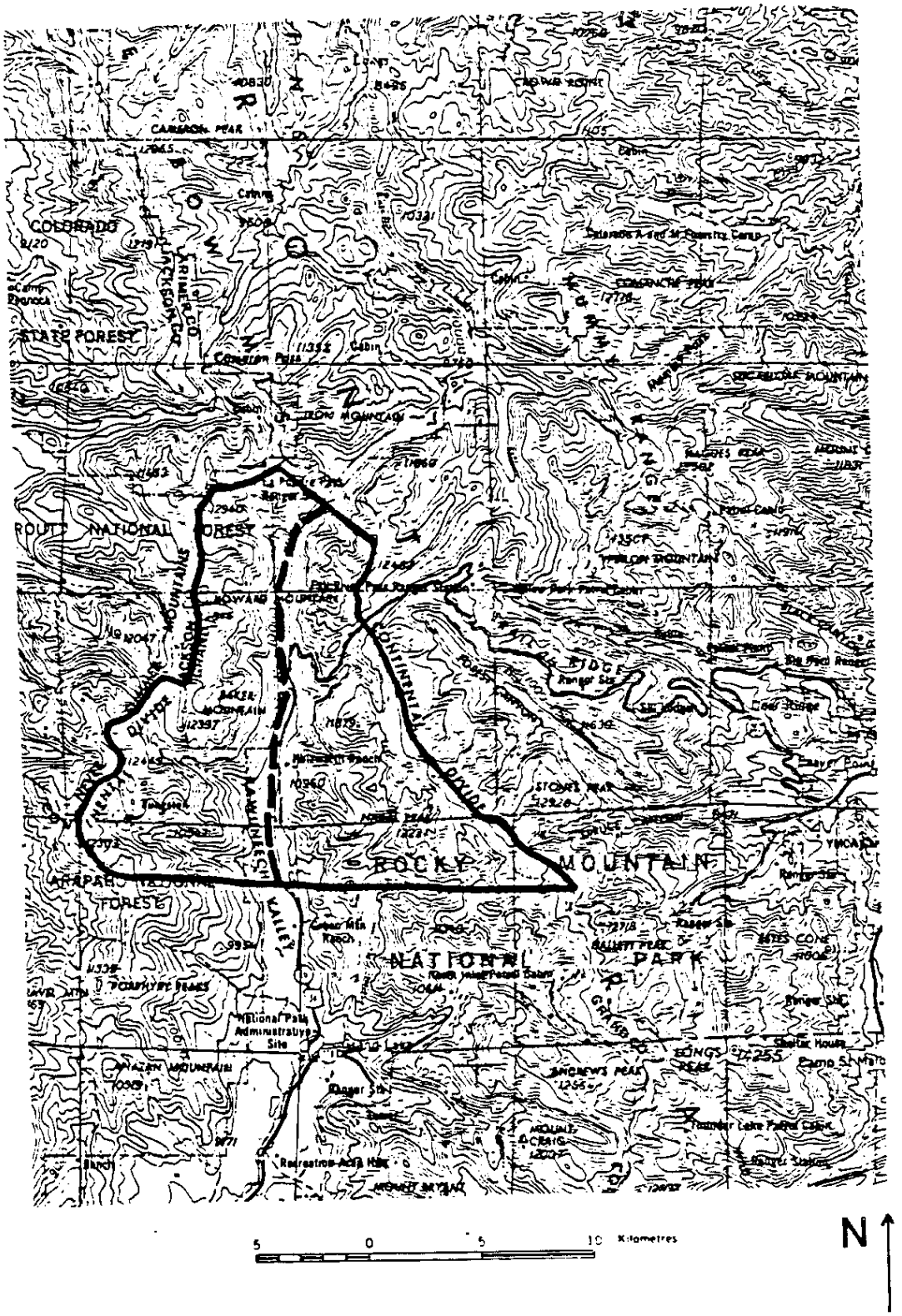

Figure 12a. Same as Figure 10a but for Upper Colorado River.

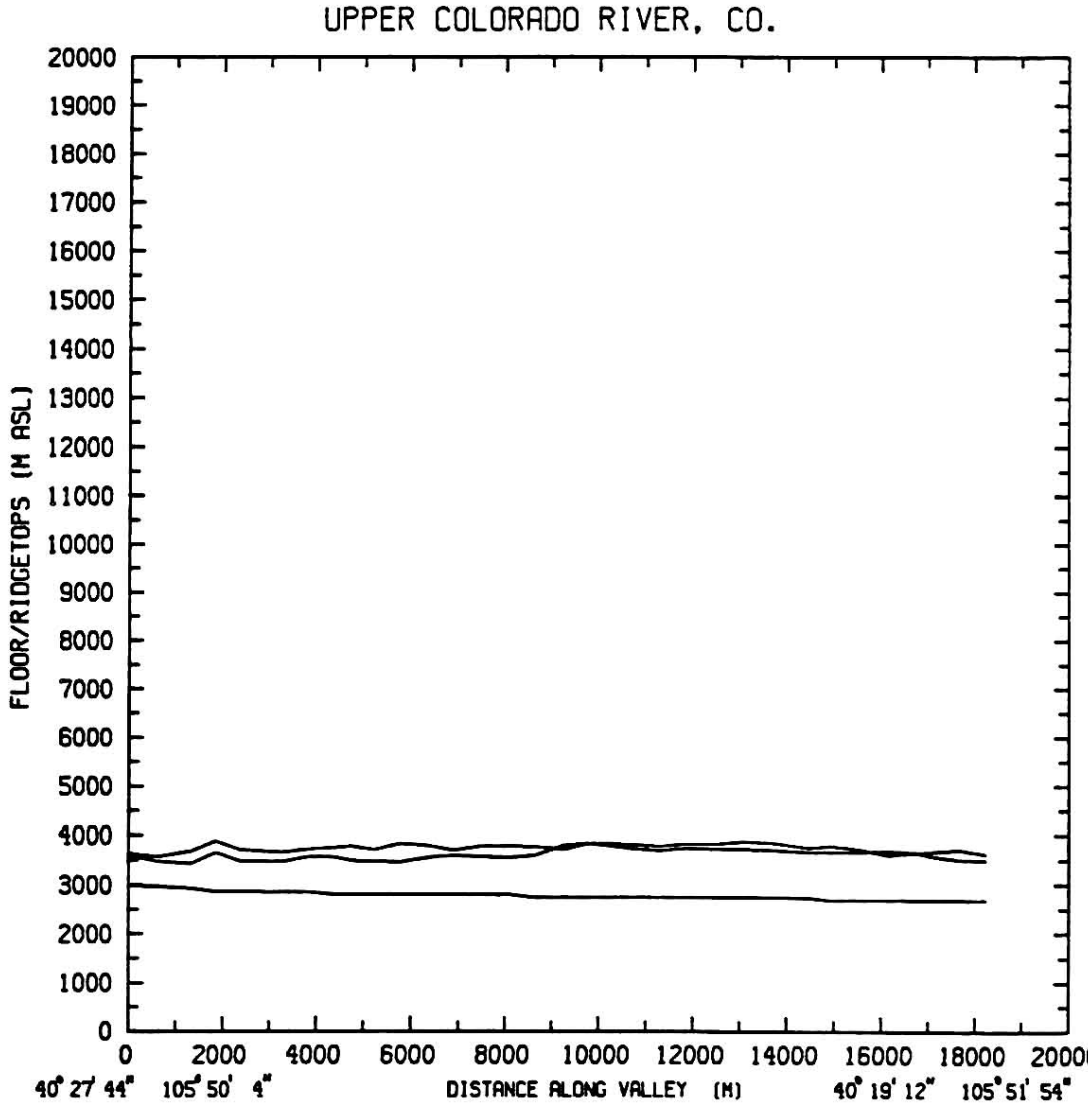

Figure 12b. Same as Figure 10c but for Upper Colorado River.

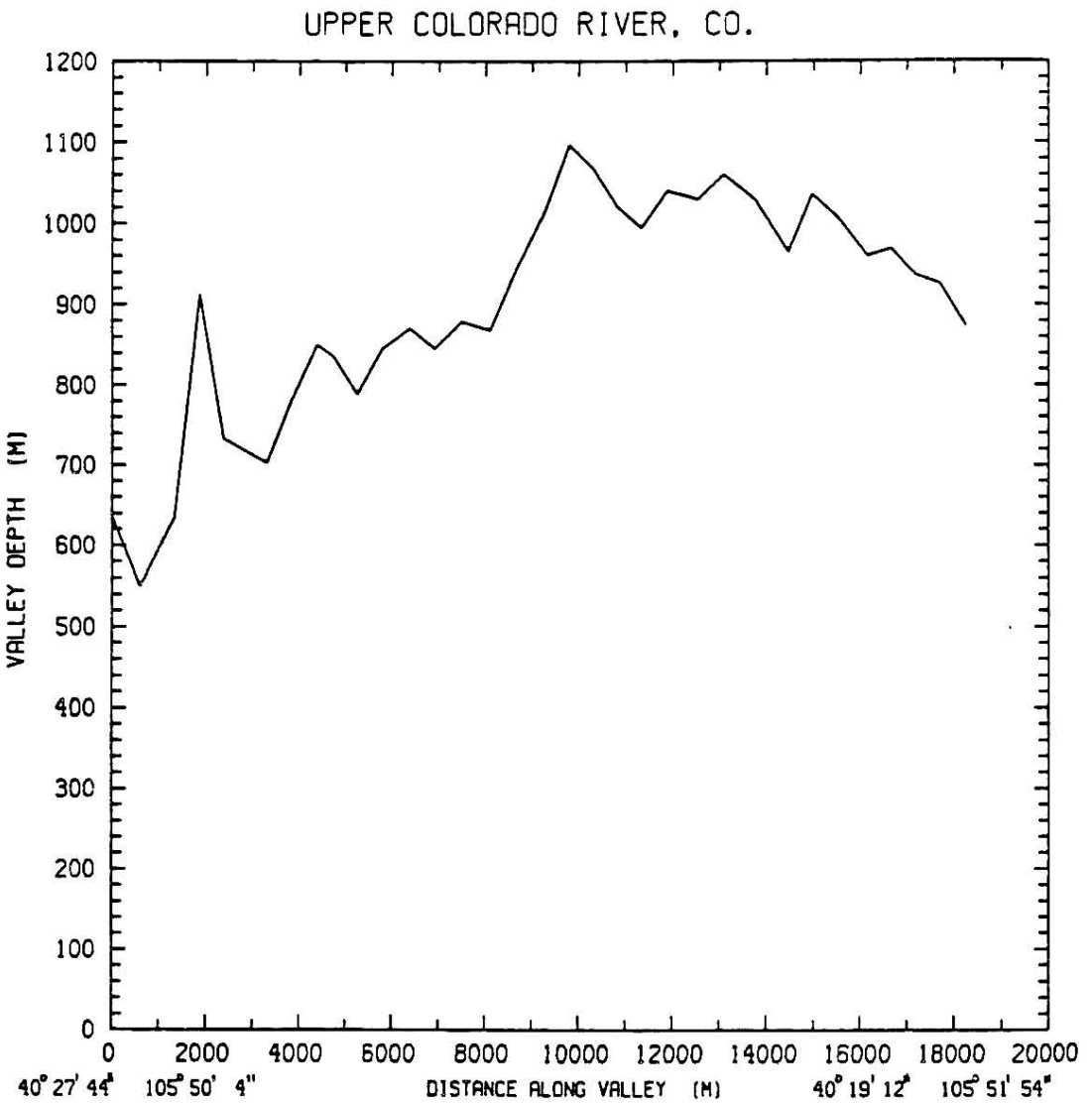

Figure 12c. Same as Figure 10d but for Upper Colorado River.

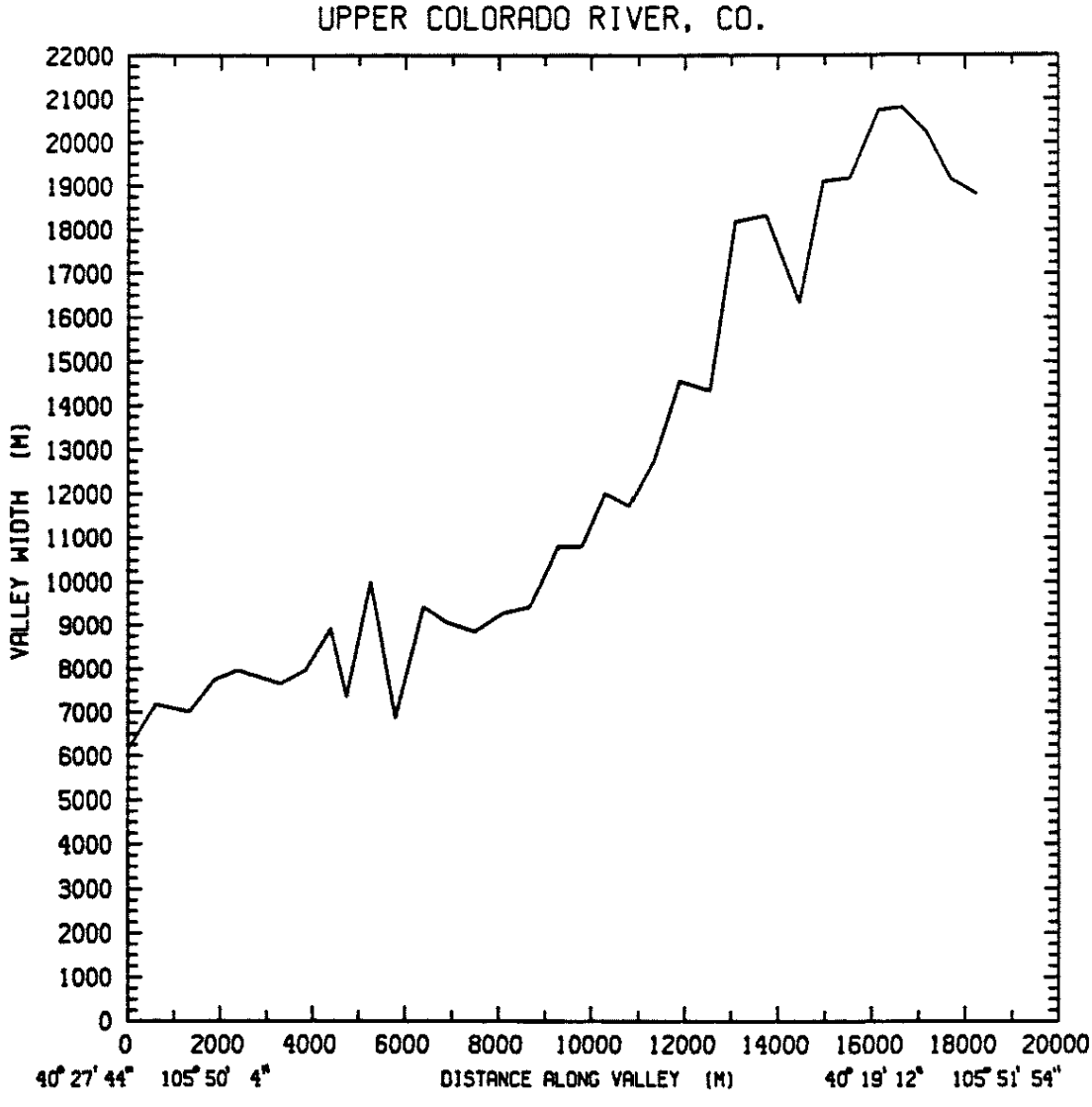

Figure 12d. Same as Figure 10e but for Upper Colorado River.

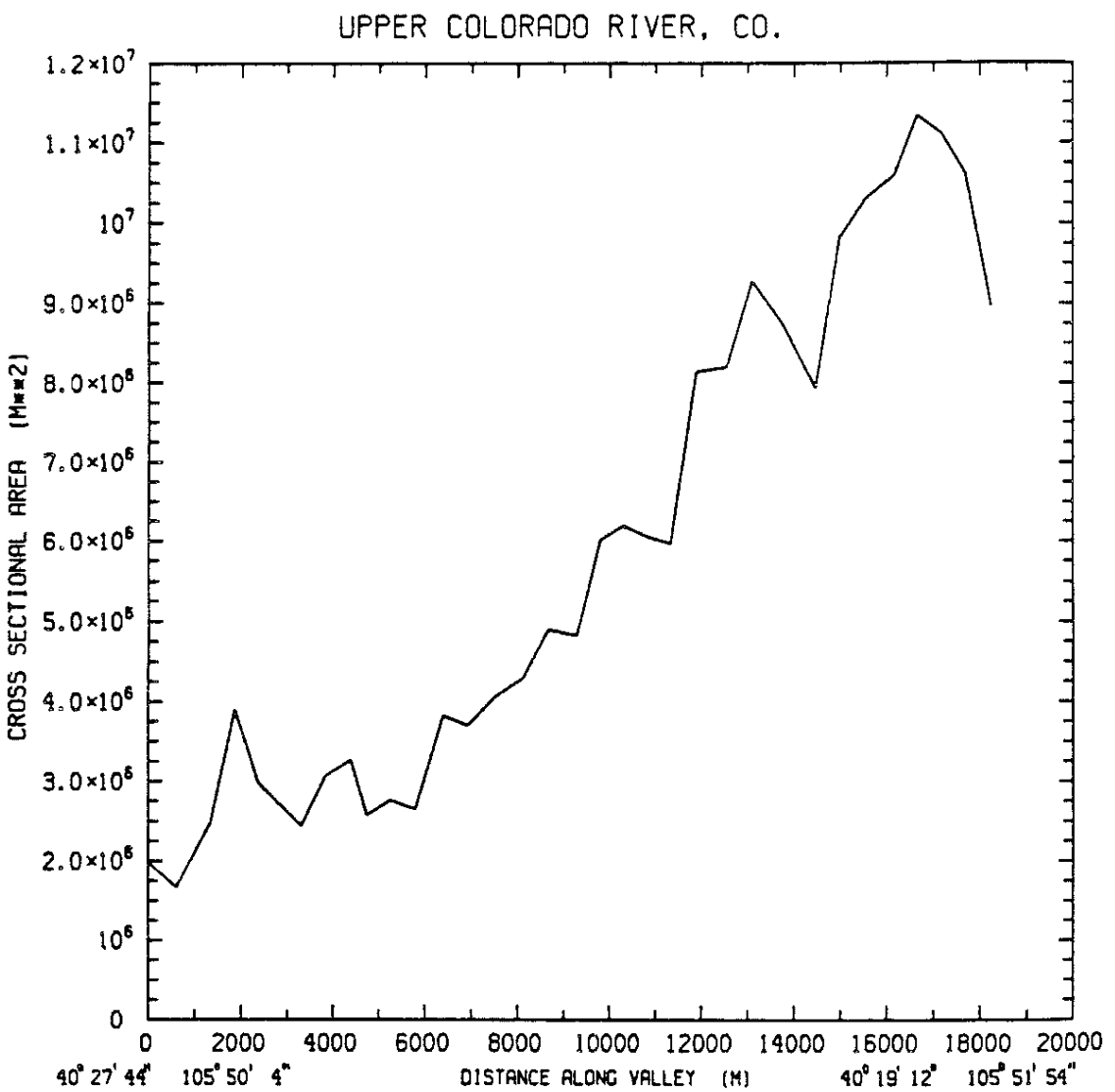

Figure 12e. Same as Figure 10f but for Upper Colorado River.

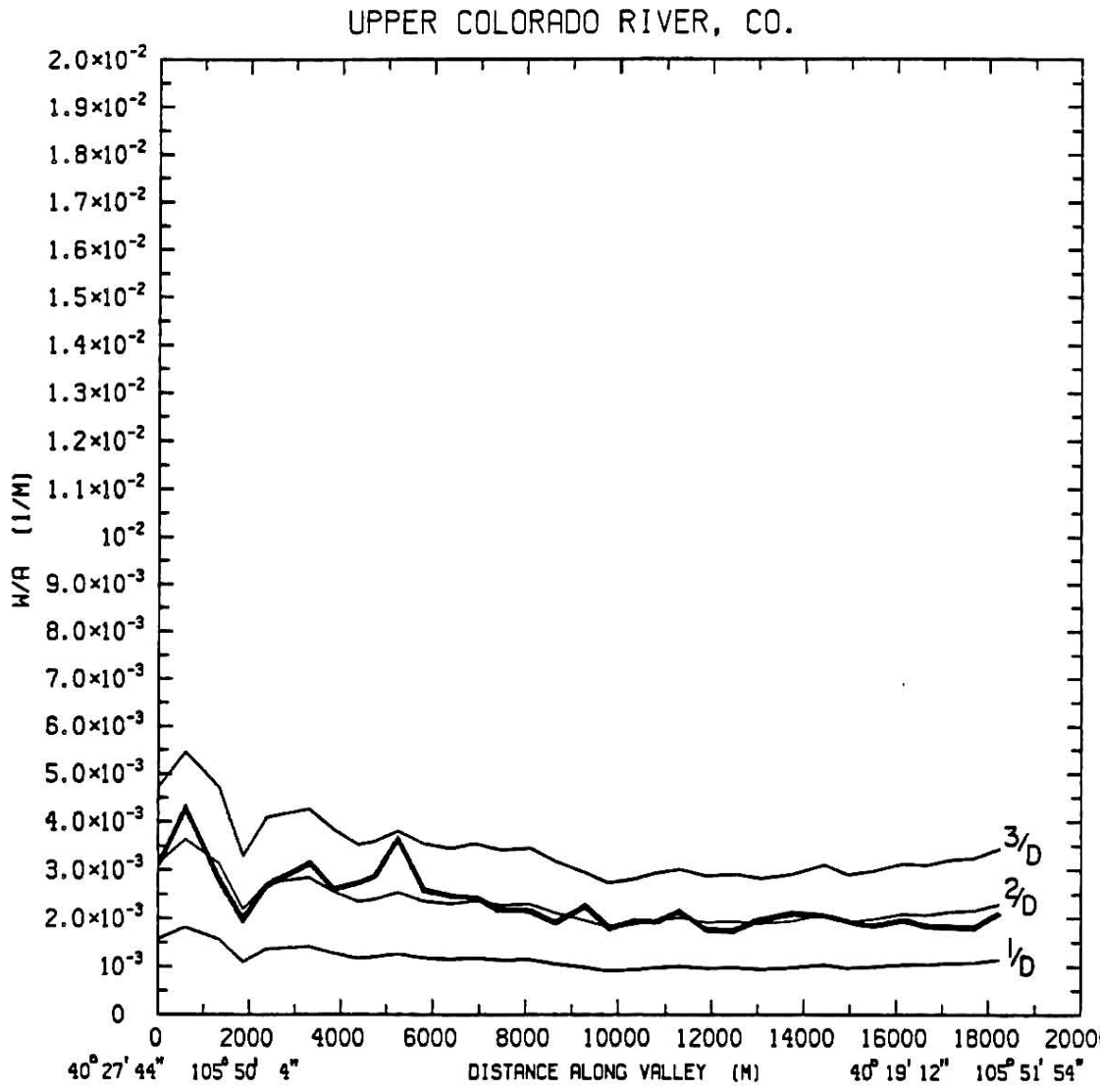

Figure 12f. Same as Figure 10g but for Upper Colorado River.

level of the lowest ridgetop fluctuates between 200 and 500 meters (Figure 13c). Observations from other Colorado valleys indicate that this depth is enough to contain the level of maximum nocturnal down-valley winds.

Figure 13g indicates that (W/A) doubles in value from 0.00275 m^{-1} to 0.0055 m^{-1} in the first six kilometers of the Yampa Valley due to a steadily decreasing cross-sectional area. This ideal pattern for a pooling valley is broken for the next four kilometers by the intrusion of Walton Creek flowing west from the Park Range. The reversal of (W/A) in this interval is a result of the large area increases as the elevation contours along the creek bend perpendicular to the Yampa Valley. Ridgelines perpendicular to the main valley are in violation of the (W/A) concept for valley cooling developed in an earlier chapter, therefore this section of the valley is not representative of the valley geometry as a whole. It is not yet clear how these side pockets affect the overall flow of the valley wind system.

Once the effect of Walton Creek is left behind, (W/A) returns to 0.0055 m^{-1}, the same value seen at the end of the rising curve in the first six kilometers. The inability of the Yampa to generate much of an along-valley wind is reflected in the 3 m/s breeze measured at the Sombrero Stable in Steamboat Springs (Figure 13h). The presence of such light winds has most likely enhanced the development of a shallow but very stable inversion layer during this snow covered sounding.

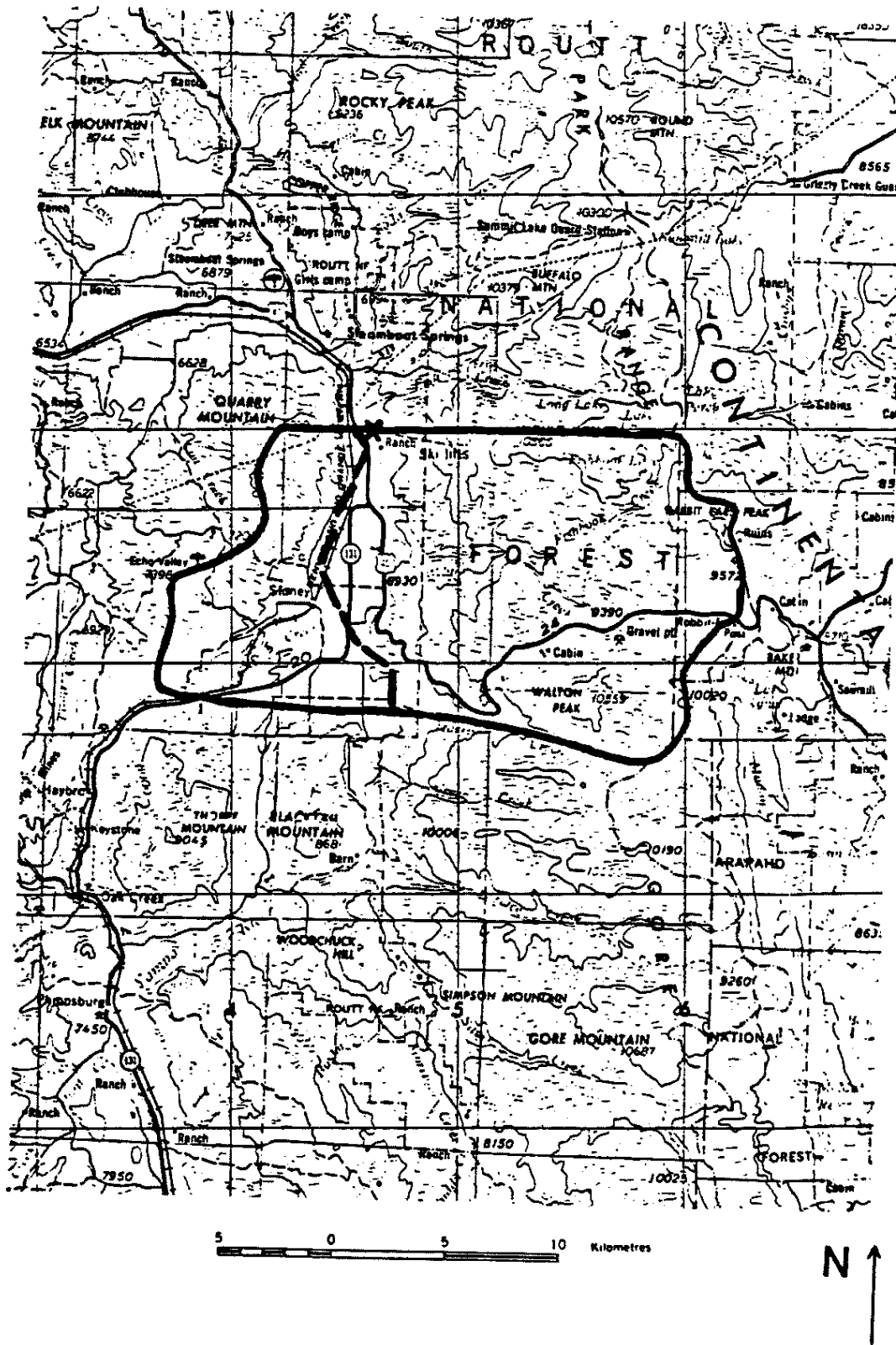

Figure 13a. Same as Figure 10a but for Yampa Valley.

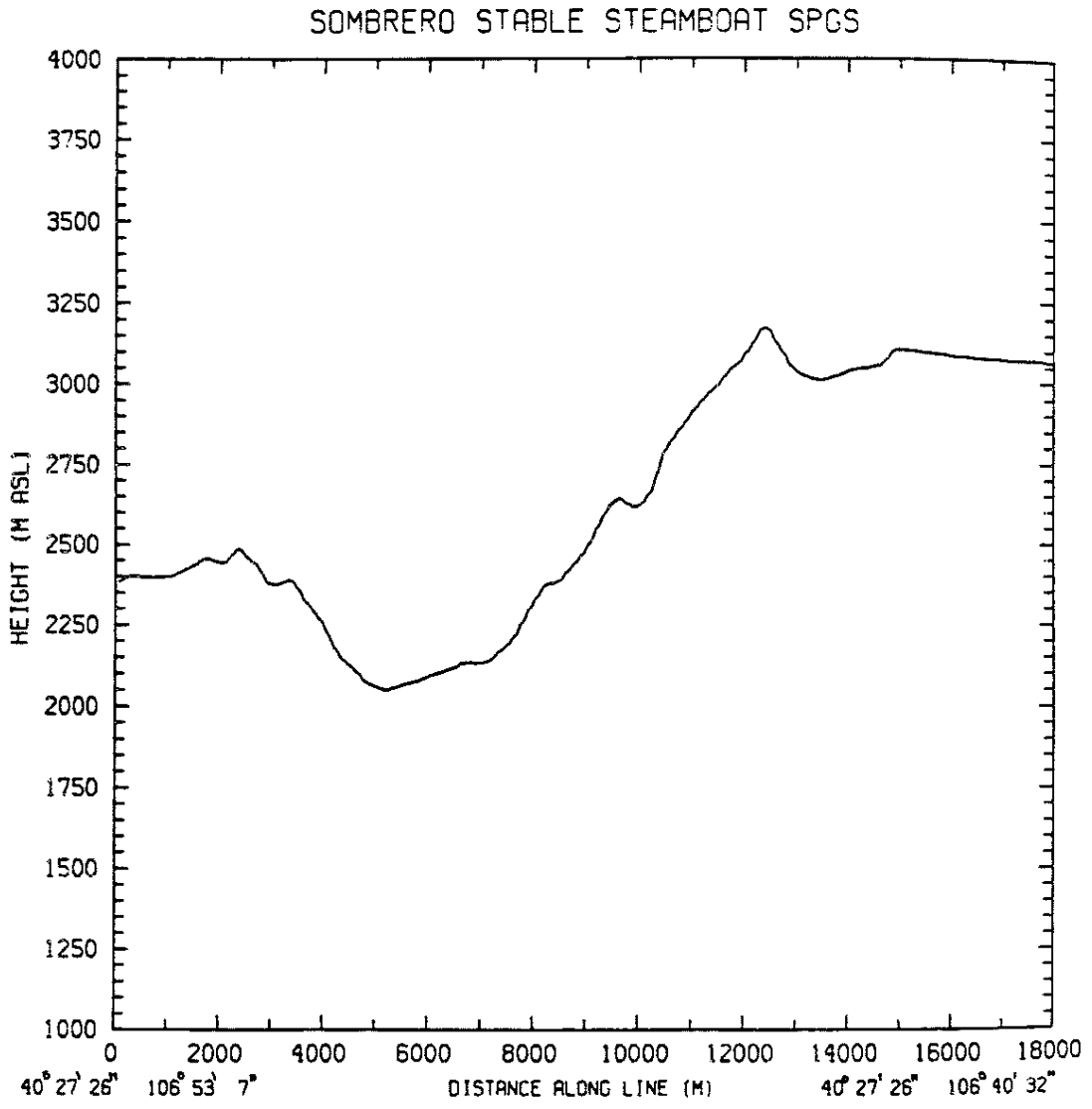

Figure 13b. Same as Figure 10b but for Yampa Valley. Sidewall slope angle is 9°.

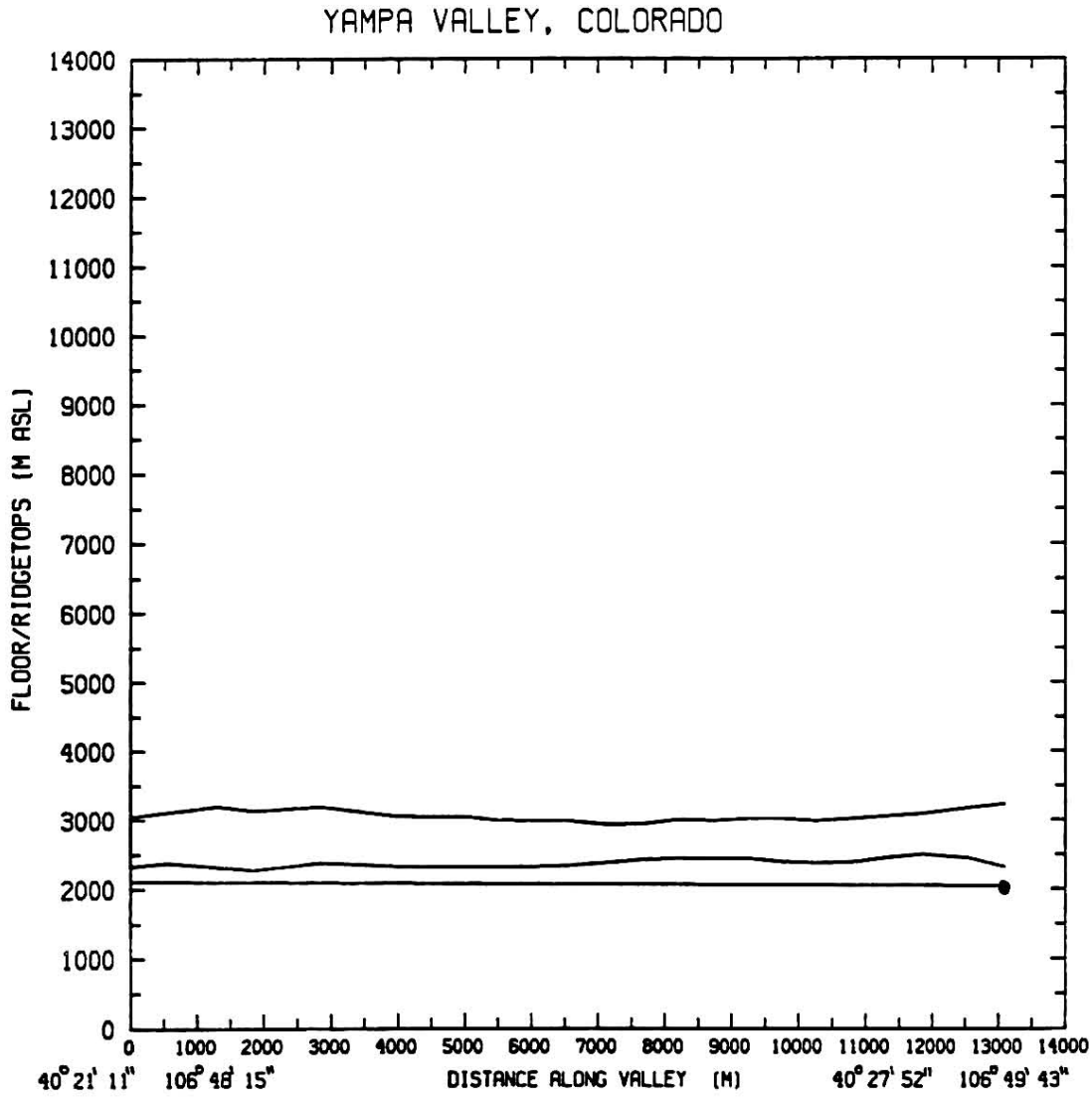

Figure 13c. Same as Figure 10c but for Yampa Valley.

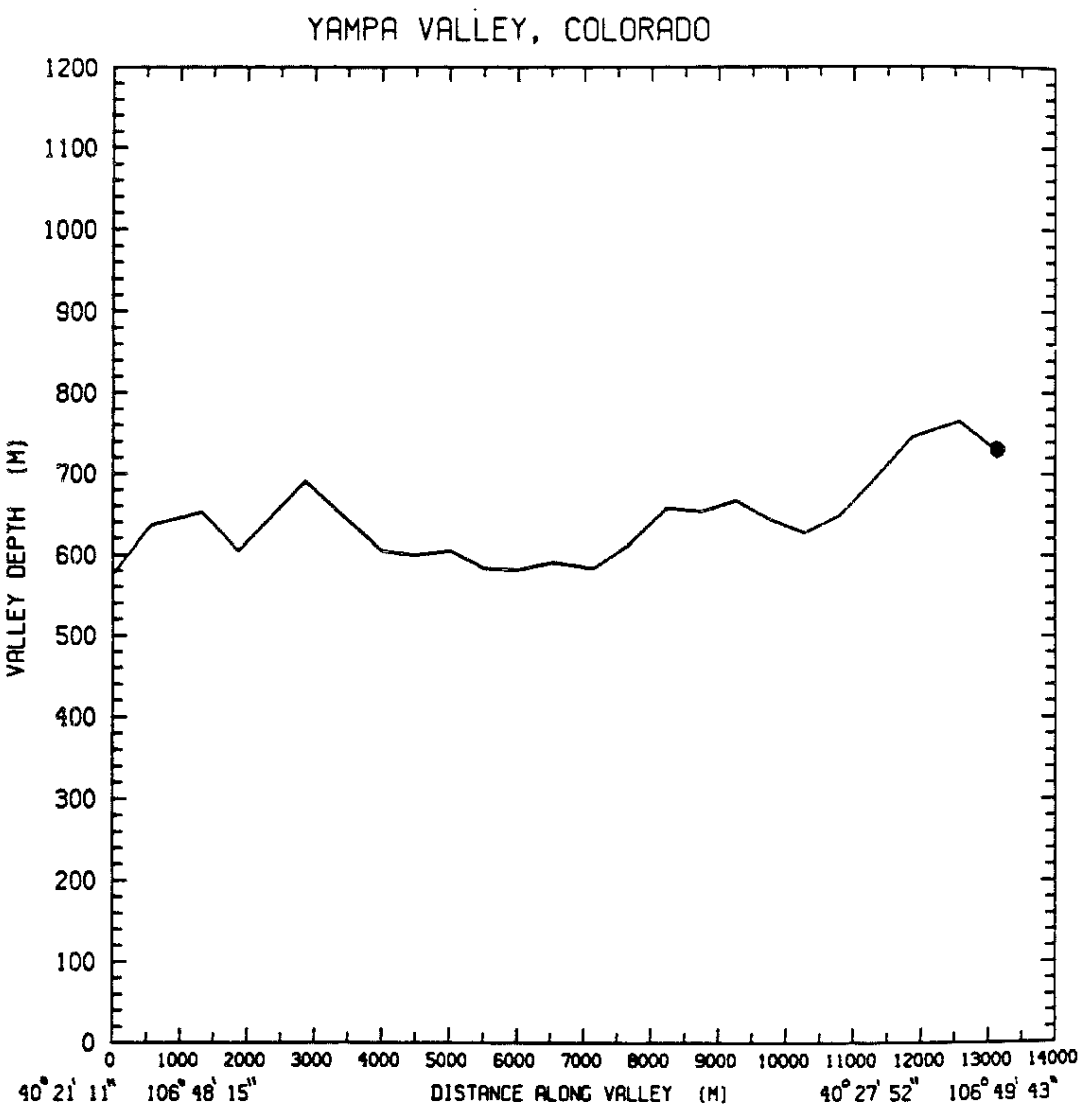

Figure 13d. Same as Figure 10d but for Yampa Valley.

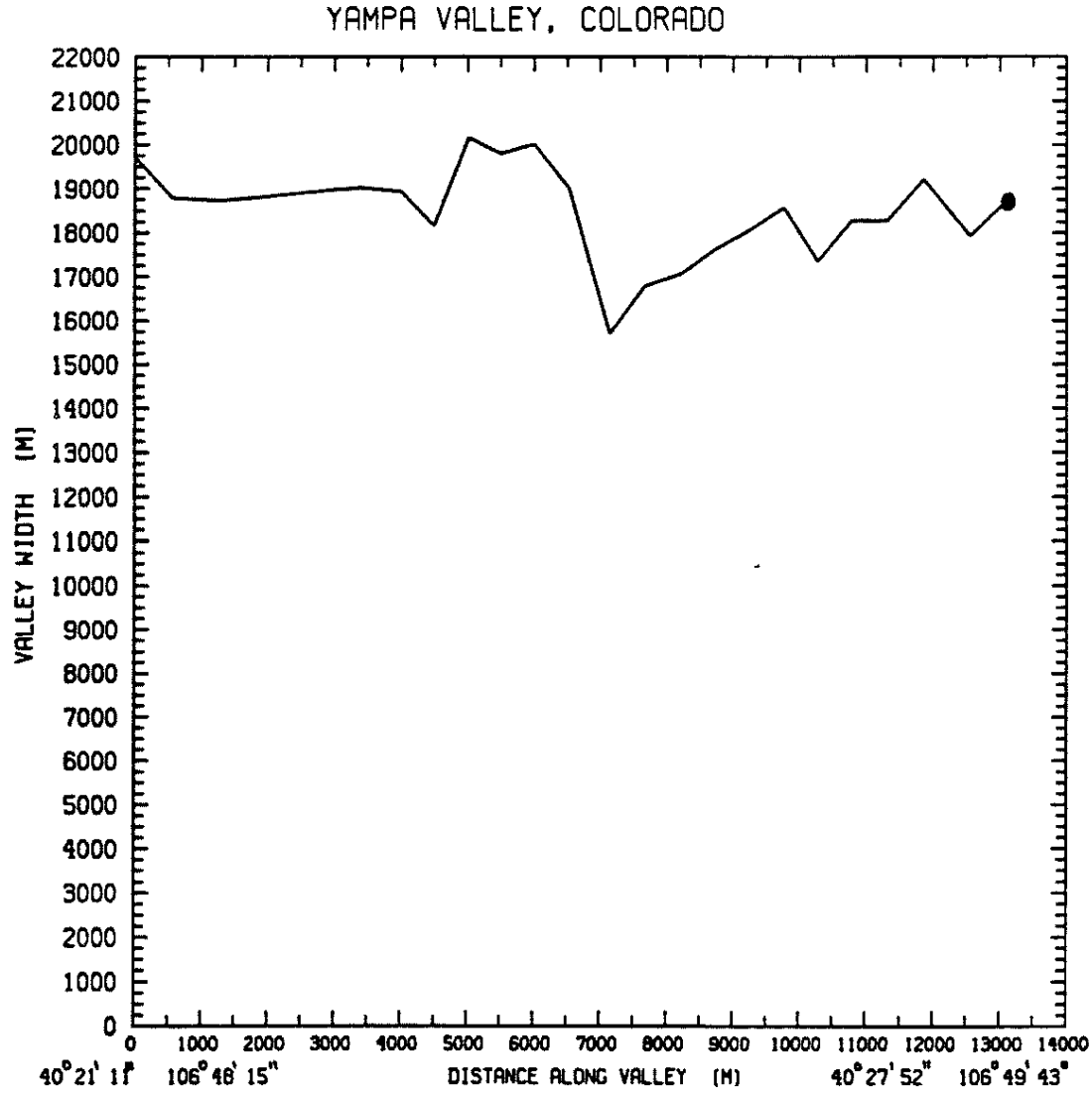

Figure 13e. Same as Figure 10e but for Yampa Valley.

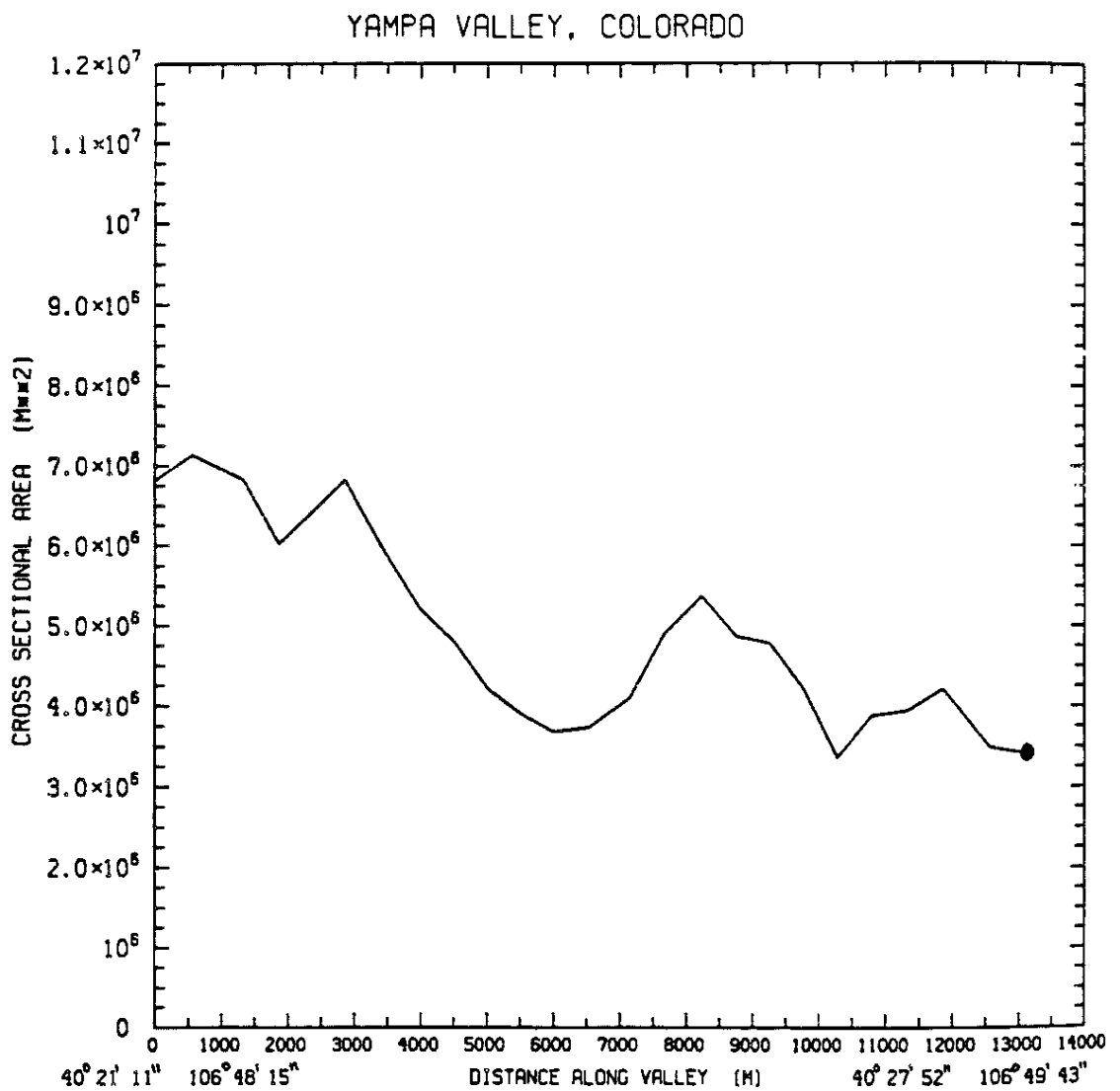

Figure 13f. Same as Figure 10f but for Yampa Valley.

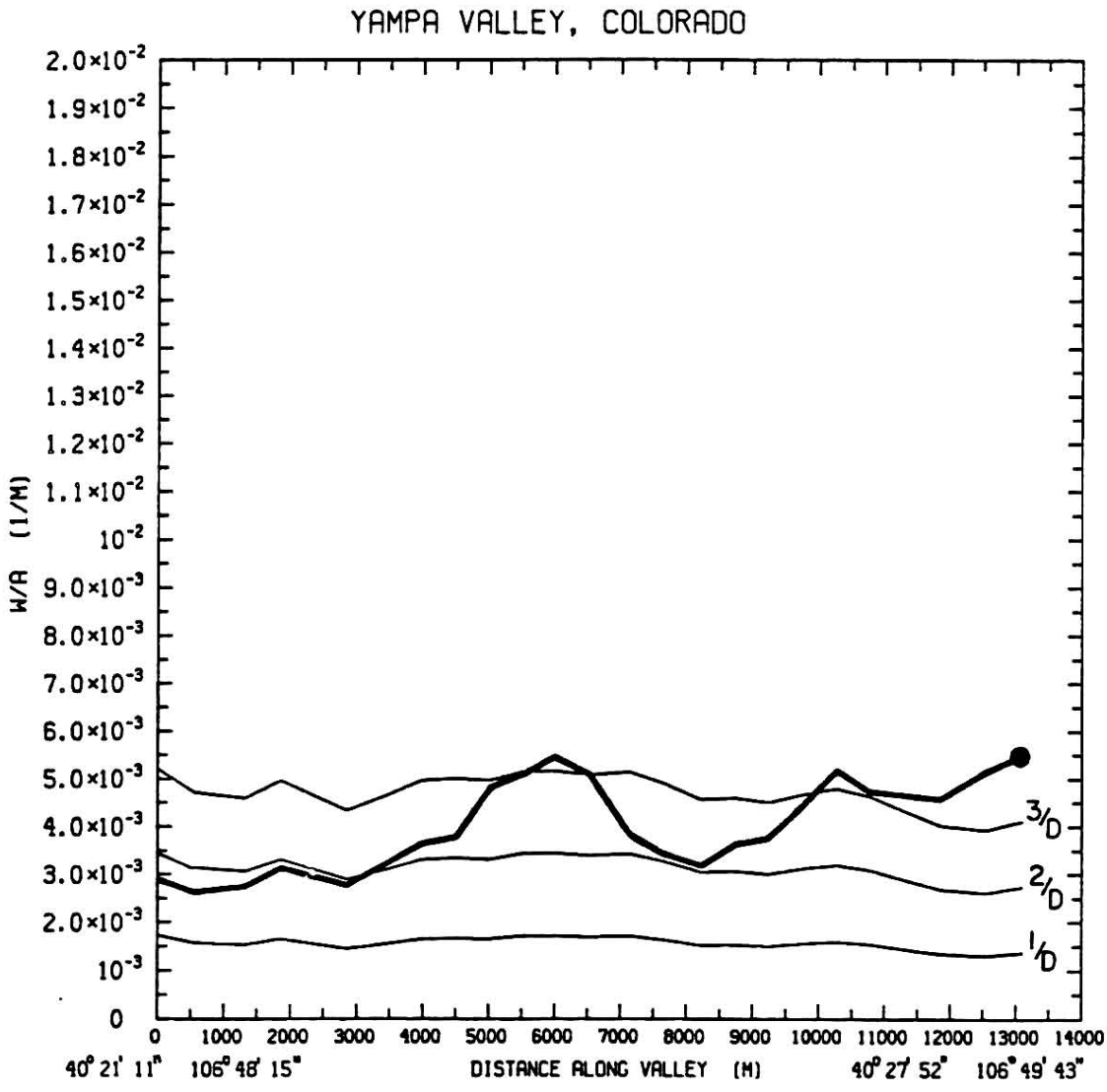

Figure 13g. Same as Figure 10g but for Yampa Valley.

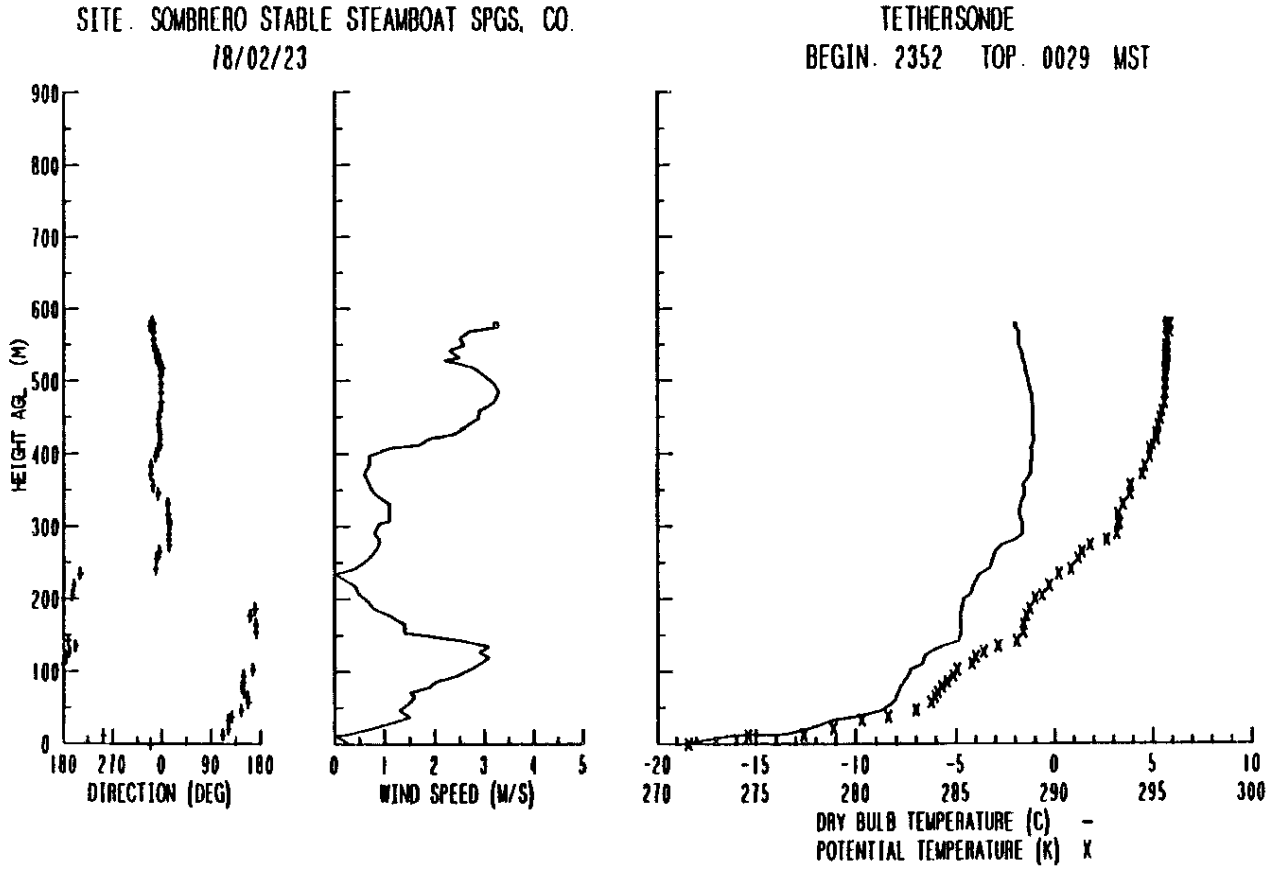

Figure 13h. Same as Figure 10h but for Yampa Valley.

2. Gore Creek

Fourteen kilometers of the Gore Creek were tested from the confluence of the Gore and Black Gore Creeks until both ridgelines begin to fall away two kilometers northeast of the merging of the Gore Creek and Eagle River. The only major disruption to the ridgelines is the intrusion of the Red Sandstone Creek from the northern edge of the watershed around the ten kilometer point. This causes a lowering of the ridgeline (Figure 14c) and a subsequent decrease in cross-sectional area in the nine to eleven kilometer stretch of the valley. Other than this brief interruption, (W/A) increases rather uniformly from 0.002 m^{-1} to 0.004 m^{-1} except for the last kilometer of the valley where the ridgelines on both sides of the creek have begun to drop. The results of an increasing (W/A) can be seen in the extremely light winds (0.5 m/s) generated at the Safeway store in West Vail (Figure 14h).

C. Data Summary

Figures 10 through 14 present the calculated values for the four valley geometrical parameters D, W, A and (W/A). However, modelers and other researchers may have occasion for a simple order of magnitude value for these quantities. Table 7 summarizes rounded values taken from the five Colorado valleys in this study. Also included in this table is the valley geometric gradient, $\partial K/\partial x$, derived from the slope of the (W/A) plots. Values cited for both the extremes and the representative values are a range taken from all the valleys. Representative values are not statistically averaged numbers but merely the median range of values found in the tested Colorado locations. It is interesting to note that despite different valley topography (W/A)

Figure 14a. Same as Figure 10a but for Gore Creek.

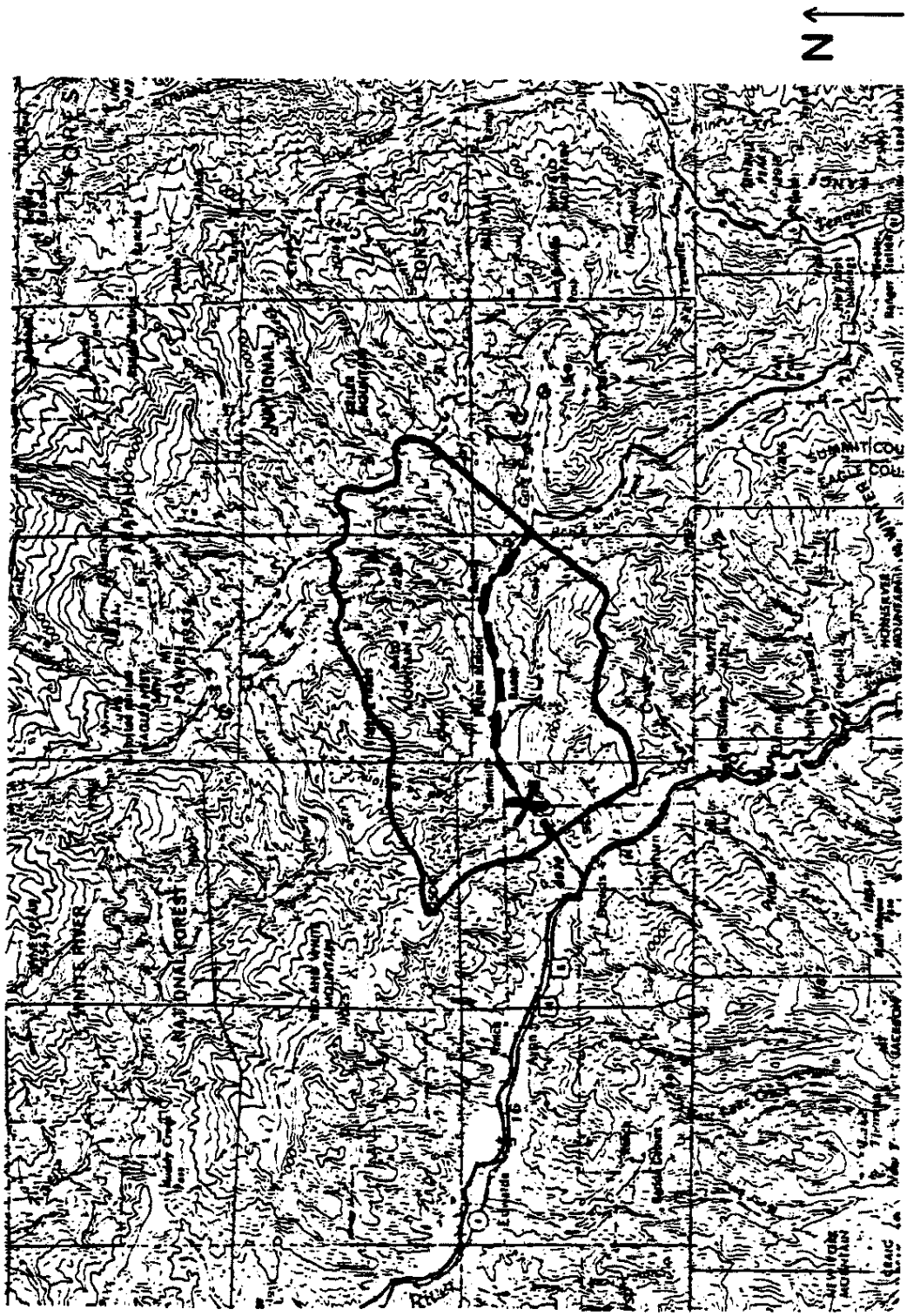
N
Kilometres

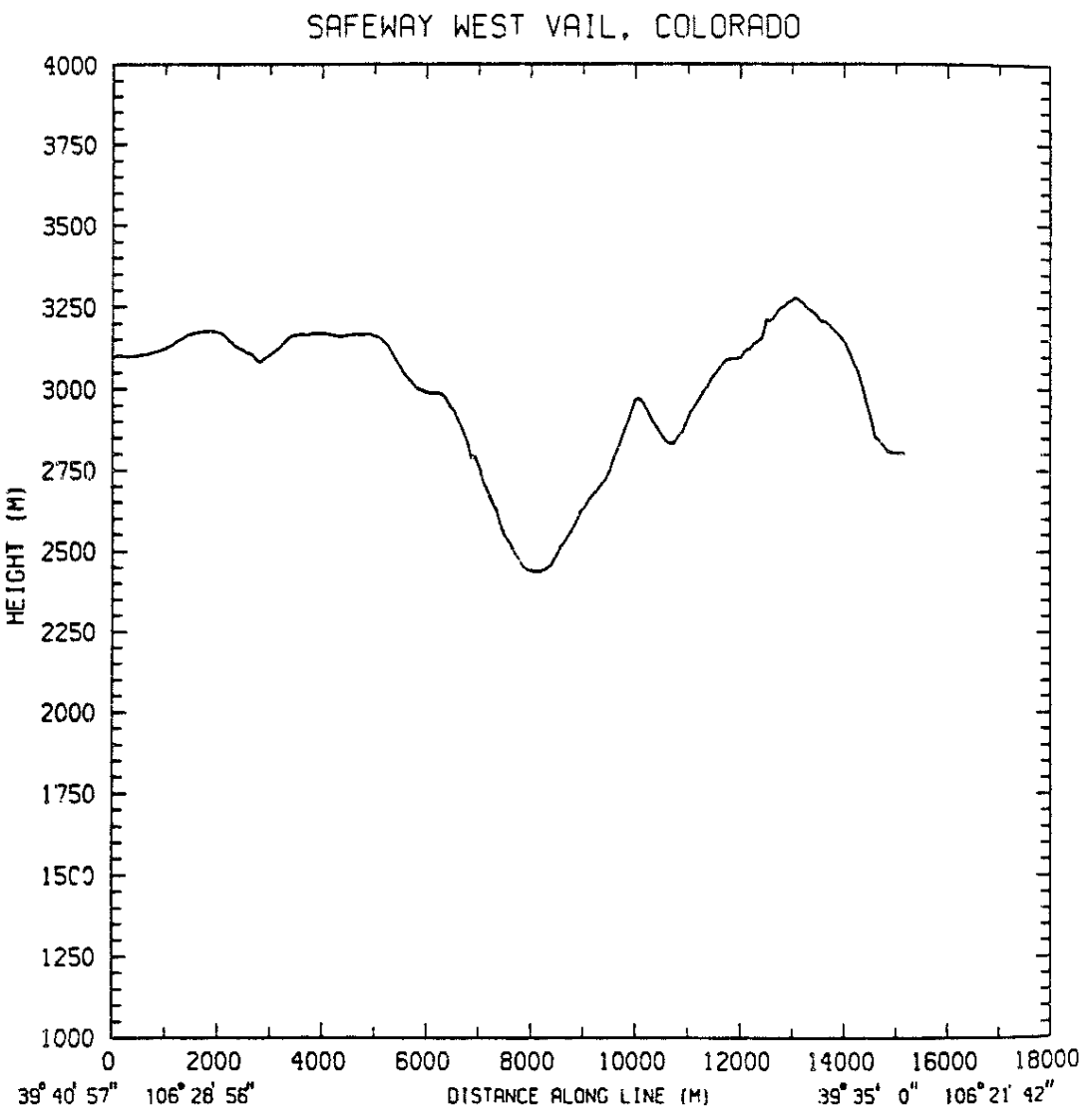

Figure 14b. Same as Figure 10b but for Gore Creek. Sidewall slope angle is 16°.

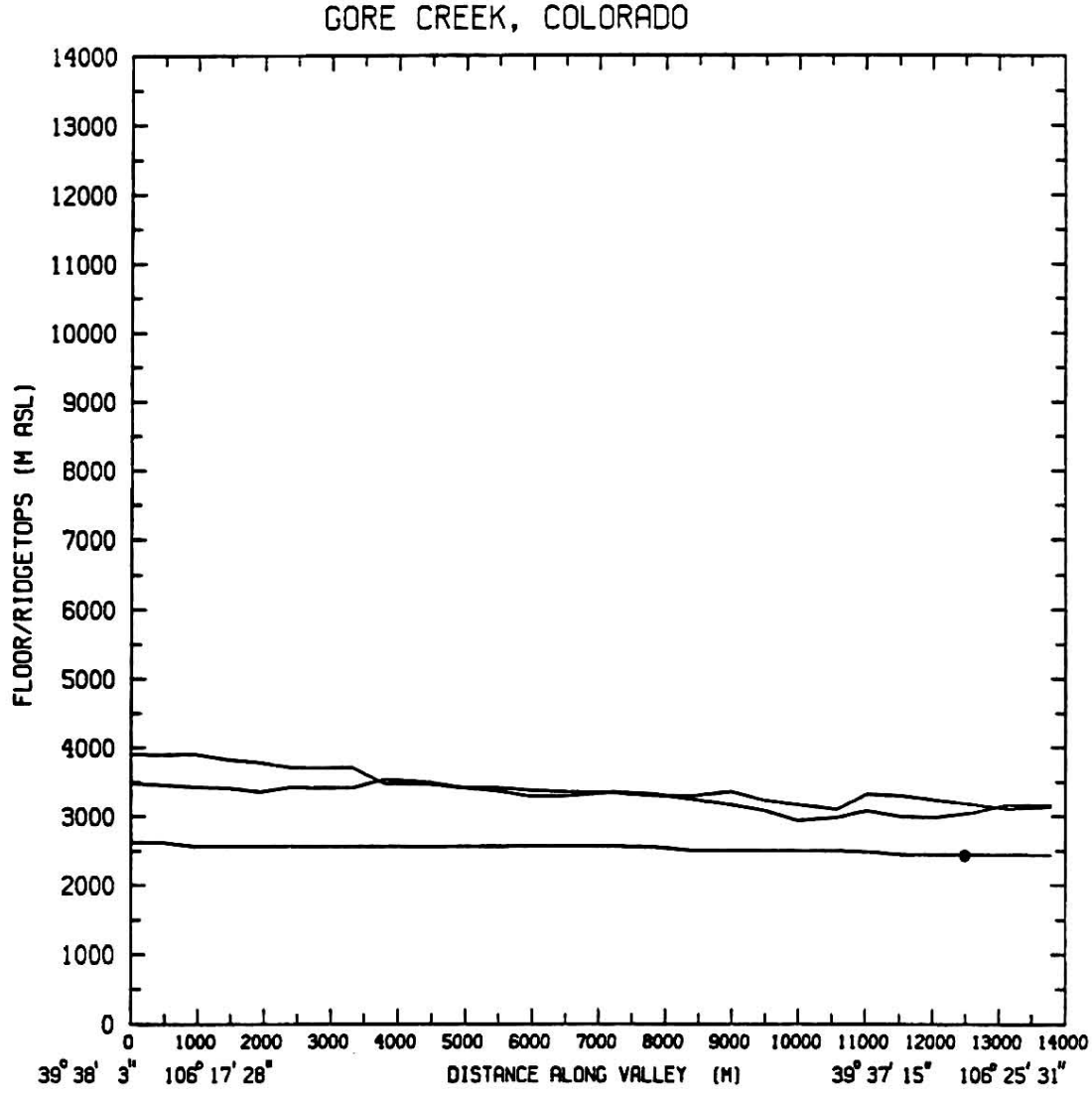

Figure 14c. Same as Figure 10c but for Gore Creek.

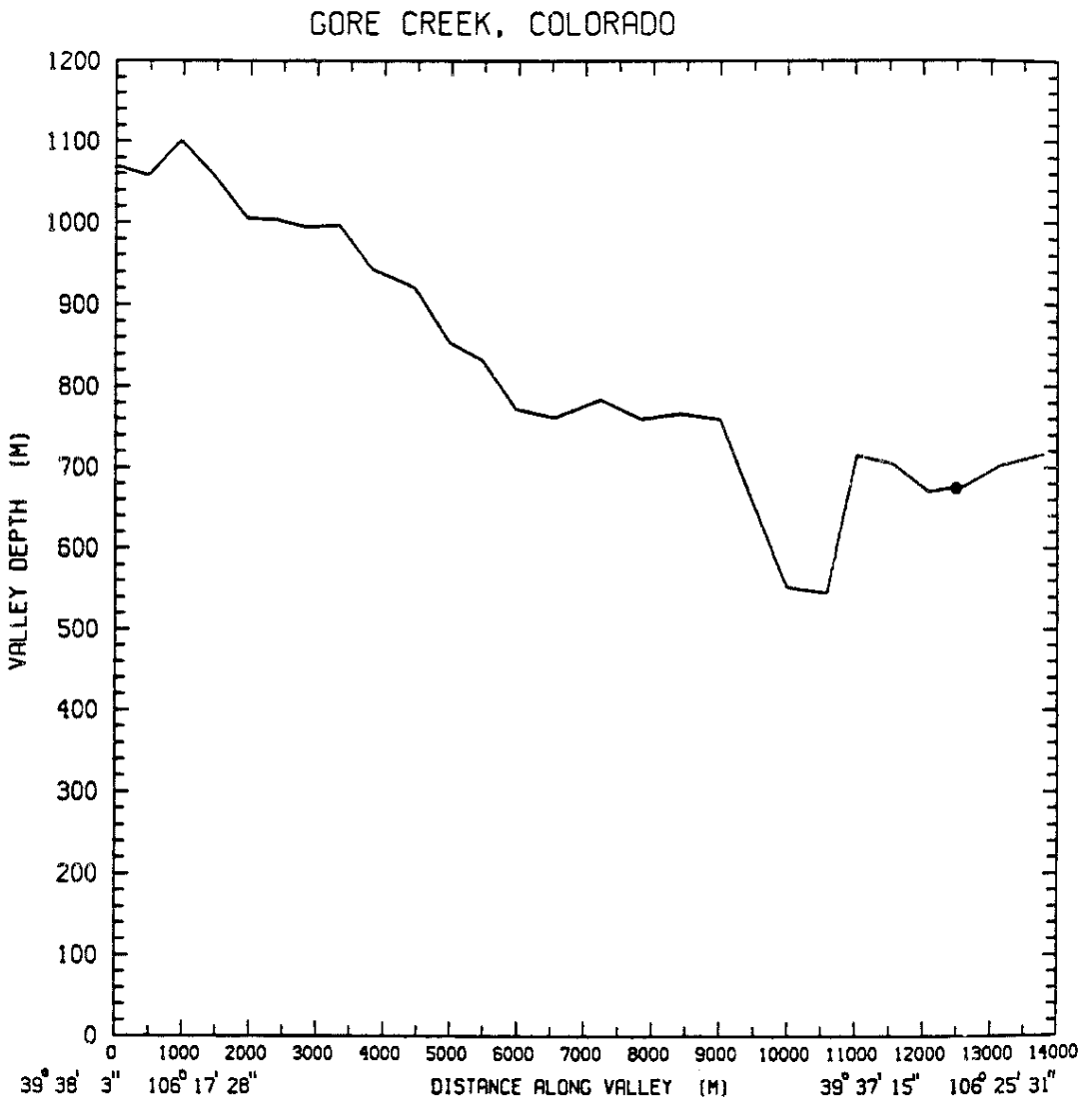

Figure 14d. Same as for Figure 10d but for Gore Creek.

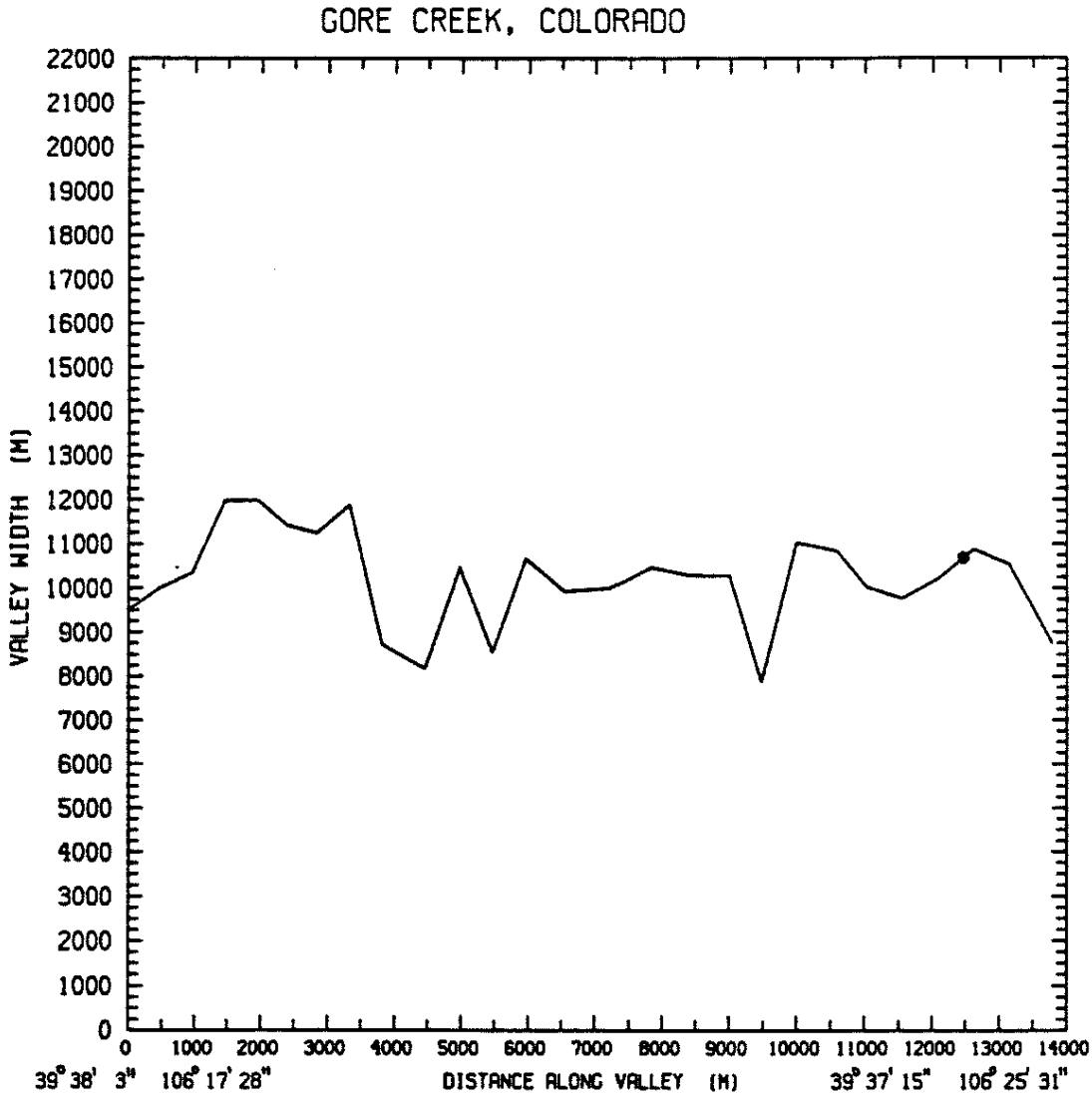

Figure 14e. Same as Figure 10e but for Gore Creek.

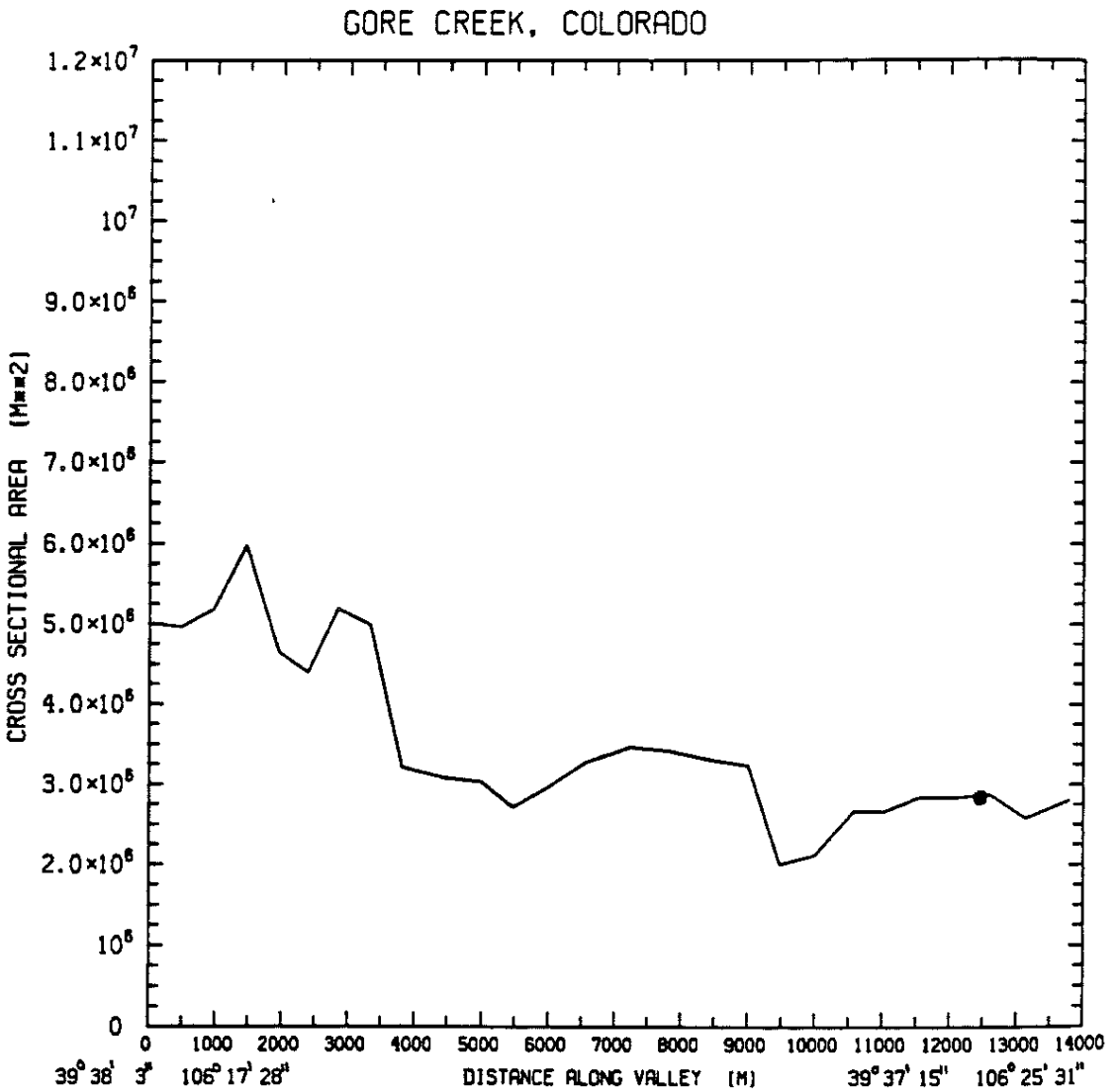

Figure 14f. Same as Figure 10f but for Gore Creek.

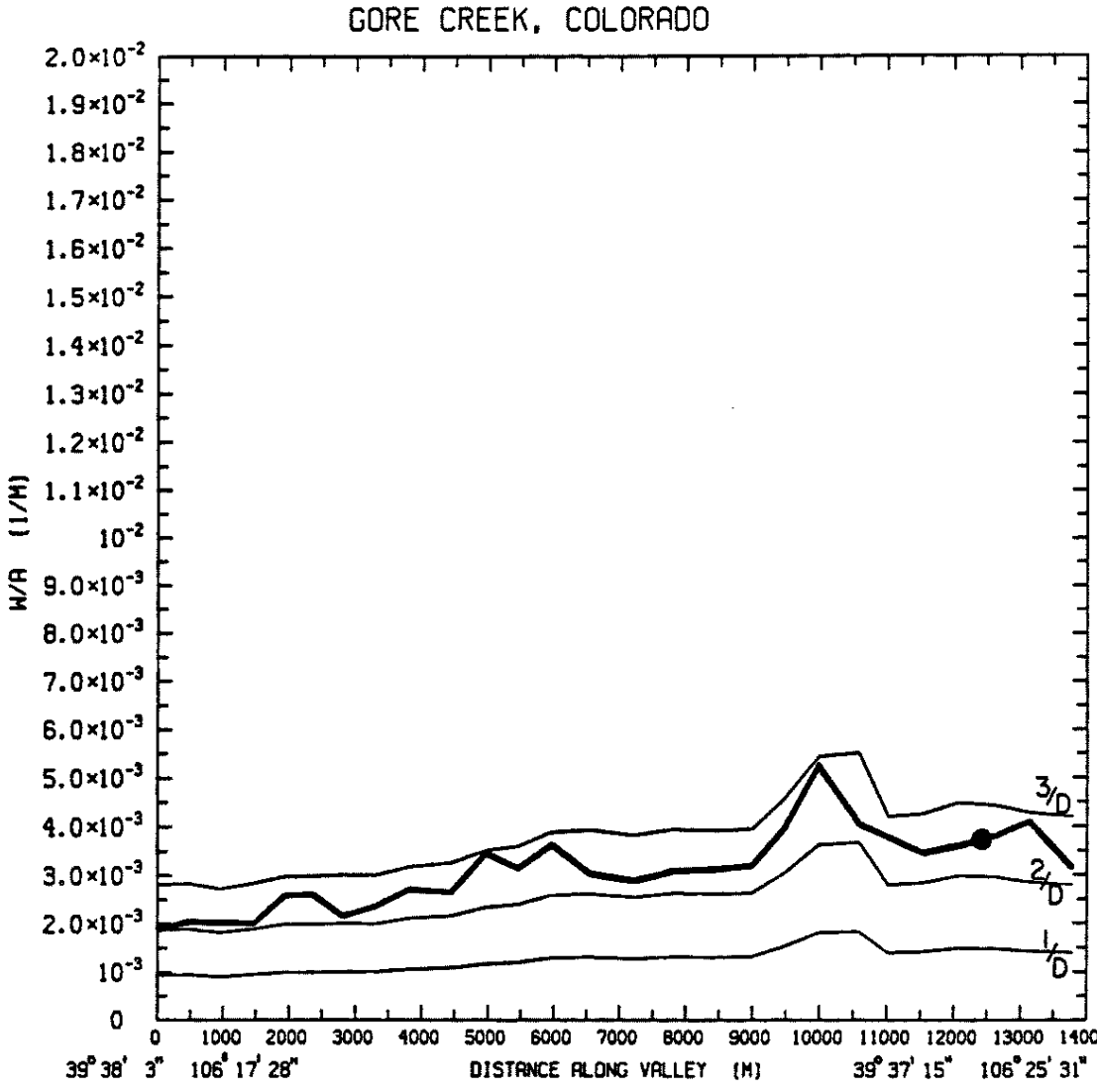

Figure 14g. Same as Figure 10g but for Gore Creek.

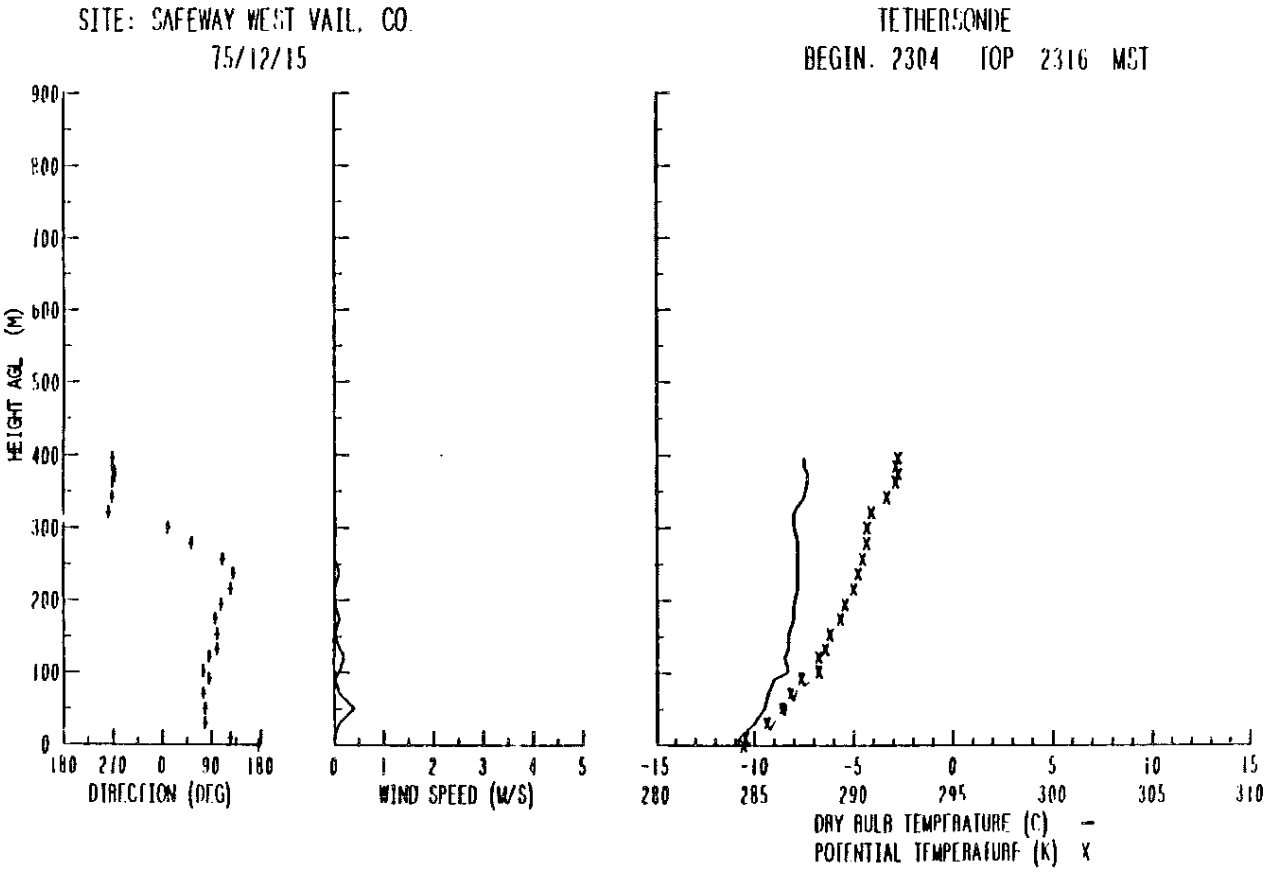

Figure 14h. Same as Figure 10h but for Gore Creek.

rarely varies outside the range of 0.002 to 0.004 m^{-1}. It would be interesting to know if this is true for mountain valleys located in other parts of the world. The five valleys included in this research had values of (W/A) that fell between 2/D and 3/D with D being the actual valley depth. This allows a rough approximation to the (W/A) ratio of a valley knowing only the valley depth, a quantity much easier to calculate than cross-sectional area.

Table 7.

Data Summary: Geometrical parameters for five Colorado valleys studied with computer program.

Valley Parameter		Extreme Value Low	Extreme Value High	Representative Value(s)
Depth (m)		200	1,100	600-800
Width (m)		2,000	21,000	10,000-18,000
Cross-Sectional Area	(m^2)	$2x10^5$	$1.1x10^7$	$1x10^6$ - $1x10^7$
W/A (m^{-1})		$2x10^{-3}$	$1.6x10^{-2}$	$2x10^{-3}$ - $4x10^{-3}$
$\partial K/\partial x$ (m^{-2})	< 0	$-1x10^{-7}$	$-1x10^{-6}$	approx. -10^{-7}
	> 0	$3x10^{-7}$	$5x10^{-7}$	approx. $+10^{-7}$

D. Suggestions for future study

Two areas of this paper could benefit greatly from additional research in the area of mountain-valley meteorology. A deficit still remains in our knowledge of the atmospheric and surface energy budget partitioning in mountain-valley environments, especially during the nighttime hours. A better understanding of the terms which can be

scaled out of the energy budget equations may influence the cooling rate expression, containing the valley geometric factor, which hydrostatically drives the valley wind system.

A second area of concern which has not been resolved in this work is how to handle merging valleys. The problem has been hinted at in the Yampa and Gore Valleys where the intrusion of side creeks has caused the valley geometric parameter, K, to abruptly change the sign of its slope. One may be able to predict whether a single valley may drain or pool but how does that valley interact with the watershed below it? It has not been demonstrated that a drainage wind in Brush Creek will mean that the valley below it (Roan Creek) will also drain. In fact, will the volume of air from two merging valleys equal the volume of the resultant stem? This idea was tested at the intersection of Brush and Roan Creeks (Figure 10a). Figure 15a displays the cross-sectional area of Roan Creek just above and just below the mouth of Brush Creek while Figure 15b shows the cross-sectional area of the last two kilometers of Brush Creek. Both area profiles were calculated at 100 meter increments to gain finer detail at the merging point. The cross-sectional area at the end of the Roan Creek segment above the Brush Creek-Roan Creek intersection is 2.25×10^6 m^2. The cross-sectional area at the end of the Brush Creek segment is 1.25×10^6 m^2. This adds up to 3.5×10^6 m^2 while the cross-sectional area of Roan Creek below the Brush Creek-Roan Creek intersection is only 3.0×10^6 m^2 or less. This would seem to suggest that air from the merging of these two watersheds must flow over the mesa tops into the free atmosphere down-valley if the air is to continue a downstream progression.

(a)

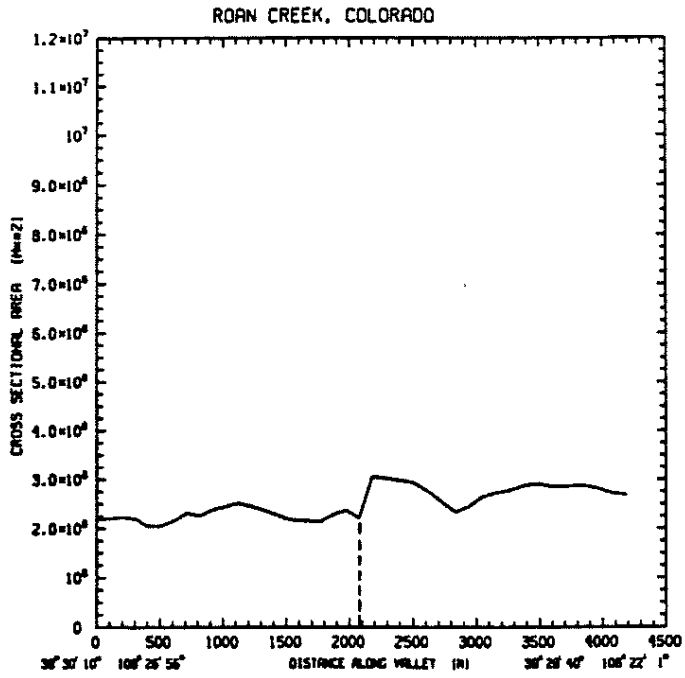

(b)

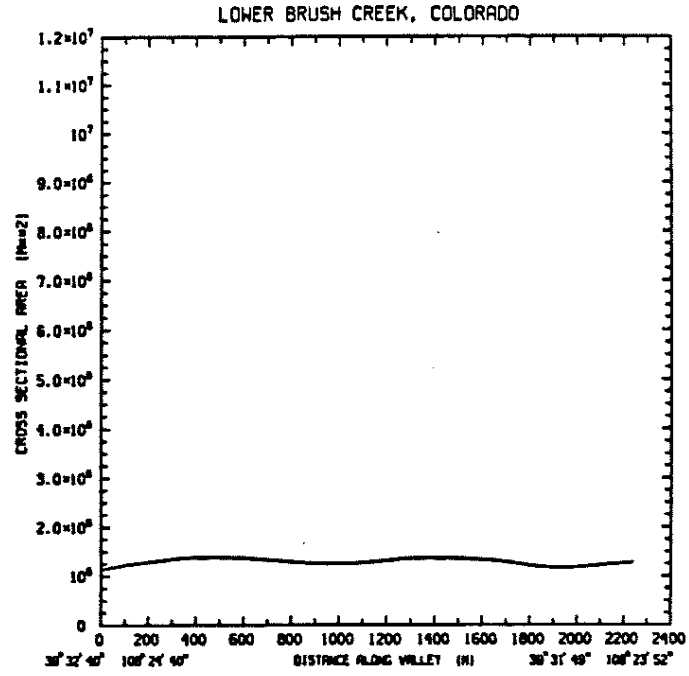

Figure 15. (a) Cross-sectional area of Roan Creek just above (left of dashed line) and just below (right of dashed line) intersection of Roan and Brush Creeks, (b) Cross-sectional area of last two km of Brush Creek.

The problem of merging valleys is basically one of falling ridgelines as one valley blends in with the valley below it. Freytag (1985) acknowledges this problem in the Inn Valley and circumvents it by placing a "lid" over the whole watershed to be used for any height calculations. This "lid" is an average height of the ridgeline above the valley floor, a ridgeline whose actual elevation can vary by more than 1000 meters along a valleys length. Definition of a standard ridge height is critical because all three calculated parameters, W, D and A, ultimately depend on the choice of ridge height.

CHAPTER VI

CONCLUSIONS

Mountain-valleys throughout the world exhibit diurnal wind systems under synoptically undisturbed conditions. Along-valley temperature and pressure gradients are established under these circumstances creating valley wind systems which reverse sign twice daily. The purpose of this research was to investigate the role that valley topography plays during the nocturnal cooling of air in the valley volume, particularly when advective processes are small such as early in the cooling period.

Commencing with the First Law of Thermodynamics and utilizing energy budgets, a unique method has been derived for the cooling rate of an air volume. In a dry environment the rate of cooling is proportional to an energy term, expressed as the difference between the net longwave radiation escaping through the top of the valley atmosphere and the ground heat flux in the valley, multiplied by a topographical term, K. The topographical parameter is defined for a cross section to be the ratio of valley width from ridgetop to ridgetop divided by the cross-sectional area.

A changing valley configuration produces a variation in the topographical parameter which allows for differential cooling rates among the valley cross sections. If the topography changes in a systematic manner, an along-valley temperature gradient will be established which will hydrostatically produce a corresponding pressure gradient driving the nocturnal valley wind. The sign of the

topographically-induced temperature gradient hinges entirely on the change of the topographic parameter along-valley. Advective changes aside, a decreasing K down-valley produces relatively cooler air in the upper portion of the valley compared to the lower portion which leads to a strong down-valley wind. An increasing K in the down-valley direction produces the opposite temperature regime and consequently light down-valley winds.

The topographic parameter was calculated for five Colorado mountain-valleys using digital elevation data and compared to tethersonde wind observations available in four of them. Good agreement was found between the changing topographic parameter and the observed strength of the valley wind system. The ability of the topographical parameter to create a localized temperature gradient within individual valleys eliminates the need to include the plain effect as an important feature in the creation of the local mountain-valley wind system.

CHAPTER VII

REFERENCES

André, J.C. and L. Mahrt, 1982: The Nocturnal Surface Inversion and Influence of Clear-Air Radiative Cooling. Journal of the Atmospheric Sciences, 39, pp. 864-878.

Bader, D. C., 1985: Mesoscale Boundary Layer Development over Mountainous Terrain. Atmospheric Science Paper No. 396. Department of Atmospheric Science, Colorado State University, Fort Collins, CO., 251 p.

Clark, R. H., 1970: Observational Studies in the Atmospheric Boundary Layer. Quart. J. Roy. Met. Soc., 96, pp. 91-114.

Dickerson, M. H. and P. H. Gudiksen, 1980: The Department of Energy's Atmospheric Studies in Complex Terrain (ASCOT) Program. Proceedings, AMS/APCA Second Joint Conference on Applications of Air Pollution Meteorology, March 24-27, 1980, New Orleans, LA. Published by American Meteorological Society, Boston, MA, pp. 469-473.

Dietrich, D. L. and J. E. Childs, 1982: Organization and Structure of the NOAA/EDIS/NGSDC 30-second Average Elevation Data. Final Report, Contract 28-K2-242, Rocky Mountain Forest and Range Experiment Station, U. S. Forest Service, Fort Collins, CO., 45 p.

Edson, R. T., 1980: Parameterization of Net Radiation at the Surface Using Data from the Wangara Experiment. Masters Thesis. Department of Atmospheric Science, Colorado State University, Fort Collins, CO., 89 p.

Egger, J., 1987: Simple Models of the Valley-Plain Circulation Part I: Minimum Resolution Model. Meteorology and Atmospheric Physics, 36, pp. 231-242.

Egger, J., 1987: Simple Models of the Valley-Plain Circulation Part II: Flow Resolving Model. Meteorology and Atmospheric Physics, 36, pp. 243-254.

Elassal, A. A. and V. M. Caruso, 1983: Digital Elevation Models. USGS Digital Cartographic Data Standards, Geological Survey Circular 895-B, 40 p.

Fleagle, R. G., 1950: A Theory of Air Drainage. Journal of Meteorology, 7 (3), pp. 227-232.

Freytag, C., 1985: MERKUR-Results: Aspects of the Temperature Field and the Energy Budget in a Large Alpine Valley During Mountain and Valley Wind. Contributions to Atmospheric Physics, 58, pp. 458-476.

Garrett, A., 1983: Drainage Flow Prediction with a One-Dimensional Model Including Canopy, Soil and Radiation Parameterizations. Journal of Climate and Applied Meteorology, 22, pp. 79-91.

Hennemuth, B., 1987: Heating of a Small Alpine Valley. Meteorology and Atmospheric Physics, 36, pp. 287-296.

Holton, J. R., 1979: An Introduction to Dynamic Meteorology, second edition, Academic Press, New York, 391 p.

Kyle, T. G., 1987: The Energy Budget in a Valley Nocturnal Flow. Tellus, 39A, pp. 226-234.

Manins, P. C. and B. L. Sawford, 1979a: A Model of Katabatic Winds. Journal of the Atmospheric Sciences, 36, pp. 619-630.

Petkovsek, Z., 1978: Relief Meteorologically Relevant Characteristics of Basins, Zeitschrift fur Meteorologie, pp. 333-340.

Petkovsek, Z., 1980: Additional Relief Meteorologically Relevant Characteristics of Basins, Zeitschrift fur Meteorologie, pp. 379-382.

Sellers, W. D., 1965: Physical Climatology, The University of Chicago Press, Chicago, 272 p.

Steinacker, R., 1984: Area-Height Distribution of a Valley and its Relation to the Valley Wind. Contributions to Atmospheric Physics, 57 (1), pp. 64-71.

Vergeiner, I., 1987: An Elementary Valley Wind Model. Meteorology and Atmospheric Physics, 36, pp. 255-263.

Vergeiner, I. and E. Dreiseitl, 1987: Valley Winds and Slope Winds-Observations and Elementary Thoughts. Meteorology and Atmospheric Physics, 36, pp. 264-286.

Vergeiner, I., E. Dreiseitl, and C.D. Whiteman, 1987: Dynamics of Katabatic winds in Colorado 's Brush Creek Valley. Journal of the Atmospheric Sciences, 44 (1), pp. 148-157.

Wagner, A., 1938: Theorie und Beobachtung der periodischen Gebirgswinde. Gerlands Beitr. Geophys. (Leipzig), 52, pp. 408-449.

Whiteman, C. D., 1980: Breakup of Temperature inversions in Colorado Mountain Valleys. Atmospheric Science Paper No. 328, Colorado State University, Fort Collins, CO., 250 p.

Whiteman, C. D. and S. Barr, 1986: Atmospheric Mass Transport by Along-Valley Wind Systems in a Deep Colorado Valley. Journal of Climate and Applied Meteorology, 25, pp. 1205-1212.

Whiteman, C. D., K. J. Allwine, J. M. Hubbe, H. P. Foote, M. M. Orgill, L. J. Fritschen, 1987: Radiation and Surface Energy Budgets for a Colorado Valley. Proceedings, AMS Fourth Conference on Mountain Meteorology, August 25-28, 1987, Seattle, Washington. To be published by the American Meteorological Society, Boston, Massachusetts.

Yamada, T., 1981: A Numerical Simulation of Nocturnal Drainage Flow. Journal of the Meteorological Society of Japan, 59 (1), pp. 108-122.

APPENDIX A

RELATIONSHIP BETWEEN θ AND T

In this appendix a relationship between θ and T is derived utilizing three simple expressions and one assumption regarding the ratio of (T/θ).

Even in mountainous terrain extensive ground slopes are generally small, say, less than 10^{o}, so that the air in the valley may be regarded as being in hydrostatic balance (Manins and Sawford 1979.) Air in the valley volume may thus be described by the hydrostatic principle

$$\frac{dP}{dz} = - \rho g \quad , \tag{A.1}$$

the equation of state

$$P = \rho RT \quad , \tag{A.2}$$

and Poisson's equation for potential temperature

$$\theta = T \left(\frac{P_o}{P} \right)^{R/c_p} \tag{A.3}$$

where R is the gas constant for dry air and P_o is a reference pressure generally taken as 1000 mb.

Taking the natural logarithm of Poisson's equation and differentiating both sides yields

$$\frac{d\theta}{\theta} = \frac{dT}{T} - \frac{R}{c_p} \frac{dP}{P} \quad . \tag{A.4}$$

Substitution of the hydrostatic relationship into the second term of the right side produces

$$\frac{d\theta}{\theta} = \frac{dT}{T} - \frac{R\rho g}{c_p P}\, dz \qquad (A.5)$$

and with the insertion of the equation of state in the same term, equation (A.5) becomes

$$\frac{d\theta}{\theta} = \frac{dT}{T} + \frac{g}{c_p T}\, dz \quad . \qquad (A.6)$$

Equation (A.6) can be rewritten as

$$d\theta \approx dT + \frac{g}{c_p}\, dz \qquad (A.7)$$

if $(T/\theta)\approx 1$. This approximation works very well at elevations near sea level but deteriorates as the pressure decreases. For valleys located below the 700 mb surface T is within 10% or less of θ.

The integration of equation (A.7) from sea level to an arbitrary height z is

$$(\theta - \theta_o) \approx (T - T_o) + \frac{g}{c_p}(z - z_o) \quad . \qquad (A.8)$$

where the subscript denotes sea-level quantities. In equation (A.8) z_o equals zero and $\theta_o = T_o$ by definition so in the lower troposphere

$$\theta \approx T + \frac{g}{c_p} z \qquad (A.9)$$

where z is defined as the height above sea level in meters. The gravitational acceleration g can be treated as constant with height over the range of mountain-valley altitudes found on earth.

2-101

PORT DOCUMENTATION PAGE	1. REPORT NO. Atmospheric Sci. Paper 416	2.	3. Recipient's Accession No

Title and Subtitle
INTRA-VALLEY TOPOGRAPHICAL CONTROL OF NOCTURNAL VALLEY WINDS

5. Report Date July 1987

6.

Author(s)
Robert D. O'Neal and Thomas B. McKee

8. Performing Organization Rept. No. Ats Paper 416

Performing Organization Name and Address
Colorado Climate Center
Department of Atmospheric Science
Colorado State University
Fort Collins, CO 80523

10. Project/Task/Work Unit No.

11. Contract(C) or Grant(G) No.
(C) ATM-839428
(G) CSU Agr. Exp. Station

Sponsoring Organization Name and Address

13. Type of Report & Period Covered

14.

Supplementary Notes

Climatology Report No. 87-2, Colorado Climate Center, Fort Collins, CO 80523

Abstract (Limit: 200 words)

Mountain valleys throughout the world exhibit diurnal wind systems under synoptically undisturbed conditions. Along-valley temperature and pressure gradients are established under these circumstances creating valley wind systems which reverse sign twice daily. The purpose of this research was to investigate the role that valley topography plays during the nocturnal cooling of air in the valley volume, particularly when advective processes are small such as early in the cooling period.

The topographic parameter was calculated for 5 Colorado mountain valleys using digital elevation data and compared to tethersonde wind observations available in 4 of them. Good agreement was found between the changing topographic parameter and the observed strength of the valley wind system. The ability of the topographical parameter to create a localized temperature gradient within individual valleys eliminates the need to include the plain effect as an important feature in the creation of the local mountain-valley wind system.

Document Analysis a. Descriptors

b. Identifiers/Open-Ended Terms

mountain-valley
digital elevation data
nocturnal cooling by topography

c. COSATI Field/Group

Availability Statement	19. Security Class (This Report) UNCLASSIFIED	21. No. of Pages 103
	20. Security Class (This Page) UNCLASSIFIED	22. Price